

**UNITED STATES AIR FORCE  
ARMSTRONG LABORATORY**

---

**Proceedings of RF and UWB  
Measurements Symposium**

**John E. Brewer  
Nancy L. Beauregard**

Illgen Simulation Technologies, Inc.  
8305 Hawks Road  
Brooks AFB TX 78235-5324

**Richard A. Tell**

Richard A. Tell Associates., Inc.  
8309 Garnet Canyon Lane  
Las Vegas NV 89129

**Sherrie S. Sorensen, Captain, USAF**

**June 1997**

**19970630 059**

*Approved for public release;  
distribution is unlimited.*

**Occupational and Environmental Health  
Directorate  
Radiofrequency Radiation Division  
8305 Hawks Road  
Brooks AFB, TX 78235-5324**

**DTIC QUALITY INSPECTED 1**

## NOTICES

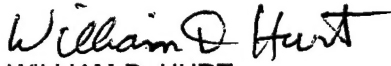
When Government drawings, specifications, or other data are used for any purpose other than in connection with a definitely Government-related procurement, the United States Government incurs no responsibility or any obligation whatsoever. The fact that the Government may have formulated or in any way supplied the said drawings, specifications, or other data, is not to be regarded by implication, or otherwise in any manner construed, as licensing the holder or any other person or corporation; or as conveying any rights or permission to manufacture, use, or sell any patented invention that may in any way be related thereto.

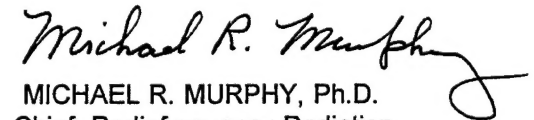
The office of Public Affairs has reviewed this report, and it is releasable to the National Technical Information Services, where it will be available to the general public, including foreign nations.

This report has been reviewed and is approved for publication.

Government agencies and their contractors registered with Defense Technical Information Center (DTIC) should direct request for copies to : Defense Technical Information Center, 8725 John J. Kingman Rd., STE 0944, Ft. Belvoir, VA 22060-6218.

Non-Government agencies may purchase copies of this report from: National Technical Information Services (NTIS), 5285 Port Royal Road, Springfield, VA 22161-2103.

  
WILLIAM D. HURT  
Project Scientist

  
MICHAEL R. MURPHY, Ph.D.  
Chief, Radiofrequency Radiation  
Division

REPORT DOCUMENTATION PAGE			Form Approved OMB No. 0704-0188	
Public reporting burden for this collection of information is estimated to average 1 hour per response, including the time for reviewing instructions, searching existing data sources, gathering and maintaining the data needed, and completing and reviewing the collection of information. Send comments regarding this burden estimate or any other aspect of this collection of information, including suggestions for reducing this burden, to Washington Headquarters Services, Directorate for Information Operations and Reports, 1215 Jefferson Davis Highway, Suite 1204, Arlington, VA 22202-4302, and to the Office of Management and Budget, Paperwork Reduction Project (0704-0188), Washington, DC 20503.				
1. AGENCY USE ONLY (Leave blank)		2. REPORT DATE June 1997	3. REPORT TYPE AND DATES COVERED Final, July 1994 - May 1995	
4. TITLE AND SUBTITLE  Proceedings of RF and UWB Measurements Symposium			5. FUNDING NUMBERS  C - F08635-91-C-0167-TFP94-24 PE - 62202F PR - 7757 TA - B3 WU - 13	
6. AUTHOR(S)  John E. Brewer, Nancy L. Beauregard, Richard A. Tell, Sherrie S. Sorensen				
7. PERFORMING ORGANIZATION NAME(S) AND ADDRESS(ES)  Illgen Simulation Technol, Inc.    Richard Tell Assocs., Inc.    AL/OERS 8305 Hawks Road                    8309 Garnet Canyon Lane    8305 Hawks Road Brooks AFB TX 78235-5324        Las Vegas NV 89129        Brooks AFB TX 78235			8. PERFORMING ORGANIZATION	
9. SPONSORING/MONITORING AGENCY NAME(S) AND ADDRESS(ES)  Armstrong Laboratory (AFMC) Occupational and Environmental Health Directorate Radiofrequency Radiation Division 8305 Hawks Road Brooks Air Force Base, TX 78235-5324			10. SPONSORING/MONITORING  AL/OE-PC-1997-0026	
11. SUPPLEMENTARY NOTES  Armstrong Laboratory Technical Monitor: William D. Hurt, (210) 536-3167				
12a. DISTRIBUTION/AVAILABILITY STATEMENT  Approved for public release; distribution is unlimited.			12b. DISTRIBUTION CODE	
13. ABSTRACT (Maximum 200 words) The radio frequency (RF) radiation and ultrawideband (UWB) measurements symposium, held during February 13-16, 1995, was sponsored by the U.S. Air Force Armstrong Laboratory at Brooks Air Force Base in San Antonio, Texas, and represented a collection of experts with day-to-day working experience in assessing RF fields and associated induced body current and contact currents as well as researchers studying improved methods and instrumentation for such measurements. In addition, specialists in the area of ultrawideband RF measurements presented information relevant to this specialized field. Mr. Richard A. Tell of Richard Tell Associates, Inc., 8309 Garnet Canyon Lane, Las Vegas, NV 89129, served as Technical Chairman of the symposium.				
14. SUBJECT TERMS Radio frequency radiation, RF, ultrawideband, UWB, RF measurements			15. NUMBER OF PAGES 134	
			16. PRICE CODE	
17. SECURITY CLASSIFICATION OF REPORT Unclassified	18. SECURITY CLASSIFICATION OF THIS PAGE Unclassified	19. SECURITY CLASSIFICATION OF ABSTRACT Unclassified	20. LIMITATION OF ABSTRACT UL	





## Table of Contents

Introductory Overview to Meeting on Current Issues in RFR and UWB Measurements and Safety, by R. Tell.....	1
RFR Meter Calibration, Methods, and Observations, by E. Mantiply.....	3
Calibration of Narda Probes at 94 GHz, by S. Sorensen.....	7
Electric Field Exposure Characterization and Induce Foot Current Measurements in the Presence of Multiple-Source and Multiple-Frequency VHF Fields, by S. Tofani.....	21
A Method for 2-Dimensional Imaging of RFR Fields, by T. Walters.....	27
A Practical Assessment of Variability Associated with Broadband RF Field Strength Survey Measurements, by R. Tell.....	29
U.S. Army Experiences in Performing RFR Field Measurements, by B. Roberts.....	33
Conclusions Drawn from Near-Field Exposure Assessment and Reduction Studies: RF (6-65 MHz) Dielectric Heaters, by D. Conover.....	35
Case Studies of Exposure to Nonuniform RF Nearfields: FM Broadcast Antenna, Heat Sealer and Cellular Telephone, by A. Guy.....	41
738 Engineering Installation Squadron Environmental Radio Frequency (RF) Measurement Capability, by J. Laycock.....	43
Extension of Narda Calibration Interval, by J. Brewer.....	45
Overview of UWB Free-Field Measurement and Signal Recording Techniques, by D. Voss.....	49
Development of Direct Means for Measuring Ankle Currents in RF Fields, by V. Anderson.....	53
Some Observations on the Measurement of Induced and Contact Currents, by J. Hatfield.....	57
Measurements of Induced Body Currents at HF/MF Broadcasting Stations and Resulting Results of Laboratory Tests, by K. Jokela.....	63
Measurement for OSHA Compliant RF Protection Programs, by R. Curtis.....	69
Development, Characteristics and Use of Air-Core RF Current Transformers for Measuring Induced Body Currents, by M. Hagmann.....	75
Calculated and Measured Currents Induced in the Human Body for VHF Plane-wave, EMP, and UWB Exposures, by O. Gandhi.....	79
Comparison of Ferrous and Non-Ferrous Inductive Probes with Stand-On Probes for Measuring Induced Currents, by J. Passour.....	97

SAR Measurements in the Field and Practical Constraints, by R. Olsen.....	101
Automated Dosimetric Scanning System for Mobile Communications, by N. Kuster.....	107
Practical Aspects of Applying Time-Averaging to Determination of Compliance with RFR Exposure Standards, by R. Woolnough.....	113
Protective Clothing Evaluations, by R. Olson.....	121
Measurements of Shielding Effectiveness of Microwave-Protective Suits, by A. Guy.....	125

## **Introductory Overview to Meeting on Current Issues in RFR and UWB Measurements and Safety**

Richard A. Tell  
Richard Tell Associates, Inc.  
8309 Garnet Canyon Lane  
Las Vegas, NV 89129, USA.

The subject of radiofrequency (RF) radiation measurements is a relatively narrow one and one not served well by any single annual symposium or specialized publication. While this topic falls within the realm of some researchers, it is predominately the focus of technicians charged with evaluating exposure of humans to a wide variety of RF fields from a standards compliance perspective. The present meeting represents a collection of experts with day-to-day working experience in assessing RF fields and associated induced body current and contact currents as well as researchers studying improved methods and instrumentation for such measurements.

In November of 1980, a workshop convened of some 33 individuals by the Environmental Protection Agency (EPA) permitted practitioners of RF measurement technology to discuss their experiences with the use, application, design and, importantly, limitations of then currently available instrumentation for assessing potentially hazardous electromagnetic fields and to participate in actual field and laboratory tests in order to compare differing instruments and measurement techniques under identical field and test conditions (1).

Subsequently, a symposium of approximately 125 attendees, also sponsored by the EPA, was held in 1984, for the purpose of further sharing information among users in the field and laboratory. The strong showing of interest at that time, despite limited advertisement of the symposium, included participation from around the world and included numerous attendees interested in learning about the subject because of their new responsibilities in RF radiation protection activities. Nonetheless, similar focused symposia have not been held. This meeting proposes to partially fill that gap.

Historically, a wide range of questionable issues have confronted those carrying out practical RF related measurements. In more recent years, with the increase in complexity of RF exposure standards and the increase in bandwidth occupied by new RF sources, these issues have only further expanded in scope. For example, the addition of requirements to limit the magnitude of induced body currents and contact currents has severely complicated the task of determining compliance with applicable guidelines on exposure in complicated environments. The following items highlight some of the many issues relevant to the subject of this meeting.

- Absolute calibration of field meters, methods and uncertainties;

- Instrument response characteristics, out of band responses;
- True RMS response relative to modulation and pulsed fields;
- Instrument responses to outside influences, like static charge and light;
- Application of uncertainty factors in compliance measurements;
- Observer introduced field perturbations during measurements;
- Instrument drift over prolonged measurement periods;
- Response time of field probes to rapidly varying fields;
- Appropriate measurement techniques for characterizing non-uniform fields;
- Minimum measurement distances for assessing RF fields, especially in the context of close proximity exposure;
- Determining exposure levels in complicated environments, like on towers;
- Induced body current measurements and suitability of instruments to the task;
- Response of body current meters to outside influences, fields;
- Problems in performing induced body currents on towers;
- Level of detail required for field and current measurements on towers;
- Interference with contact current measurements by local high strength fields;
- Spatial resolution of complex RF fields as a function of frequency;
- Practical aspects of SAR measurements in real-world RF environments;
- Measurement approaches for multiple frequency RF fields
- Measurement approaches for ultra wide band (UWB) fields;
- Appropriate measurement parameters for quantifying potential for RF burns;
- Induced body currents in the VHF range;
- Relating point SAR measurements to whole-body average SAR;
- Sufficient evidence of compliance for certain complex exposure conditions;
- Accuracy of induced and contact current measurements with simulated body impedances;
- Instrument aging relative to calibration stability;
- Practical issues related to exposure averaging times in the millimeter wave bands;

While many of these topics will be addressed by the participants at this meeting, a remaining question to be discussed will be the perceived desirability and usefulness of subsequent similar meetings which would provide a forum for specialists in RF measurements to exchange information.

## Reference

1. Radiofrequency Measurements Workshop Summary. U.S. Environmental Protection Agency report EPA 520/2-82-010, July 1982, Office of Radiation Programs, Las Vegas, NV 89114.

# RADIOFREQUENCY RADIATION METER CALIBRATION, METHODS, AND OBSERVATIONS

Edwin D. Mantiplly  
U.S. Environmental Protection Agency  
National Air and Radiation Environmental Laboratory  
Montgomery, Alabama

**Introduction.** In the early 1980's, the EPA developed laboratory radiofrequency (RF) standard field generation systems for the evaluation and calibration of RF electric and magnetic field survey instruments. Commercially available survey instruments were procured and characterized in the laboratory and in real field measurement conditions near various transmitter installations. The purpose of this paper is to review the practical problems and limitations of these instruments and provide some background on the calibration systems.

**Calibration Systems.** The field generation systems at EPA include three transverse electromagnetic (TEM) cells, three large rectangular waveguides, and eight standard gain microwave horns to cover the frequency range of 10 kHz to 26 GHz. These are "standard field" systems; that is, the value of the field strength is calculated from electrical measurements and theory using the geometry of the cell, waveguide, or horn. In the cells and waveguides, measurements of the complex reflection coefficients of the terminations are used to correct for standing wave errors. In the standard gain horn systems, errors due to reflection from microwave absorbers were measured but not incorporated as a system correction.

**Cross-checks.** Cross-checks of the field generation systems were performed with the National Institute of Standards and Technology (NIST). Two Holaday model HI-3001 and two Narda model 8616 with 8621 probes were calibrated at EPA, shipped to NIST and calibrated, and returned to EPA and calibrated again. The Holaday meters were used from 10 to 1120 MHz and the Narda meters from 1.12 to 18 GHz. Representative results of these tests are shown in Figure 1. Generally, the cross-check shows good agreement between the NIST and EPA systems. Both EPA and NIST normally quote standard field accuracy as  $\pm 1$  dB, so a difference of 2 dB is acceptable. Relatively large differences at some VHF and microwave frequencies could probably be explained as

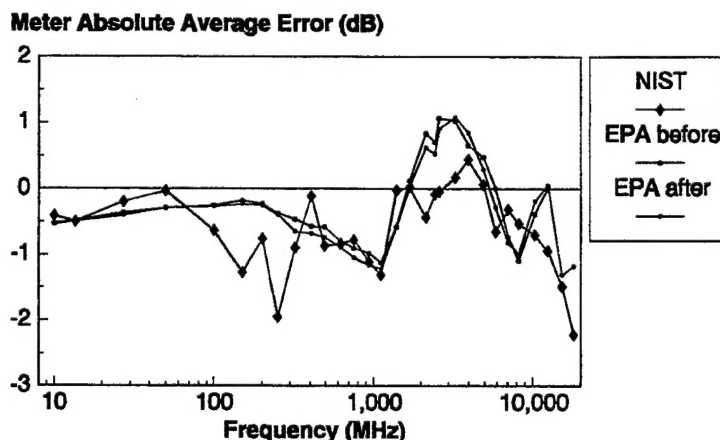


Figure 1. NIST/EPA cross-check results.

systematic errors.

**Instrument Problems.** Results for the absolute calibration of survey instruments in their specified frequency range are generally within the manufacturer's accuracy specification if the instrument is tested by the same basic methods that the manufacturer uses. However, more extensive tests in the laboratory and field experiences have revealed various serious problems with RF survey instruments. These are generally fundamental problems that result from the sensor configuration and are not due to electronic problems in the readout instrument. With a good understanding of these problems, the user can normally achieve excellent measurement results.

### Potential Sensitivity.

The low frequency failure of high-resistance leads to isolate electric field probes is termed "potential sensitivity." The resulting survey meter behavior is a tendency to detect the RF potential difference between the probe and readout instrument, rather than the electric field strength at the probe. Figure 2 shows the results of fields tests for potential sensitivity near a standard AM broadcast

antenna operating at 720 kHz [1]. The best estimate of the field is 25 V/m vertically polarized. The Instruments for Industry EFS-1 readings may be used as a reference because, for the EFS-1, the probe and meter are integrated in a single unit. For the other instruments, with the meter hand-held, there is an exaggerated increase in the field strength displayed as probe height above ground is increased. The largest error observed was about +16 dB. Bundling the meter and probe together on a nonconductive stand with the probe axis horizontal and stepping back to take a reading improves the situation somewhat. Readings tend to be low in this configuration -- the largest error observed was -7 dB. Tests in a TEM cell were used to determine how potential

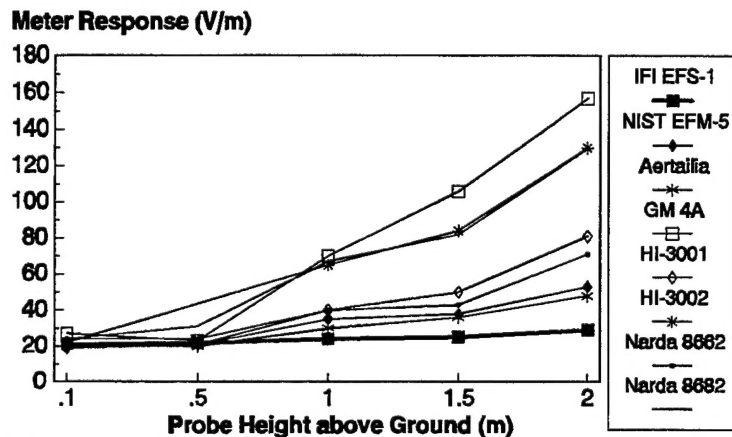


**Figure 2. Potential sensitivity measurement near AM tower.**

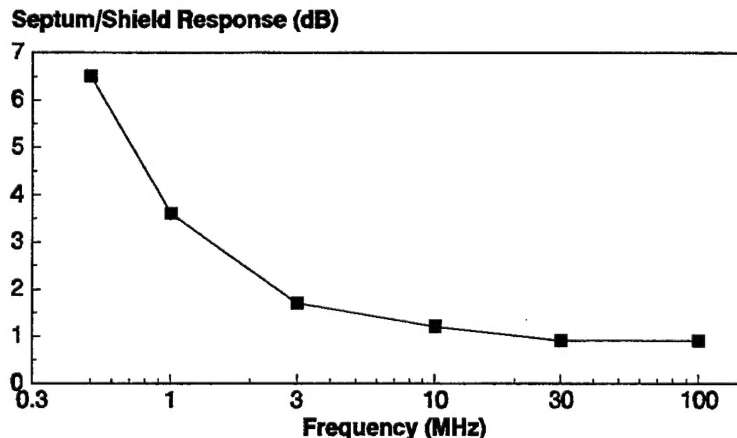


**Figure 3. Potential sensitivity measurement in TEM cell.**

sensitivity varies with frequency [2]. The probe was moved in the cell so that its cover either touched the cell shield or septum. Figure 3 shows the differences in response. Actual field change at the two probe locations in the cell is about 0.8 dB. The meter tested was a NIST EFM-5 and the cell was an IFI 101.5 with 40 cm between the septum and shield.

**Out-of-Band Response.** Large errors in measurement can occur if significant field sources operating at frequencies well above the normal band of a survey instrument are present. Figures 4 and 5 show calibration results, out-of-band, for a Holaday and a Narda magnetic field probe. Figure 6 gives similar data for an IFI EFS-1 electric field meter with the "long" element in use. In the opposite frequency direction, the response of RF electric field survey meters to power frequency electric fields near transmission lines can be significant. The IFI EFS-1 response is only about 20 dB down at 60 Hz, and for other meters the power frequency response is unpredictable because of potential sensitivity. Electrostatic fields can also cause problems.

**Other Problems.** Zero stability, anisotropy, and non-sinusoidal response are other lower priority issues that require evaluation and careful operation. Zero drift for thermocouple-based meters is a problem for relatively low field measurements and when the source is not controlled by the surveyor. Here the probe must be shielded and re-zeroed during measurements. Errors of about - 3 dB due to anisotropy in some magnetic field probes have been observed. Positive errors of 1 to 2 dB can be seen in non-sinusoidal fields such as multiple signal environments and amplitude modulated fields.

**Summary.** In summary, cross-checks indicate good agreement between calibration systems at EPA and NIST. Several problems can seriously affect the

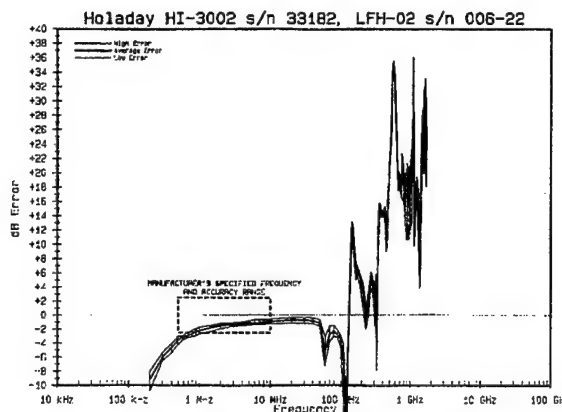


Figure 4. Holaday low frequency magnetic field probe response.

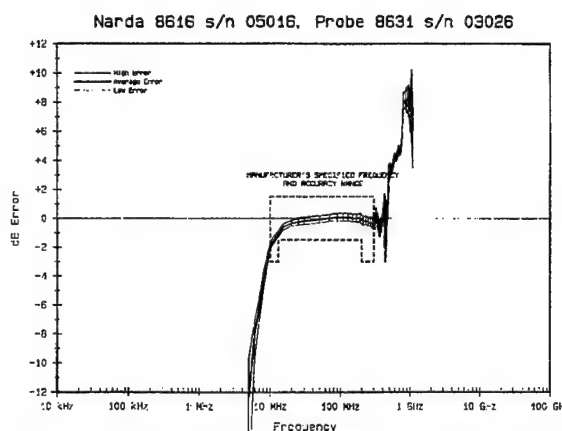


Figure 5. Narda magnetic field probe response.

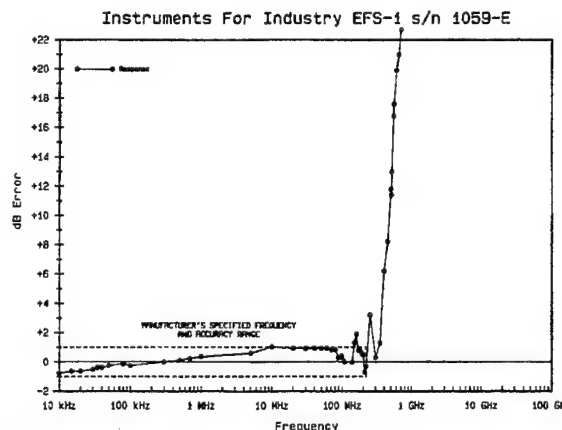


Figure 6. IFI electric field sensor response.

performance of RF hazard survey meters. These problems include: potential sensitivity, out-of-band response, zero stability, anisotropy, and non-sinusoidal response.

**References.**

- [1] E. D. Mantipliy, "Characteristics of Broadband Radiofrequency Field Strength Meters," in IEEE Engineering in Medicine & Biology Society 10th Annual International Conference., CH2566-8/88/0000--889, pp. 889-891, Aug. 1988.
  
- [2] E. D. Mantipliy, An Automated TEM Cell Calibration System., U. S. Environmental Protection Agency, Office of Radiation and Indoor Air, EPA 520/1-84-024, pp. 65-66, Oct. 1984.



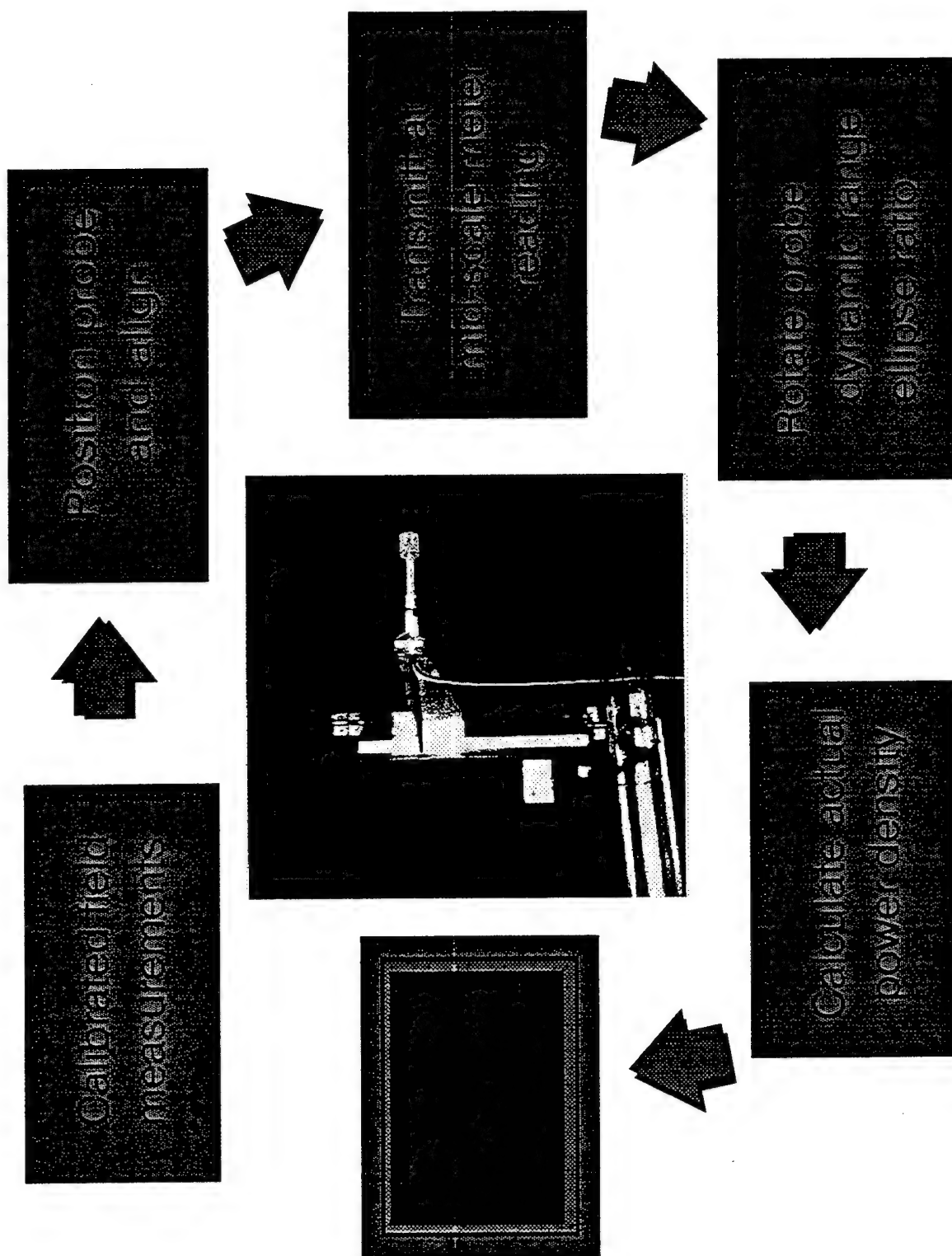
# **Calibration of Narda Probes at 94 GHz**

**Presented by Capt S. Sorensen  
to  
RFR and UWB Measurements  
Symposium**

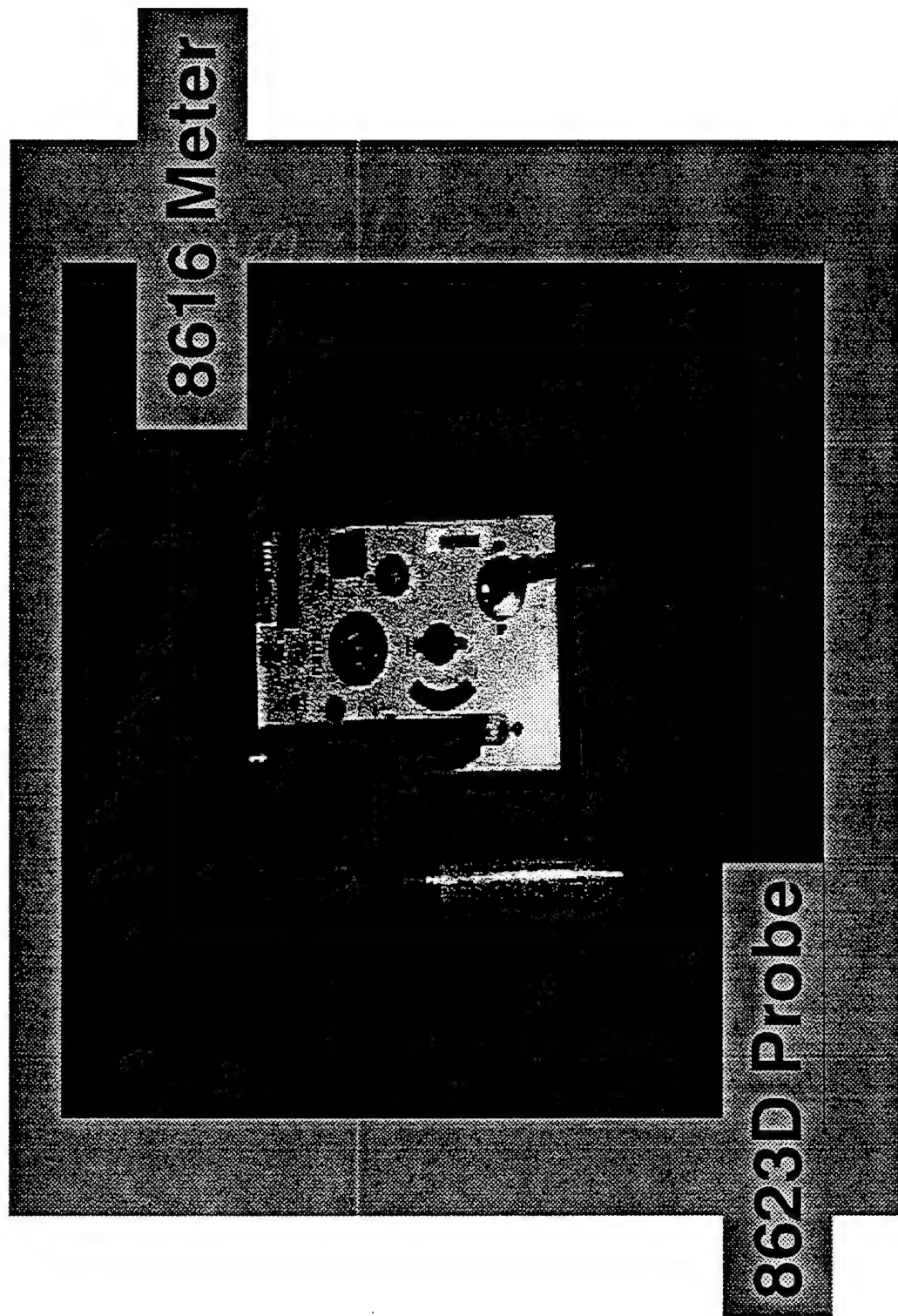
Capt Sherrie Sorensen  
Mr Richard Strickland\*  
Mr Edward Aslan\*  
TSgt Alan Johnston

\* Loral-Microwave Narda, Happague, NY

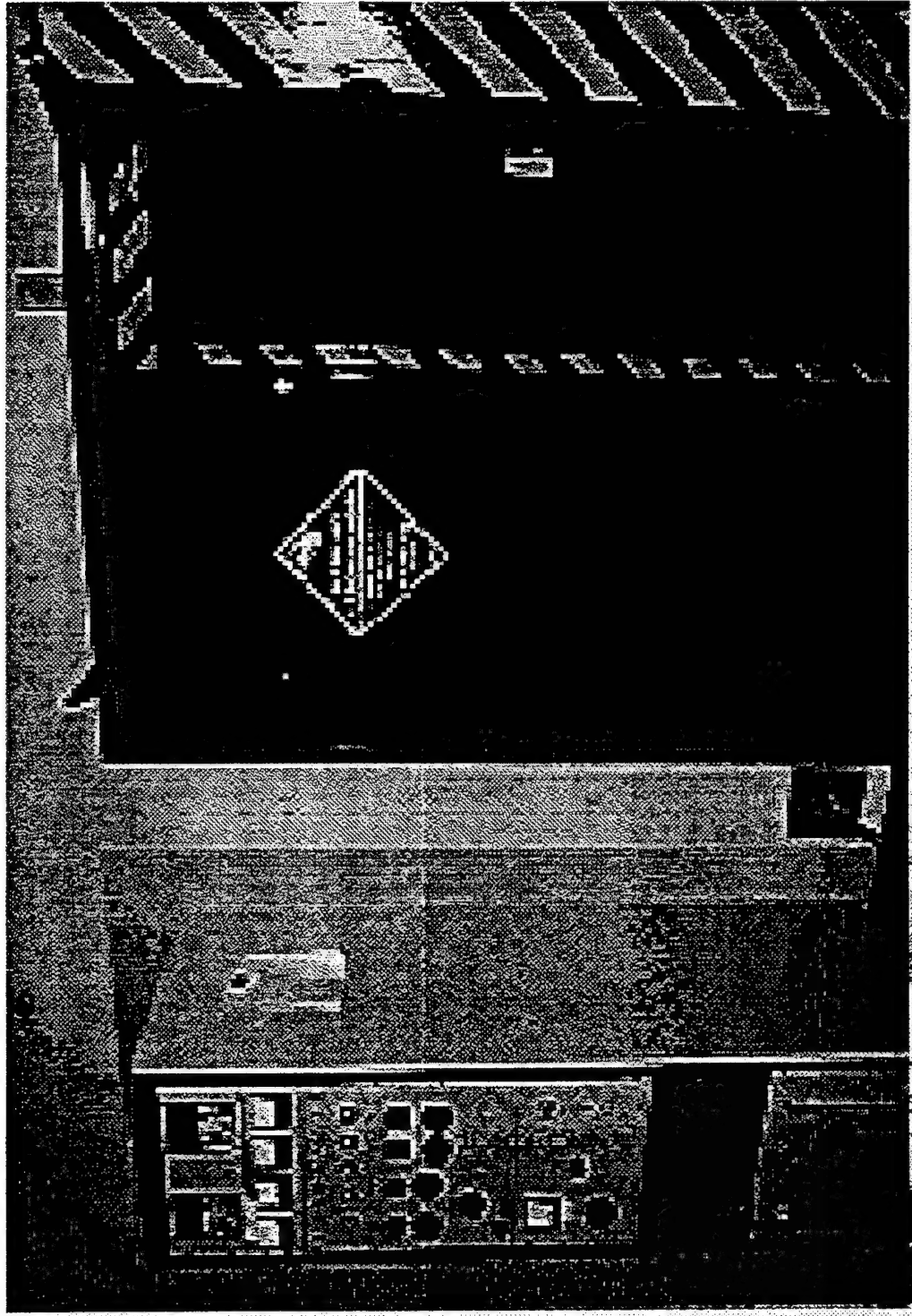
# 94 GHz Calibration Process



# Narda Electric Field Density Probe



# 94 GHz Transmitter and Anechoic Chamber



# 94 GHz Transmitter

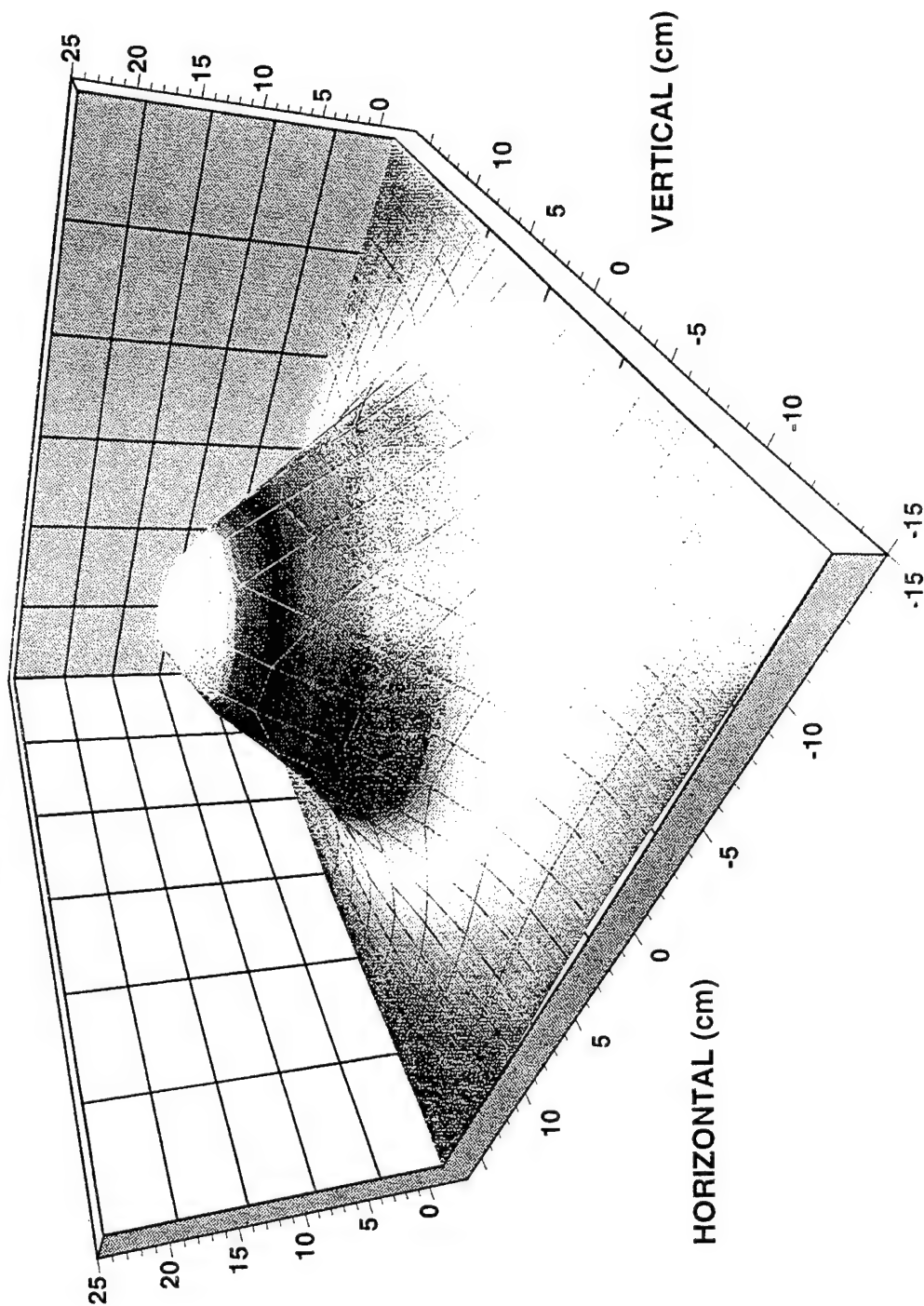
- ◆ Klystron tuned for 94.37 GHz
- ◆ 45 W Maximum Forward Power
- ◆ Horizontally polarized
- ◆ Circular horn, 2.54 cm dia. aperture
- ◆ Gain = 315.02 or  $G = 24.983$  dB
- ◆ Far Field Point ( $2d^2/\lambda$ ) = 40.588 cm
- ◆ Wavelength  $\lambda = 0.3179$  cm

# 94 GHz Source, Grid Map #2

Pout=8.58 W, Distance=97.26 cm

DLL, 'L'WSR, 27-Sep-94

POWER DENSITY (mW/sq. cm)

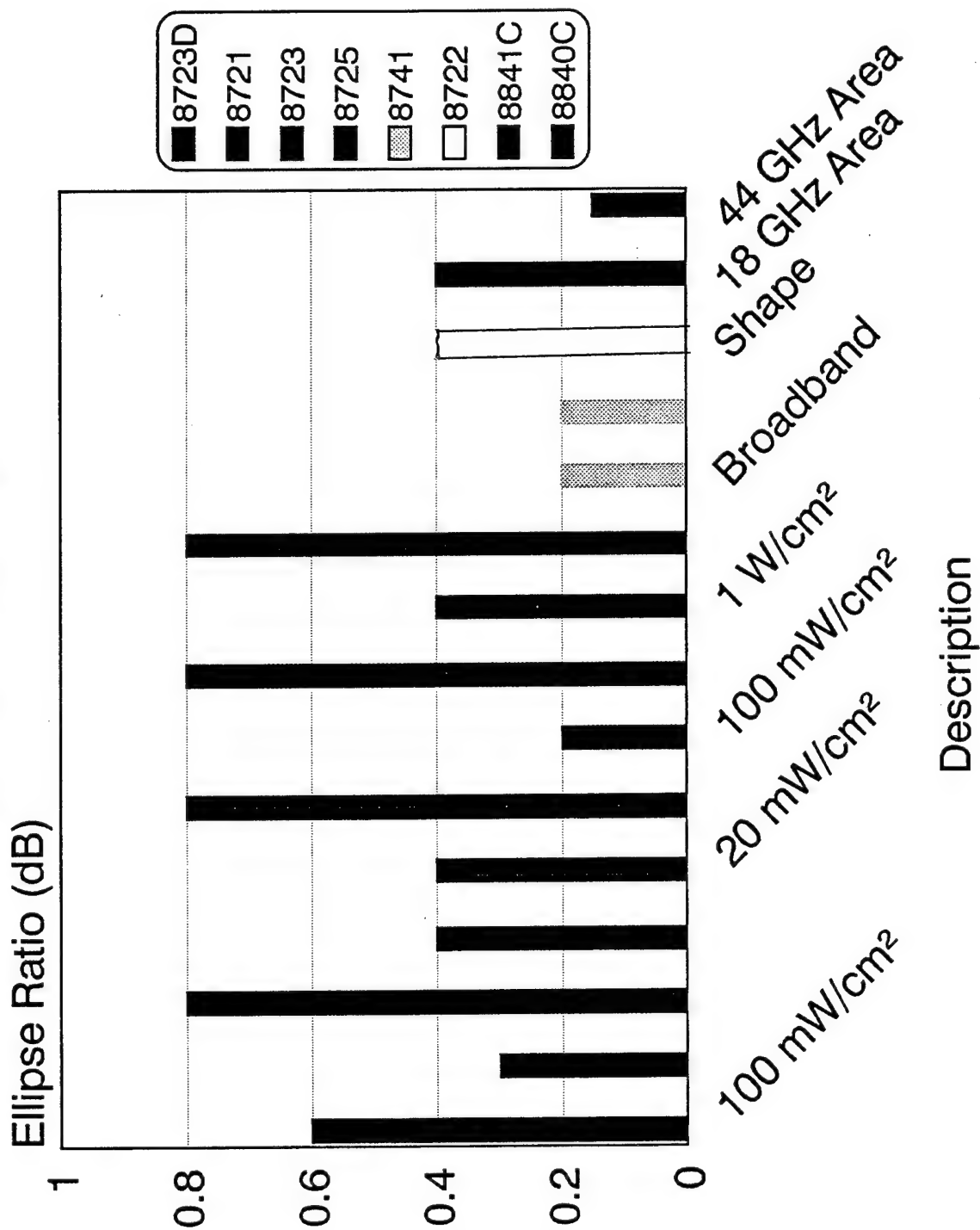


# Dipole Antenna Elements

- Structural Arrangement
  - Traveling wave effect on dipoles oriented along Poynting vector
  - Offset decreased sensitivity of dipole as frequency rises
- Orthogonal arrays of interconnected, resistive thermocouple dipoles
- Provides broadband isotropic response
- Relatively constant sensitivity across broadband of frequencies

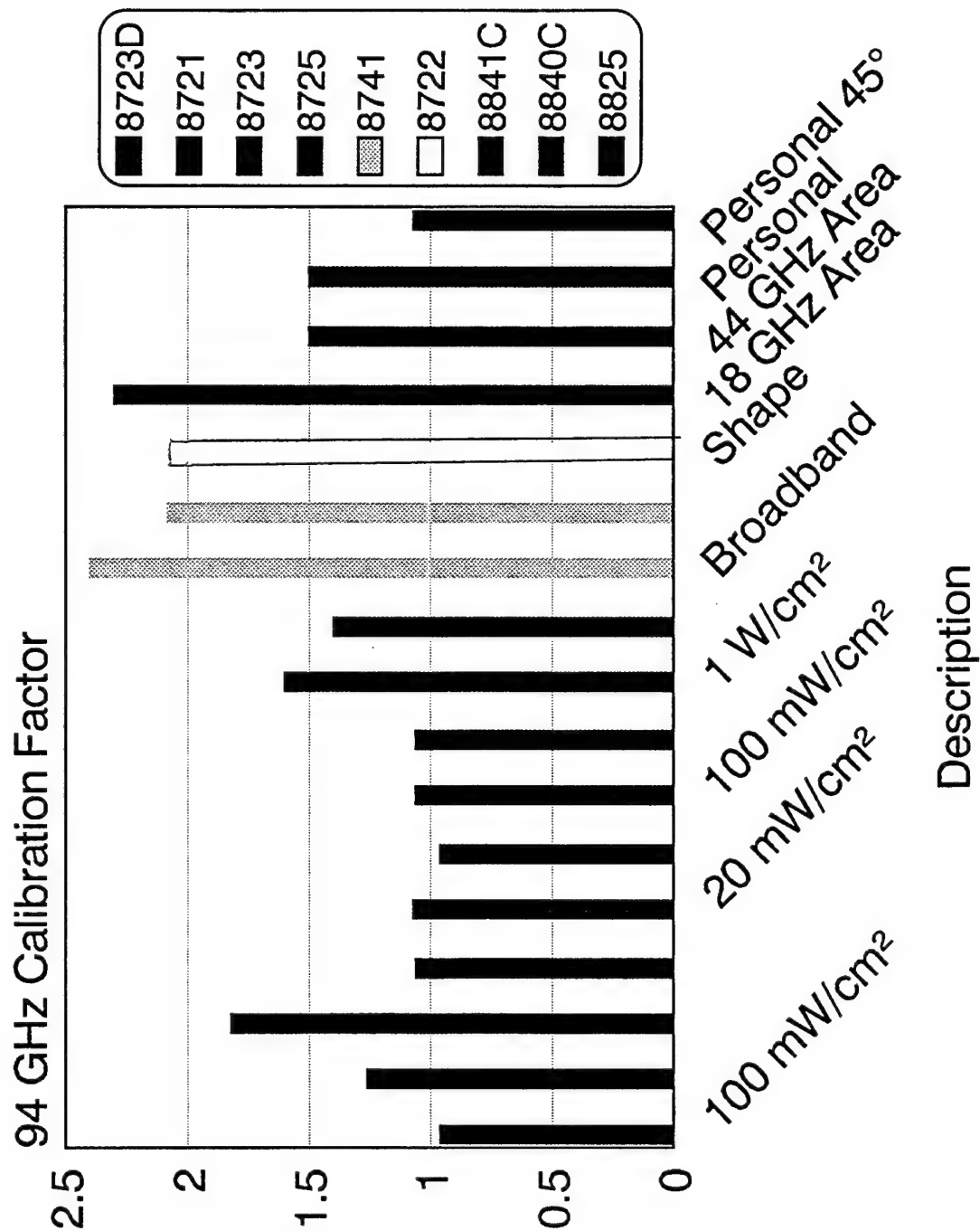
patent 4,629,978

# Comparison of Calibration Factors at 94 GHz





# Comparison of Calibration Factors at 94 GHz



# Narda Probes

- ◆ Standards recommend isotropic equipment
- ◆ Accomplished by three mutually orthogonal antenna arrays
- ◆ Thermocouple detectors
- ◆ true RMS detectors - low overload capability
- ◆ New invention - increase overload capability
- ◆ 1000% of meter full scale
- ◆ Theoretical response at 94 as effective as 35 GHz

U.S. Patent Dec. 16, 1986

Sheet 2 of 2

4,629,978

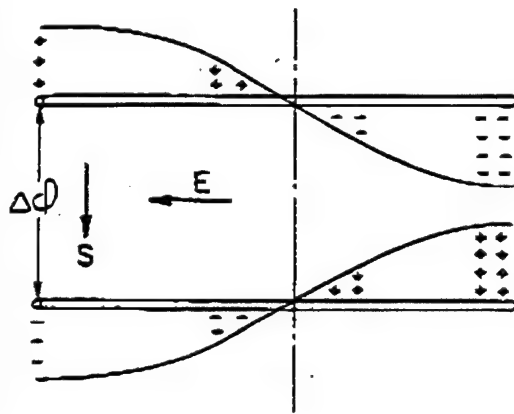


FIG. 4A

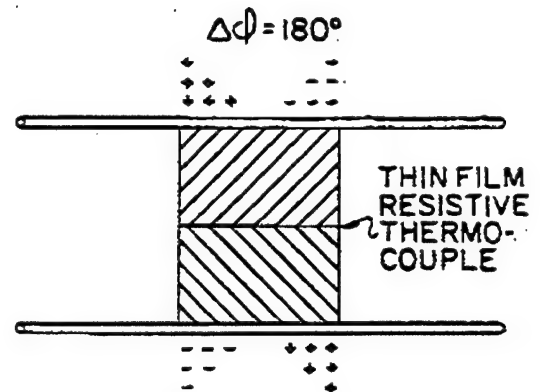


FIG. 4B

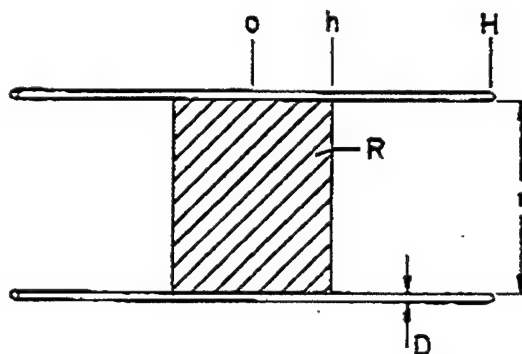


FIG. 5

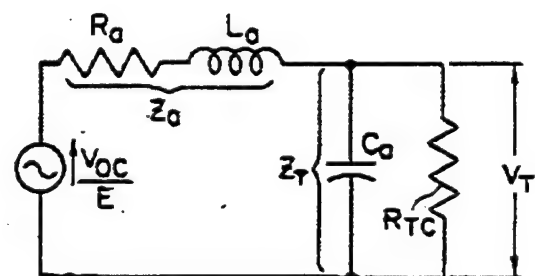


FIG. 6

U.S. Patent Dec. 16, 1986

Sheet 1 of 2

4,629,978

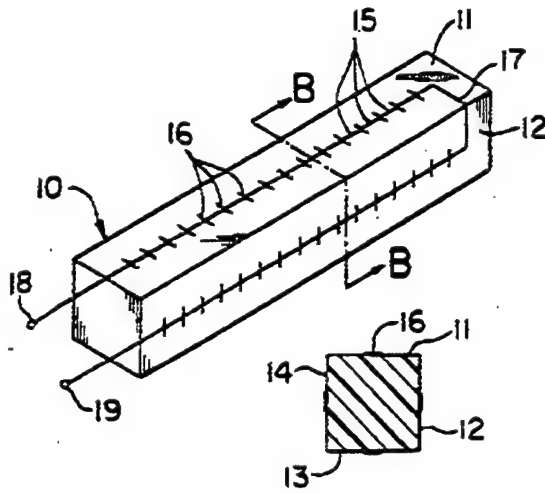


FIG. 1A

FIG. 1B

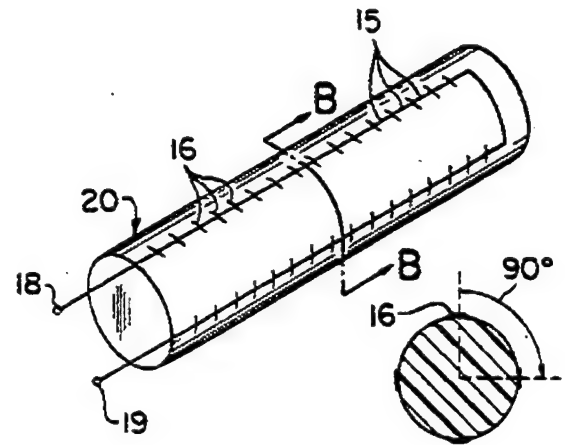


FIG. 2A

FIG. 2B

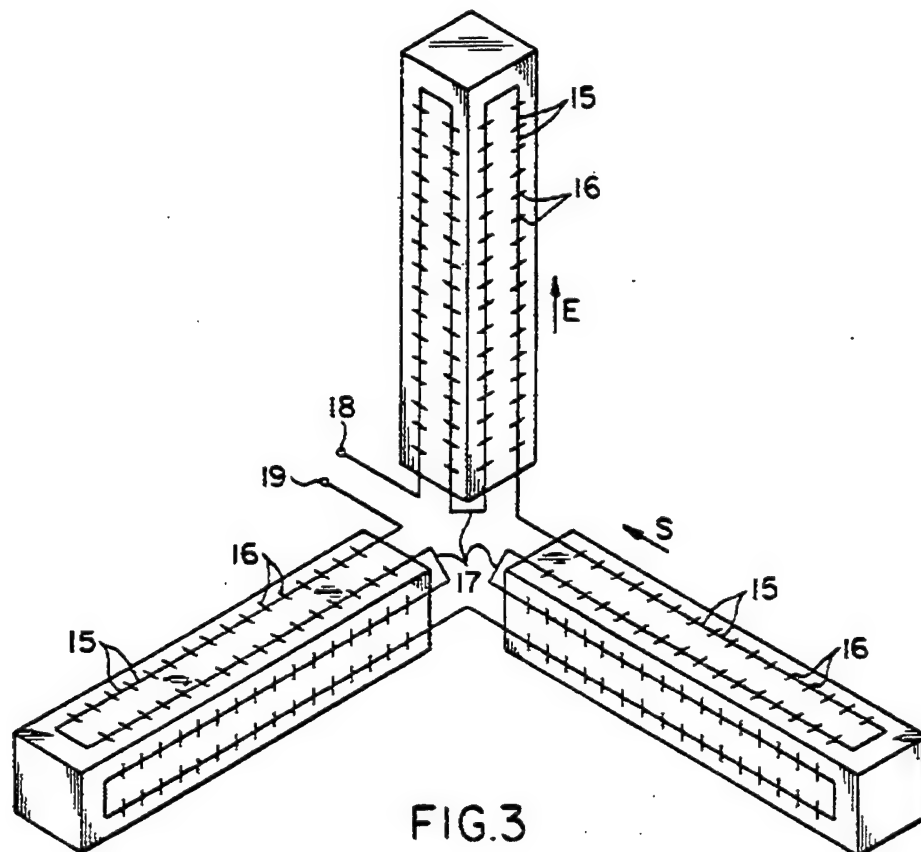
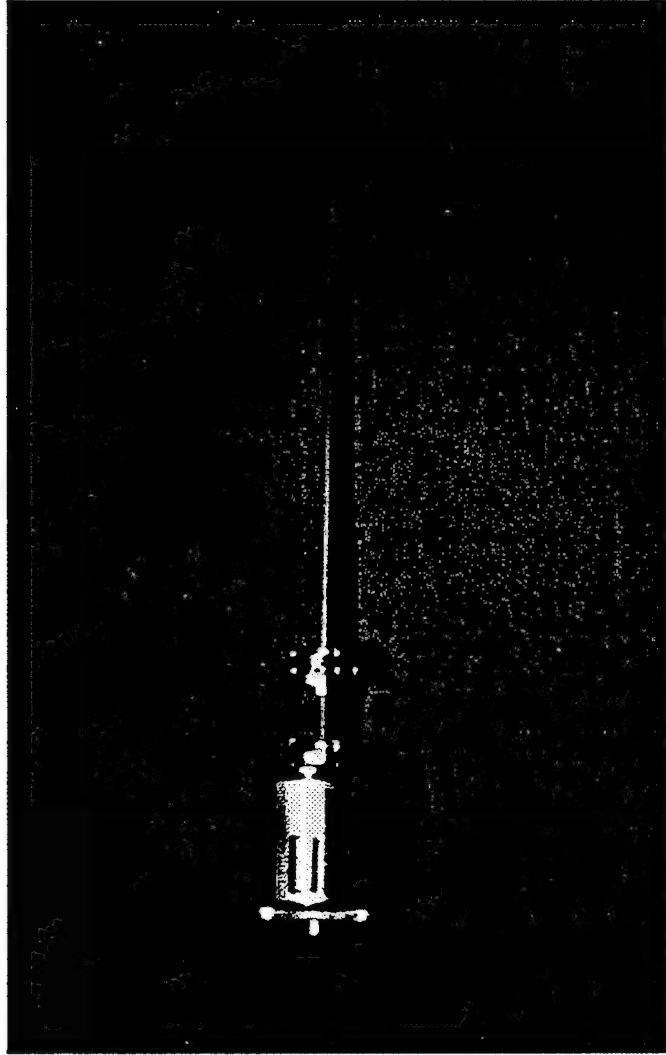


FIG. 3

# 94 GHz Open-Ended Waveguide and Thermistor



# Patent Charts - 3 elements

The broadband characteristics are obtained by distributing resistive thermocoupled dipoles along the length of the elements at spacings that will permit no resonance lengths over the range of frequencies within which the probe is intended to operate. The spacing  $< \frac{1}{4}\lambda$  of the highest frequency to be measured. The probe may be viewed as a group of series connected small resistive dipoles or as a very low Q resonant circuit.

# **ELECTRIC FIELD EXPOSURE CHARACTERIZATION AND INDUCED FOOT CURRENT MEASUREMENTS IN THE PRESENCE OF MULTIPLE-SOURCE AND MULTIPLE-FREQUENCY VHF FIELDS.**

*Santi Tofani*

*Servizio di Fisica Sanitaria - Regione Piemonte Azienda USL 9  
Servizio Sanitario Nazionale - 10015 Ivrea - Italy*

## **Abstract**

Multiple-source, multiple-frequency antennas used in telecommunication system produce very complicated field structures with reactive (stored) and real (propagated) components, standing waves, and unknown phases and field polarization. Measurements of these fields and the correspondent induced foot-current as a function of frequency are influenced by many parameters and can be difficult to reproduce.

Outdoor measurement procedures for assessing both the electric field and the foot current intensities require the simultaneous use of both narrow- and broad-band systems calibrated to characterize complex field environments.

The calibration procedures adopted to characterize the response of the field and current meters are reported.

The procedures followed to measure the electric field strength as well as the foot current intensity in practical exposure situations are also presented together with the corresponding results of the monitoring activity carried out in 46 different complex electromagnetic environments.

The obtained results confirm that the adopted measurement procedures allow the assessment, in presence of multiple-source and multiple-frequency VHF fields, of the electric field strength and of the foot current with an accuracy of about 2 dB.

## 1. Introduction

The concentration of antennas broadcasting Radio and TV programs is very high in Italy where for a 60 million inhabitants we have about 60.000 stations.

As a consequence in many places, mostly in hills surrounding big towns we have transmitting sites with a huge number of antennas. As an example close to Turin there is a transmitting site where in an area of 0,1 Km<sup>2</sup> there are 70 antennas emitting a total power of nearly 190 kW.

People living in the surrounding areas are exposed to very complicated (multiple source and multiple frequency) complex electromagnetic environments with field structures having reactive (stored) and real (propagated) components, standing waves, and unknown phases and field polarization.

Measurements of these fields and the corresponding induced foot current as a function of frequency are influenced by many parameters and can be difficult to reproduce.

This paper reports on the adopted procedures employed by our Laboratory for the measurements of human exposure (electric field strength and foot current ) in complex electromagnetic environments. The influence of different parameters on the measurement accuracy will also be analyzed and discussed.

## 2. Electric field measurements

Precise measure of VHF electric field as a function of frequency in a space occupied by the human body is difficult to make since isotropic antenna to use in such situations are very difficult to manufacture.

Errors relative to the antenna cable behavior are difficult to determine due to the fact that conditions of exposure (dependent upon the configurations of transmitting antennas and their characteristics, as well as, upon the characteristics of the surrounding area) are difficult to reproduce in Laboratory.

Problems of this kind do not apply to broad-band field meters which are more compact, and rigid and therefore can be calibrated in the Laboratory in the same configuration as they are used, in the open environment.

For this reason, the broad band field meter may be used as a means of comparison in testing the reliability of the adopted procedure of narrow-band measurements made by using a spectrum analyzer.

To obtain an isotropic response of the antenna used for narrow-band measurements a biconical antenna (EMCO mod. 3604) is used as a dipole that, at each measurement point supplies three electrical field values corresponding to the x,y and z Cartesian axes having the origin in the electrical center of the antenna itself.

By rotating the antenna during the measurements independent measurements of the fields for three mutually orthogonal polarizations could be obtained.

The antenna is calibrated indoor using exposure conditions similar to those found close to



a large number of VHF transmitting antennas with the procedure described in [1].

The antenna factor AF is defined as:

$$AF = \frac{\sqrt{(V_x^2 + V_y^2 + V_z^2)}}{E_M}$$

where  $V_x$ ,  $V_y$ , and  $V_z$  are the three rms signals (expressed in volts) corresponding to the three polarizations x, y, z of the biconical antenna, and  $E_M$  is the mean electric field strength incident on the biconical antenna (evaluated as the mean of seven measurements, at each frequency, carried out with the traveling standard).

In the real exposure situations the narrow-band antenna is used following the procedure above described. The total rms field is evaluated using the equation:

$$E = \sqrt{\sum_{i=1}^n (E_i)^2}$$

where n is the total number of sources and  $E_i$  is the rms electric field strength value expressed in V/m and calculated as follows:

$$E_i = 10^{(A+AF+CA-13.01)/20}$$

where A is the dBm signal amplitude measured by the spectrum analyzer, AF is the antenna factor, CA is the cable attenuation and the coefficient -13.01 represents the conversion from dBm to dBV in a 50 ohm system.

E is compared with that measured in the same point by using a broad band field meter.

The narrow-band antenna is connect to a spectrum analyzer (HP 8562A) located inside an electromagnetic radiation analysis van. The van has a shielding effectiveness of about 15 dB. The broad-band field meter is linked to a repeater via a 10 m long fiber-optic cable. From a detailed error analysis the asseigned total systematic error in the field assessment is 1.82 dB [1].

Measurement results are then accepted when the ratio between the narrow- and broad-band field values are within 1.82 dB. This criterium of acceptance is possible since the adopted measurement procedure is based in the use of two different and independent measurement systems (broad- and narrow-band).

In order to achieve so precise measurement, apart from the calibration of narrow-band antenna, the use of periodically calibrated broad-band field meter is very important. If the

meter is not periodically calibrated the above reported accuracy may be well exceeded. In fact results of calibrations carried out by our Laboratory over 42 field meters show that only 40% of them respond correctly, while the other 60% measure with additional errors that can range up to 2 dB (48% of the sensors) and up to 4 dB (12% of the sensors). Results of more than 267 measurements carried out by our Laboratory in the last 3 years in 46 different sites characterized by multiple-source and multiple-frequency VHF fields show that the ratio between broad- and narrow-band measurements agree for 60% of cases within 1 dB, and for 85% of cases within 2 dB [2]. These results confirm the validity of the adopted procedures.

### **3. Induced foot current measurements**

Foot current induced in people exposed to multiple-source, multiple -frequency VHF EM Fields is measured by using a stand on foot current meter developed at the University of Utah [3], which consists of a polyethylene sheet of thickness 6 mm that was sandwiches between copper plates of size 30x30 cm, placed in series with an RF millimeter. The spectral analysis of foot current is made by connecting a spectrum analyzer (model HP 8562A) directly to the two copper plates of the stand-on meter, whose impedance is 6  $\Omega$  at the considered frequencies.

The foot-current meter is calibrated in the Laboratory to evaluate its response versus amplitude and frequency of the current by monitoring its response to an injected known current as reported in .

The influence of different parameters (grounding, human dimension, electric contact between feet and the top copper plate) on the foot current measurements results has been analyzed [4].

The grounding of the meter is improved by interposing an additional copper sheet between the meter bottom plate and the ground. A proper dimension for this copper sheet is 50x50 cm, above this dimension the increment of foot current reading is negligible (about 1% for a sheet of dimension 70x70 cm).

The influence of body dimension, electric contact between feet and meter can be evaluated by making measurements of foot current induced in different people.

For each person the current measured as a function of frequency is compared with the correspondent electric field, measured in the same point using the procedures above reported to give the induced foot current  $F_v$  for an exposure to an unitary electric field strength.

Results obtained following this procedure for nine different subjects (bare footed and wearing leather and rubber sole shoes) exposed in 5 different sites characterized by multiple-source and multiple-frequency VHF fields, (frequency range from 90 to 104 MHz) considering field with a total number of frequencies of 26 (Electric field strength greater than 0.5 V/m) show a decreasing trend of  $F_v$  as a function of frequency and an increasing trend of  $F_v$  with the height of the person.

For a person of 1.75 m tall the foot current induced by unitary electric field ranges from 46 to 3.45 mA (V/m) in the frequency range 90 to 104 MHz. If the person has an height of 1.9 m the  $F_v$  ranges from 5.42 to 4.45 in the same frequencies range.

These values are refereed to bare foot situations, and decrease of 19.1 % if wearing rubber soled shoes or 10.5% with leather shoes.

The standard deviation of  $F_v$  for a considered subject taking into account for all the different measurement performed ranges from 0.68 dB to 2.8 dB. The mean standard deviation for all the considered subjects is 1.9 dB.

This mean standard deviation can be taken as the statistical error on foot current measurement for the unitary electric field exposure. This is very satisfactory since the error on  $E$  measurement is 1.8 dB so it allows to believe that the measurement of foot current is subjected to a smaller error.

An additional validation of the measurement data was obtained by comparing the measured foot current values with those obtained by making numerical (FDTD) calculations using anatomically based model of the human body.

The agreement between the experimental and numerical values of  $F_v$  is resulted to be within  $\pm 12\%$  that is considered very good since it is well inside the measurement accuracy.

The combined measurement of Electric Field strength and induced foot current at different frequencies of VHF Fields have shown that current in excess of the RF safety guidelines would results both for controlled and uncontrolled environments if the incident electric fields were purely vertical and of maximum values given in the safety guidelines (ANSI/IEEE C 95.1-1992).

#### 4. References

- [1] S. Tofani and P. Ossola, "Accuracy in outdoor isotropic measurements of multiple-source, multiple-frequency EM fields", IEEE Trans. Electromagn. Compat, vol 34 pp.299-303, 1992.
- [2] S. Tofani, P. Ossola, G. d'Amore and L. Anglesio, "Standardization and Accuracy in measurements of Electromagnetic Fields in Bioelectromagnetics. Proceedings of the COST 244 Meeting on "Mobile Communications and Extremely Low Frequency Field & Instrumentation and Measurements in Bioelectromagnetics Research". Sponsored by the European Union (DG XIII). Dina Simunic (Ed.), pp. 296-303, 1994.
- [3] O.P. Gandhi, J.Y. Chen, and A. Riazi, "Currents induced in a human being for plane-wave exposure conditions 0-50 MHz and for RF sealers", IEEE Trans. Microwave Theory Tech., vol. 37, pp 174-180, 1989.
- [4] S. Tofani, G. d'Amore, G. Fiandino, A. Benedetto, O.P. Gandhi and J.Y. Chen, "Induced Foot-Current in Humans Exposed to VHF Radio-Frequency EM Fields". IEEE Trans. on Electromagn. Compat. Vol 37, No 1, February 1995.



## A Method for 2-Dimensional Imaging of RFR Fields

T.J. Walters<sup>1</sup>, C.J. Sherry, J.L. Kane<sup>1</sup> and J. E. Brewer<sup>2</sup>

<sup>1</sup>Systems Research Laboratories, San Antonio, Texas and

<sup>2</sup>Armstrong Laboratory, Radiofrequency Radiation Division,  
Brooks Air Force Base, Texas, 78235-5324

The study of the effects of RFR on biological systems requires that the RFR fields be well characterized. At the very least knowledge of the location of the center of the beam is needed. The use of conventional methods e.g., Narda probes, to map RFR fields can be extremely time consuming, as it not only requires careful records of probe locations, but also "off-line" reconstruction of the field map. One of the major complications in studying the biological effects of RFR is the perturbations to the fields caused by test equipment, monitoring devices, and in the case of conscious animals, restrainers or cages. In many case it is not possible to actually make determinations of RFR field strength or geometry within the experimental device in which the animal is contained.

In this paper we report on a method we have developed that can be used to quickly visualize RFR fields, allowing rapid determination of their location, as well as visualizing the interactive effect of restrainers, test equipment, etc. The method involves the use of cotton cloth covered with a temperature sensitive dye. The cloth is stretched over a piece of Styrofoam and saturated with distilled H<sub>2</sub>O. When placed in the RFR field, the water couples with the RFR and heats up, as it does the color of the cloth changes, resulting in a clear image of the RFR fields. This method enables the experimenter to immediately determine the limits of the field and its geometric shape. The relative strength of the field can be obtained by capturing serial video images of the screen recorded during RFR exposure. The captured images are digitized using a PC and a video capture system (Silicon Graphics). By superimposing the serial images, the relative intensity of the RFR field can be visualized. Subsequent superimposition of these composite images over images of the biological system of interest allows rapid visualization of the RFR fields encountered during an RFR exposure, as well as a method of predicting the shape and relative strength of the fields that will be encountered during future exposures.

This method can also be used to setup experiments with the use of only a video camera and monitor. First, the cloth is placed at the desired distance from the RFR antenna, with the video camera focused on the cloth, the cloth is exposed to the RFR. The outline of the image of the RFR field is then traced on the screen of a video monitor using a water soluble marker (a video recorder is helpful so that the image can be "paused" while tracing). Finally the experimenter can then move the experimental setup into the exact location desired by viewing this process on the video monitor (with the tracing of the image of the RFR field).

We have been able to validate this method using RFR frequencies ranging from 915 MHz through 94 GHz. A variety of additional applications will be discussed to demonstrate the utility, as well as the limitations, of this method.



# **A PRACTICAL ASSESSMENT OF VARIABILITY ASSOCIATED WITH BROADBAND RF FIELD STRENGTH SURVEY MEASUREMENTS**

Richard A. Tell  
Richard Tell Associates, Inc.  
8309 Garnet Canyon Lane  
Las Vegas, NV 89129, USA.

## **Abstract**

An analysis of RF field measurement data obtained during a field survey in Portland, Oregon, is presented with an emphasis on the degree of variability in measured field magnitudes obtained at the same measurement location, using the same instrumentation with measurements performed by the same individual but with different orientations of the observer relative to the measurement point. A broadband electric field probe equipped with a data logger was used to acquire measurements of the minimum, maximum and average square of the RF field strengths along a vertical path two meters in height with the observer facing the measurement point from four different directions. Measurements were performed at 171 different locations along neighborhood streets near a VHF broadcast site with six FM radio stations. Observer induced field perturbations accounted for a mean value of 71 percent (2.3 dB) variation in the spatial average measurement of RF fields (ratio of maximum spatial average to minimum spatial average obtained from four successive vertical scans at each measurement point). RF fields were found to be non-uniform over the body dimension with a mean value of the ratio of the maximum to minimum field readings of 10.3 (10.1 dB). These variabilities in measured fields should be carefully considered when interpreting measurements for showing compliance with applicable human exposure standards.

## **Summary**

Environmental measurements of RF fields are subject to several factors that can lead to uncertainty in the measurement results. These factors include, among others, accuracy of the probe calibration, non-linearity in probe response and perturbation of the incident fields introduced by the presence of the observer. This study relates to local field perturbations caused by the individual performing the measurements and is based on data obtained during a broadband RF field survey near high-power VHF broadcast facilities (comprising a total of six FM radio stations) in a neighborhood in Portland, Oregon. One of the main objectives of the study was to use a methodology which would result in measured values of the RF fields that had a high potential for replication by others who might make similar measurements in the future.

A common problem associated with RF field surveys is replication of the measurement results by others after the initial survey has been completed. This is often related to subsequent measurements not being taken at the same exact point in space and can be a function of the presence of nearby reflective objects, including the body of the

person performing the measurements. The measurement approach used in this study consisted of repeated vertical scans with a broadband field probe (Holaday Industries, Inc. Model HI-3001) connected to a data logger at each measurement point. Four vertical scans of the fields were taken at each of 171 measurement locations within the neighborhood, one scan being taken with the observer facing the measurement point from each of four different directions, 90 degrees apart. Measurement points were generally located in the middle of local streets, each being marked with a survey nail driven into the asphalt. The probe was slowly moved along a vertical line above the measurement point at a uniform speed beginning at the ground surface up to a height of 2 meters such that the scan took 10 seconds. The data logger recorded a total of 40 readings of the square of the electric field strength during each vertical scan and was programmed to determine and record the minimum, maximum and average readings from each scan. Hence, the process resulted in a total of 160 field readings at each measurement point or a total of 27,360 individual readings for all of the 684 vertical scans.

Analysis of the data consisted of forming the ratio of the maximum to minimum values of the average of each vertical scan at each measurement point to assess apparent ability to obtain similar field readings, depending on the direction from which the measurement observer faced the measurement point, and, hence, to obtain a measure of possible field perturbation introduced by the presence of the observer. These ratios ranged from a low of 1.05 (0.2 dB) to a high of 23.5 (13.7 dB) with a mean value of 1.71 (2.3 dB) (standard deviation of 1.99 or 3.0 dB). Thus, on average, this study revealed that, even at the same precise measurement location, RF field measurements taken by the same observer varied by as much as 71 percent in terms of equivalent power density (2.3 dB), just depending on the orientation of the observer relative to the measurement point. For different observers, of different physical stature, greater variation could be expected. Figure 1 illustrates the ratios of maximum spatial average values to minimum spatial average values for the 171 measurement points in the study.

An additional analysis of the data was performed by examining the ratio of the absolute maximum field reading to the absolute minimum field reading at each measurement location. This analysis was done to assess the degree of field non-uniformity over the height of a person exposed to the incident fields from the various broadcast stations. From the entire data set, a total of 105 locations yielded data useful for determining this ratio; at some locations the fields at particular points within the vertical scans indicated zero on the meter and, hence, could not be used in forming the ratio discussed. The result of this analysis showed that that mean value of the ratio of maximum to minimum field values was 10.3 (10.1 dB) with a standard deviation of 8.13 (9.10 dB).

These results indicate that the variability in common RF field measurements induced by field perturbation can be significant and should be taken into consideration when performing measurements to show compliance with guidelines on human exposure. This is especially true when attempting to compare measurement results obtained by different observers who may also be using different instrumentation and different



measurement techniques. An obvious conclusion also supported by the data is that typical RF field exposures produced by the broadcast stations in this study are not uniform over the size of the body. These data help establish the magnitude of typical field non-uniformity associated with commonly performed environmental RF field surveys of VHF broadcast stations and provide insight for interpreting whole-body specific absorption rates (SARs) and induced body currents.

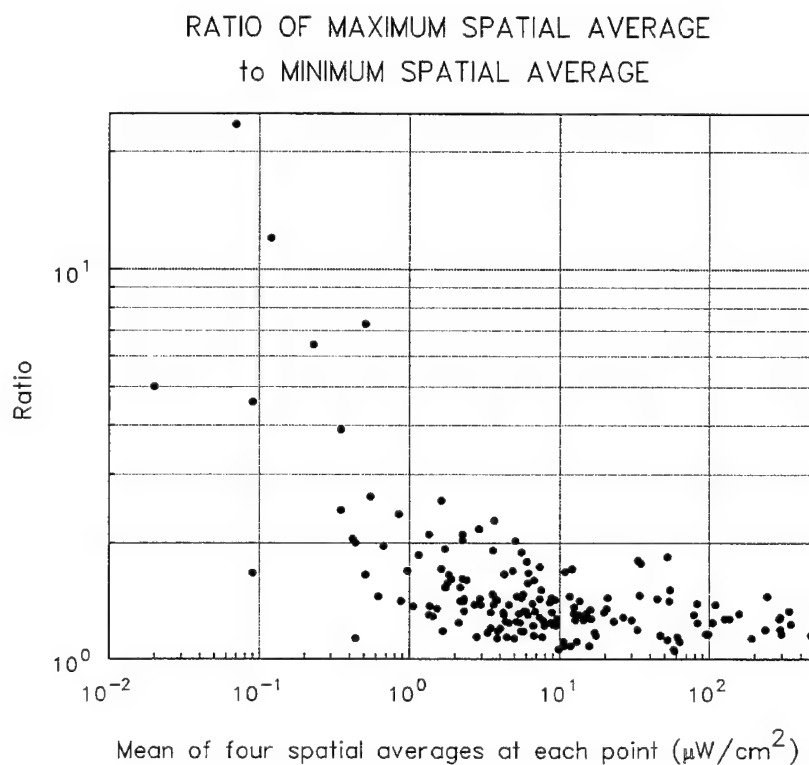


**Figure 1.** Ratio of maximum spatial average to minimum spatial average values of the squares of RF field strengths obtained at 171 measurement locations near a VHF FM broadcast facility in Portland, Oregon.



## **U.S. Army Experiences in Performing RFR Field Measurements**

Brad Roberts, Radiofrequency Program

U.S. Army Center for Health Promotion & Preventive Medicine  
Aberdeen Proving Ground, MD

The U.S. Army Center for Health Promotion and Preventive Medicine (USACHPPM), formerly U.S. Army Environmental Hygiene Agency (USAEHA), has been the backbone of the U.S. Army's nonionizing radiation protection program for over 25 years. The Radiofrequency Branch of CHPPM is responsible for determining the necessary radiation protection programs for all RF sources in the Army inventory, i.e., from low frequency heat sealers to air defense and millimeter wave radar systems. This responsibility entails getting involved at the systems concept level and staying involved throughout the lifetime of the system. Involvement usually starts with a theoretical assessment of the system technical characteristics to determine the potential of the system in producing field intensities greater than permissible exposure limits. If the analysis shows that the system can emit levels greater than permissible exposure limits, the system is then evaluated as to the potential for personnel to be exposed. Performing field intensity measurements on a prototype or existing system is one of the methods used in determining the fields present and the compliance with current standards. Measurements are always conducted in cases of suspected overexposure. This presentation addresses the experiences and approaches of the U.S. Army in conducting various RF measurements. These measurements include power density, E- and H-field, and induced current measurements. Particular attention is paid to whole-body and partial-body exposures and to spatial and non-uniform fields. Measurements made in frequency bands outside of the broad-band measuring instruments are also addressed. Problems and concerns encountered when performing all of these types of measurements are discussed



CONCLUSIONS DRAWN FROM NEAR-FIELD EXPOSURE ASSESSMENT AND REDUCTION STUDIES: RF (6-65 MHz) DIELECTRIC HEATERS. David L. Conover, Richard M. Edwards, Peter B. Shaw, W. Gregory Lotz, Dwight M. Werren and Diana L. Snyder. National Institute for Occupational Safety and Health (C-27), 4676 Columbia Parkway, Cincinnati, OH 45226 USA.

Research at the National Institute for Occupational Safety and Health (NIOSH) has addressed difficult exposure assessment and reduction problems for operators of radiofrequency (RF) dielectric heaters. All of the research involved heaters used to produce plastic products and operators who received near-field exposure (operators located within 1 m of heaters). Helpful conclusions drawn from these exposure assessment and reduction studies are given below. Two types of exposure assessment studies were conducted.

First, field strength measurements were taken for heater operators. Field strengths (electric and magnetic) were measured at the eyes, neck, chest, waist, groin, knees and ankles of operators. The results showed that measuring at a few isolated anatomical locations can fail to detect higher field strengths (electric or magnetic) at other locations because the spatial distribution of fields is quite nonuniform. Fields from adjacent heaters can be comparable to the fields from the heater being evaluated. Failure to measure both electric and magnetic field strengths can result in significant exposure being completely neglected. Approximately 96% of the heaters exceeded an electric field strength of 50 V/m and about 80% exceeded a magnetic field strength of 0.15 A/m.

Second, foot current levels were assessed for heater operators. Only the heater being studied had RF power on during foot current measurements. Surprisingly, foot current levels above 100 mA were generated in operators of adjacent heaters located up to 9 meters away (without their RF power on). Nearly 27 percent of the heaters generated operator foot current that exceeded 200 mA, the limit recommended by the International Electrical and Electronics Engineers (IEEE) for such exposures. Twenty percent of the heaters induced foot current that exceeded 350 mA.

Two types of exposure reduction studies were conducted. First, a shield was designed and installed on a heater used to produce waterbed mattresses and its effectiveness in reducing worker exposure was evaluated. Shielding this type of heater is particularly difficult since the waterbed mattress is a large and bulky product and cannot be contained inside the shield. Operator exposure was measured before and after installing the shield. The average reduction factors were: electric field strength ( $E^2$ )- 213 times, magnetic field strength ( $H^2$ )- 10.8 times, and foot current- 4.3 times. Interestingly, shielding the heater under study also reduced exposure at other locations up to 9 meters away (with only the shielded heater operating). The average reduction factors at these other locations were: electric field strength ( $E^2$ )- 12.1 times, magnetic field strength ( $H^2$ )- 7.5 times, and foot current- 6.0 times.

Second, a work practice control was investigated for reducing operator foot current for RF heaters. The dependence of foot current on operator hand position was studied for heater operators. Operator posture (relative to the RF heater) and foot current readings were documented by simultaneous video tape recordings. Foot current was at a maximum with the operator's hands closest to the heater. With the operator's hands farthest from the heater (i.e., in his/her lap), the foot current was at a minimum and was typically reduced by 30 percent. Thus, simply having the operator's hands in his/her lap while RF fields are being generated would reduce foot current. Likewise, it was also determined that foot current decreased as the operator's upper torso was positioned farther from the heater. Therefore, installing a wooden or plastic table between the operator and heater can be effective in keeping the operator's upper torso farther from an RF heater and thus reduce foot current. Finally, this study shows that to obtain meaningful exposure evaluations for heater operators, health professionals must determine the dependence of foot current on common hand and upper torso positions.

## SUMMARY

### Introduction

Radiofrequency (RF) radiation in the frequency range 10 kHz - 300 GHz is employed in a multitude of industrial, scientific and medical applications. RF dielectric heaters operating at frequencies of 3 - 100 MHz are used to heat, melt, or cure nonmetallic (dielectric) materials that are poor conductors of heat and electricity, such as plastic, rubber, and glue.<sup>(1)</sup> In RF dielectric heating, materials are heated uniformly and quickly. Generally, the RF energy is applied to an object for several seconds to heat the material. The RF source then remains off until the next piece of material is processed.

There are about 100,000 RF heaters in use in the U.S. and over 250,000 workers exposed to RF emissions.<sup>(1)</sup> Operators of RF dielectric heaters are most often exposed under near-field conditions (i.e., typically within 1 meter of the heater). For near-field conditions, operators can receive high RF exposure due to their close proximity to the RF source.<sup>(2)</sup> Because of the potential for high exposures and the number of workers exposed, NIOSH scientists measured exposures (field strengths) for operators of RF heaters.

### Electric and Magnetic Field Strength Measurements

Electric and magnetic field strengths were measured for operators of RF heaters used to produce plastic products.<sup>(3)</sup> Detailed survey monitor specifications and measurement procedures, as well as a measurement example, are given elsewhere.<sup>(3-5)</sup> In the NIOSH study, over 1000 measurements were made for a total of 82 heaters.<sup>(3)</sup> Only the RF heater being evaluated had RF power on during the few seconds required for each measurement. Measurements were taken at the eyes, neck, chest, waist, groin, knees and ankles of operators. The maximum field strength for each anatomical location was recorded. All field-strength readings were corrected for duty factor and the frequency response of probes.

Several conclusions can be drawn from the measurement data and from observations made during the measurements. Measurements at a few isolated anatomical locations can fail to detect higher field strengths (magnetic or electric) at other locations because the spatial distribution of fields is quite nonuniform and thus unpredictable. This could lead to a false sense of security. To determine "worst-case" field strengths, measurements must be made with the different dies, processed materials, heater power output, etc. normally used during heater operation. Fields from adjacent heaters can be comparable to the fields from the heater that the worker is operating. Both the electric and magnetic field strengths must be measured to determine compliance with published exposure guidelines, e.g. those from the ACGIH or IEEE.<sup>10,11</sup> Failure to measure both field strengths can result in very significant exposure being completely neglected. Approximately 96% of the heaters exceeded an electric field strength of 50 V/m and about 80% exceeded a magnetic field strength of 0.15 A/m.<sup>(3)</sup> Likewise, other researchers have shown that field strength levels for dielectric heat sealers can exceed occupational exposure limits.<sup>(6-8)</sup>

### Foot Current Measurements

To provide a more complete characterization of heater operator exposure, NIOSH and other scientists have used a relatively new exposure assessment method.<sup>(2,7,9)</sup> The exposure assessment method involves the measurement of current induced in the workers' body by incident RF fields. The measurement of induced body current is a new element

of the most recent recommendations from the ACGIH and IEEE for work place exposure limits.<sup>(10-11)</sup> Recommended exposure limits are based on the RF energy absorption rate or specific absorption rate (SAR).<sup>(10-12)</sup> The IEEE foot current guideline (200 mA through both feet) was derived based on an allowable ankle SAR.<sup>11</sup> Although the ankle SAR cannot be measured directly for heater operators, foot current measurements are readily conducted in the work place.

NIOSH scientists have conducted induced foot current measurements for operators of RF dielectric heaters.<sup>(2,13)</sup> Detailed measurement procedures are available.<sup>(2,5,7)</sup> Current through both feet to ground (foot current) was measured while operators stood where they normally worked. Since operators were located close to heaters (usually within 1 meter) they received near-field exposures. Foot current measurements were real-time, non-invasive and only required the operator to place his or her feet on the sensor. Only the RF heater being studied had RF power on during foot current measurements. Foot current levels above 100 mA were generated in operators of adjacent heaters (without their RF power on) that were located up to 9 meters away.<sup>(13)</sup> Nearly 27 percent of the heaters generated operator foot current that exceeded 200 mA.<sup>(2)</sup> Twenty percent of the heaters induced foot current that exceeded 350 mA. In addition, other foot current measurements for heater operators from the United States, Australia, the United Kingdom and Sweden also exceeded the level recommended by various organizations as an exposure limit.<sup>(7,9,14-16)</sup> Consequently, control technology methods were studied in an attempt to reduce foot current values below occupational limits.

#### Engineering Controls (Shielding)

Shielding was selected for a NIOSH study because of its demonstrated effectiveness in reducing exposure from RF heaters used for many different applications.<sup>(1,5,17)</sup> The objective of this study was to design and install a shield on an RF dielectric heater used in the waterbed industry and to determine its effectiveness in reducing worker exposures.<sup>(13)</sup> There were two reasons for selecting this industry to carry out the study. First, in prior field studies high exposures were reported.<sup>(18)</sup> Second, this industry presented a challenge to design an effective shield for a procedure where the product being heated could not be enclosed inside the shield.<sup>(1,17)</sup>

Most RF shields are designed for heaters where the product being processed fits inside the shield. In such applications, a box shield is very effective in reducing worker exposure because the product and the RF applicator (radiation source) are both enclosed inside the shield. However, the waterbed mattress is a large and bulky product and cannot be contained inside the shield. Thus, the shield required a slot or opening to allow passage of the material between the applicator plates for sealing while minimizing the leakage of RF radiation. A shield satisfying these requirements was carefully designed, fabricated, and installed. The shield was installed on a heater utilizing a common sealing process and producing high worker exposures. Operator field strength (electric and magnetic) and foot current values were measured before and after installing the shield to determine the shield's effectiveness in reducing RF exposures. The average reduction factors were: electric field strength ( $E^2$ )- 213 times, magnetic field strength ( $H^2$ )- 10.8 times, and foot current- 4.3 times.<sup>(13)</sup> These data demonstrate that the shield was effective in reducing the operators' exposure (field strength and foot current) from the heater. Only the RF heater being studied had RF power on during field strength and foot current measurements. Interestingly, shielding the heater under study also reduced field strength and foot current levels at other locations up to 9 meters away. The average reduction factors at these other locations were: electric field strength ( $E^2$ )- 12.1, magnetic field strength ( $H^2$ )- 7.5, and foot current- 6.0. In addition to these short-term results, follow-up foot current measurements were made to evaluate long-term durability and effectiveness of the shield

under actual work place usage conditions. The long-term follow-up measurements were conducted approximately 2 years after installation of the shield. The shield was still effective in reducing operator foot current.

### Work Practice Controls

For some applications of RF heaters it is more practical to reduce operator exposure with work practice controls rather than with shielding. Consequently, NIOSH scientists investigated the use of work practice controls to reduce operator exposure from heaters.<sup>(19)</sup> Typical work practice controls include the following: controlling operator exposure time; establishing safe working zones where exposures are below specified limits; installing physical, electrically non-conductive barriers (e.g., wooden or plastic walls and tables) to ensure that operators maintain a minimum separation distance from the RF heater; and other strategies for controlling the distance between the operator and heater. The latter aspect concerning distance from the heater was studied by NIOSH scientists.

The dependence of foot current on operator hand position was studied for near-field conditions where the operator was close to the heater.<sup>(19)</sup> A stand-on foot current sensor was used. Operator posture (relative to the RF heater) and foot current readings were documented by simultaneous video tape recordings. Foot current was at a maximum with the operator's hands closest to the heater. With the operator's hands farthest from the heater (i.e., in his/her lap), the foot current was at a minimum and was typically reduced by 30 percent. Likewise, it was also determined that foot current decreased as the operator's upper torso was positioned farther from the heater.

The simultaneous videotape recordings of the operator's posture and corresponding foot current readings were particularly helpful to document the dependence on the operator's upper torso position. These recordings showed that simply having the operator's hands in his/her lap, while RF fields are being generated, would reduce foot current. Likewise, installing a wooden or plastic table between the operator and heater can be effective in keeping the operator's upper torso farther from an RF heater and thus reduce foot current. These results are consistent with previous measurements and calculations.<sup>(7,14,16,20-22)</sup> Thus, work practice or work station modifications that keep the operator's hands and upper torso farther from an RF heater can reduce foot current.

In addition to its relevance to reducing worker exposure, the dependence of foot current on worker posture has important practical implications for health professionals evaluating exposures.<sup>(19)</sup> The strong dependence of foot current and ankle SAR on operator posture cannot be detected by only measuring field strength. Unfortunately, very often health professionals do not evaluate the dependence of foot current on operator posture. Thus, such near-field exposure evaluations will give erroneous conclusions. These errors are more common since foot current evaluation techniques are relatively new and the dependence of foot current on worker posture and exposure conditions is even less widely known. Nevertheless, to obtain meaningful exposure evaluations for heater operators, health professionals must determine the dependence of foot current on common hand and upper torso positions.



## References

1. Wilson, T.L.: Radiofrequency Dielectric Heating in Industry, Report No. EM-4949, pp. 1-1, B-1 to B-11. Electric Power Research Institute, Palo Alto, CA (1987).
2. Conover, D.L.; Moss, C.E.; Murray, W.E.; Edwards, R.M.; Cox, C.; Grajewski, B.; Werren, D.M.; Smith, J.M.: Foot Currents and Ankle SARs Induced by Dielectric Heaters. *Bioelectromagnetics* 13(2):103-110 (1992).
3. Conover, D.L.; Murray, W.E.; Foley, E.D.; et al.: Measurement of Electric- and Magnetic-Field Strengths from Industrial Radiofrequency (6-38 MHz) Plastic Sealers. *Proc. IEEE* 68(1):17-20 (1980).
4. National Council on Radiation Protection and Measurements: A Practical Guide to the Determination of Human Exposure to Radiofrequency Fields. NCRP Report No. 119, NCRP, Bethesda, MD (1993).
5. International Commission on Non-Ionizing Radiation Protection (ICNIRP): Practical Guide for the Safe Use of RF Dielectric Heaters and Sealers. Prepared for the International Labour Office by ICNIRP, Geneva, Switzerland (1995).
6. Cox, C.; Murray, W.E.; Foley, E.D.: Occupational Exposures to Radiofrequency Radiation (18-31 MHz) from RF Dielectric Heat Sealers. *Am. Ind. Hyg. Assoc. J.* 43:149-153 (1982).
7. Williams, P.; Mild, K.H.: Guidelines for the Measurement of RF Welders, Report No. 1991:8. National Institute of Occupational Health, Department of Medicine, Umea, Sweden (1991).
8. Eriksson, A.; Mild, K.H.: Radiofrequency Electromagnetic Leakage Fields from Plastic Welding Machines--Measurements and Reducing Measures. *J. Microwave Power Electromagn. Energy* 20(2):95-107 (1985).
9. Gandhi, O.P.; Chen, J.Y.; Riazi, W.: Currents Induced in a Human Being for Plane-Wave Exposure Conditions 0-50 MHz and for RF Sealers. *IEEE Trans. Biomed. Engr.* BME-33(8):757-767 (1986).
10. American Conference of Governmental Industrial Hygienists: 1993-1994 Threshold Limit Values for Chemical and Physical Agents and Biological Exposure Indices--Radiofrequency/Microwave Radiation. ACGIH, Cincinnati, OH (1993).
11. Institute for Electrical and Electronics Engineers: IEEE Standard for Safety Levels with Respect to Human Exposure to Radio Frequency Electromagnetic Fields, 3 kHz to 300 GHz. IEEE C95.1-1991, IEEE Standards Coordinating Committee 28, IEEE, New York, NY (1991).
12. National Council on Radiation Protection and Measurements: Biological Effects and Exposure Criteria for Radiofrequency Electromagnetic Fields--Exposure Criteria and Rationale. NCRP Report No. 86, NCRP, Bethesda, MD (1986).
13. Murray, W.E.; Conover, D.L.; Edwards, R.M.; Werren, D.M.; Cox, C.; Smith, J.M.: The Effectiveness of a Shield in Reducing Operator Exposure to Radiofrequency Radiation from a Dielectric Heater. *Appl. Occup. Environ. Hyg.* 7(9):586-592 (1992).

14. Olsen, R.G.; Griner, T.A.; Van Matre, B.J.: Measurement of RF Current and Localized SAR Near a Shipboard RF Heat Sealer. In: The First World Congress for Electricity and Magnetism in Biology and Medicine, June 14-19, 1992, paper P-303, page 151, Lake Buena Vista, FL (1992).
15. Joyner, K.H.: Measurement of Induced Current Flows in the Ankles of Humans Exposed to Radiofrequency Fields, Report #8000. Telecom Research Laboratories, Australian Telecommunications Corporation, Clayton, Victoria, Australia (1991).
16. Allen, S.G.; Blackwell, R.P.; Chadwick, P.J.; Dimbylow, P.J.; Unsworth, C.: Body Currents from HF/VHF Antennas and RF Heat Sealers. In: Bioelectromagnetics Twelfth Annual Meeting, June 10-14, 1990, paper P-9, page 78, San Antonio, TX (1990).
17. Ruggera, P.S.; Schaubert, D.H.: Concepts and Approaches for Minimizing Excessive Exposure to Electromagnetic Radiation for RF Sealers. Rockville, MD: Food and Drug Administration. DHHS Publication No. (FDA) 82-8192 (1982).
18. Grajewski, B.; Cox, C.; Schrader, S.M.; Murray, W.E.; Edwards, R.M.; Turner, T.W.; Smith, J.M.; Shekar, S.S.; Evenson, D.P.; Simon, S.D.; Conover, D.L.: Semen Quality Study of Radiofrequency Heat Sealer Operators. National Institute for Occupational Safety and Health, Division of Biomedical and Behavioral Science, Cincinnati, Ohio, Final Report (1991).
19. Conover, D.L.; Edwards, R.M.; Shaw, P.B.; Snyder, D.L.; Lotz, W.G.: The Effect of Operator Hand Position and Workstation Furniture on Foot Current for Radio Frequency Heater Operators. Appl. Occup. Environ. Hyg. 9(4):256-261 (1994).
20. Conover, D.L.; Murray, W.E.; Edwards, R.M.; Werren, D.M.: The Effects of Operator Posture and Workplace Variables on Foot Current for RF Heater Operators. In: Bioelectromagnetics Twelfth Annual Meeting, June 10-14, 1990, paper C-1-6, page 32, San Antonio, TX (1990).
21. Gandhi, O.P.: RF Currents and SARs in an Anatomically-Based Model of Man for Leakage Fields of a Parallel-Plate Dielectric Heater, Final Report. National Institute for Occupational Safety and Health, Division of Biomedical and Behavioral Science, Physical Agents Effects Branch, Cincinnati, Ohio, 38 pages (1988).
22. Gandhi, O.P.; Chen, J.Y.: SAR and Induced Current Distributions for Operator Exposure to RF Dielectric Sealers, Final Report. National Institute for Occupational Safety and Health, Division of Biomedical and Behavioral Science, Physical Agents Effects Branch, Cincinnati, Ohio, 51 pages (1989).

# brooks4.ms

## **Case Studies of Exposures to Nonuniform RF Nearfields: FM Broadcast Antenna, Heat Sealer and Cellular Telephone**

Arthur W. Guy, Ph.D.  
Bioelectromagnetics Consulting  
Seattle, Washington

This paper discusses three different methods that were used for determining compliance or non-compliance of RF exposures to highly nonuniform nearfields with the ANSI C95.1-1991 Safety Standard. The methods include (1) NEC Method of Moments for quantifying level of exposure to high power FM transmitting antenna, (2) measurement of fields and averaging over frontal plane of exposed person to determine exposure to heat sealer and (3) FDTD method for determining SAR levels in head of cellular telephone user. Details are as follows:

### **(1) Exposure to FM Transmitting Antenna**

The double precision NEC2D code installed on a DEC Model 3000-800 Alpha workstation was used to analyze the exposure of a man at a few feet away from a "roto roter" type FM transmitting antenna with an input power of 16 kW. The code was expanded to include up to 64 elements with each element separated into 3 to 26 sub-elements to represent the antenna elements, supporting boom structure, 3 sections of the tower and a ladder at the side of the tower. The power density in the vicinity of the antenna both inside and outside of the tower were calculated, displayed and plotted in 2-dimensional graphical form by means of TECPLOT Graphics software to a resolution of 1 cm.

To quantify whole body exposure, the frontal plane of the exposed person was determined based on actual body dimension measurements made by the author on a person of similar height and weight chosen from data obtained from nearly 300 human volunteers. Computer integration of the "worst case" exposure power density over the frontal plane area of the subject indicated a whole-body-average exposure of 313 mW/cm<sup>2</sup> and a peak exposure of the lower right arm of 5000 mW/cm<sup>2</sup>. The "worst case" whole-body-average exposure within the tower was calculated to be 38.3 mW/cm<sup>2</sup> with a peak exposure of 51.9 mW/cm<sup>2</sup>.

### **(2) Exposure to Heat Sealer**

To determine the exposure of a heat sealer operator under conditions where the shield or grounding plate was both in the normal operating position and removed, a series of electric and magnetic field measurements were made in a vertical plane at the location of closest proximity of the operator's body with respect to the machine during normal operation. Holaday E and H field strength meters, probes and Data Logger were used to record the average rms field strength at a number of positions during the short on time of the machine while typical plastic sheets were being sealed. Measurements were made every 6 inches in both vertical and horizontal directions over the 36 by 84 inch plane of closest operator proximity to the machine. The fields were time averaged for the normal operating cycle of heat sealing operation and scaled two-dimensional contour plots were made of the fields superimposed over drawings of the machine and outline of the operator's body. The shape and size of the frontal plane of the operator's body and the whole-body-average and peak exposures were determined in the same manner as described for case (1) above. It was found that the exposures were in compliance with the IEEE/ANSI C95.1-1991 Standard when the grounding plate was intact but they weren't in compliance when the plate was removed.

### **(3) Exposure of Head to Cellular Telephone**

Dr. Om Gandhi has employed an advanced numerical method called the finite difference time domain (FDTD) technique to many different exposure situations. The case of head exposures to cellular telephones

can be handled especially well by this method. In application to cellular telephones, the method divides the model, for this case the human head and shoulders, into more than a million small cells or elements, in which the average SAR in each can be calculated through numerical analysis on a computer. Lacking the availability of such a sophisticated technique, I did some of my own analyses with a public domain antenna analysis code (NEC Method of Moments) on some simple dipole sources. For example, the most fundamental source one can employ is probably a half-wave dipole, which is a very efficient radiator. I theoretically analyzed a case where a half-wave dipole with an input power of 0.6 W, the maximum possible cellular telephone output, was located about one inch away from the flat surface of a semi-infinite medium of brain tissue simulating the head. In that example the SAR was calculated to be a maximum of approximately 4 W/kg at the model surface adjacent to the feedpoint, dropping off rapidly with depth into the tissue. Several investigators have used similar and slightly more advanced multi-layered models, all of which indicate that the SAR exceeds the IEEE exposure standard for the uncontrolled environment, *i.e.*, a peak value of 1.6 W/kg, at the surface of the exposed tissue. The maximum SAR varies sharply with distance between the dipole to the surface of the tissue. For example, at 15 mm away, the maximum SAR approaches 8 W/kg, and at 30 mm it's below 3 W/kg.

Though the latter still exceeds the IEEE standard, it turns out that an ideal center-fed half-wavelength long dipole radiating into a semi-infinite tissue medium is quite a bit different from a hand-held cellular telephone, operating with an end-fed antenna slanting away from the head of a human. A more sophisticated approach is required to model the actual exposure situation.

Gandhi (1995) analyzed the SAR pattern in a realistic human torso and head model with the FDTD method and found that most of the energy is absorbed in the ear, where the top of the cellular telephone is placed. Some energy also is absorbed in the brain, but much less than in the ear. The highest tissue SARs found in the analysis of eight different cellular telephones approached about 1 W/kg (specifically, 849 mW/kg in the ear), but in the brain itself, the SAR levels were down to 0.3 W/kg. This value is consistent with the analysis by Balzano (1994) based on actual measurements. Gandhi also did some measurements that confirmed his calculations. On the other hand, Niels Kuster (1994), using the same model as Balzano, measured SAR values well over 1 W/kg in the ear and brain tissues when looking at the highest exposure situation. However, to obtain these higher values, Kuster placed the cell telephone antenna at distances much closer to the model head (atypical for most cell phone users) than used by Gandhi and Balzano. He also tested a phone with a shorter one quarter wavelength long antenna (not used in the United States) which results in higher SAR near the base of the antenna. This issue is one that has to be resolved through agreement on antenna types and locations of the antenna relative to the head, typical of cellular telephone use.

## References:

Kuster N., Balzano Q., 1992, Energy absorption mechanism by biological bodies in the near field of dipole antennas above 300 MHz, IEEE Transactions on Vehicular Technology 41(1):17-23.

Gandhi O. P., 1995, Some numerical methods for EM dosimetry: Extremely low frequencies to Microwaves, Radio Science Vol 30: Jan/Feb 1995.

Balzano Q., 1995, Garay O., Manning T., Electromagnetic energy exposure of simulated users of portable cellular telephones. IEEE Transactions on Vehicular Technology, In Press

## **738 Engineering Installation Squadron Environmental Radio Frequency (RF) Measurement Capabilities**

James W. Laycock  
Senior Electronics Engineer  
738 EIS, Keesler AFB, MS

The 738 Engineering Installation Squadron (EIS) (formerly the 1839 Engineering Installation Group) located at Keesler AFB MS provides a wide range of measurements and specialized engineering services (MSES) for the Air Force and other federal agencies including radio frequency (RF) radiation measurements. Measurements are performed near high powered emitters to define the areas which exceed the permissible exposure limits (PELs) for personnel or areas hazardous to electroexplosive devices and fuel handling operations.

Over the past three decades, the 738 EIS has developed expertise in the measurement of the power density and field intensity of radiated fields. Methods have been developed for RF radiation measurement of radar systems which provide beam stopped peak and average power density as well as time average power density, all without requiring the radar antenna to be stopped. This measurement method allows detailed measurements without disrupting the normal operation of the radar system.

The 738 EIS maintains a vast test equipment inventory of broadband radiation monitors as well as calibrated frequency selective receivers, antennas and associated equipment to support radiation over the frequency range of 20 Hz to over 40 GHz. In addition to electronic test equipment, the 738 EIS has three self contained special purpose measurement vehicles with telescoping pneumatic antenna masts and internal power generators. The newest of these vehicles provides a 55 foot antenna mast and an 80 decibel electromagnetically shielded laboratory. The shielded area is used to protect susceptible digital test equipment and in some cases test personnel from the high peak pulse field intensities produced by pulsed radars. Where greater test antenna heights are needed to access high level fields, high reach vehicles from the 738 EIS motor pool can be used.

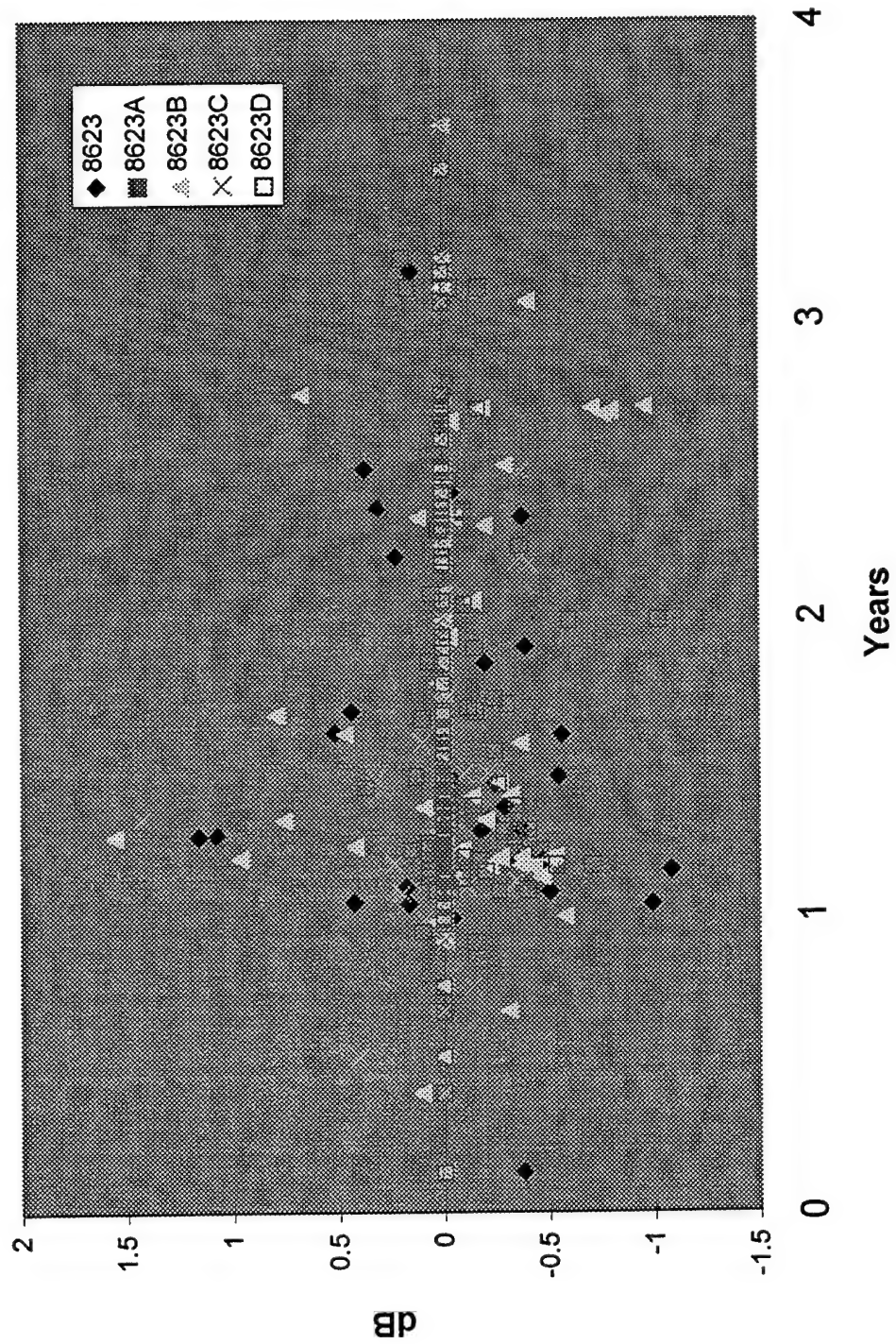


Extension of NARDA Calibration Interval  
Mr John Brewer  
Illgen Simulation Technologies Inc.

1. We evaluated a suggestion to extend the calibration interval of NARDA probes used by the USAF. We recommend extending the present recommended calibration interval from one year to two years. Although these probes are subject to failure and drift, all failure modes seem to result in the meter not being able to be zeroed and therefore obvious to the user; and any drift seems to be well within the stated accuracy of the probe. We feel that a longer calibration period will provide acceptable accuracy and reliability.
2. To conduct the study, we contacted all MIL Spec. calibration facilities to see if sufficient historical calibration information was on hand. Currently, no facility maintains data longer than one year except NARDA Corp. NARDA's MIL Spec. calibration procedure is to record the probe response, adjust the center frequency response to unity, and then record the new response. By resetting the probe response to unity each year, the drift is the difference between the two response checks (minus calibration uncertainty). We used this probe drift in our study.
3. In our retrospective evaluation we used the historical data for an entire year of calibrations at Narda Microwave Corporation. To collect the data, we first manually recorded the calibration information and serial number of every Narda model 8623 probe calibrated (without repair) in the last year. We could not use the data from repaired probes since the probe element is replaced during repair. Then we searched the previous three years billing records to find the last time the probe had been calibrated. Of the more than 200 probes that were calibrated, we were able to confirm the calibration interval of 151 probes. Our analysis showed that no probe drifted beyond the probe's measurement uncertainty of two dB. Less than 4% drifted more than one dB. Additionally, the drift did not seem to increase for probes that were calibrated at two or three years compared to the probes that were calibrated at one year. A plot of all probe drifts is attached.

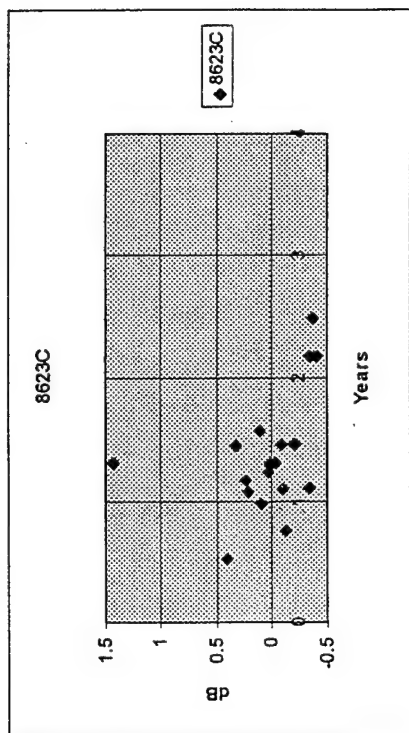
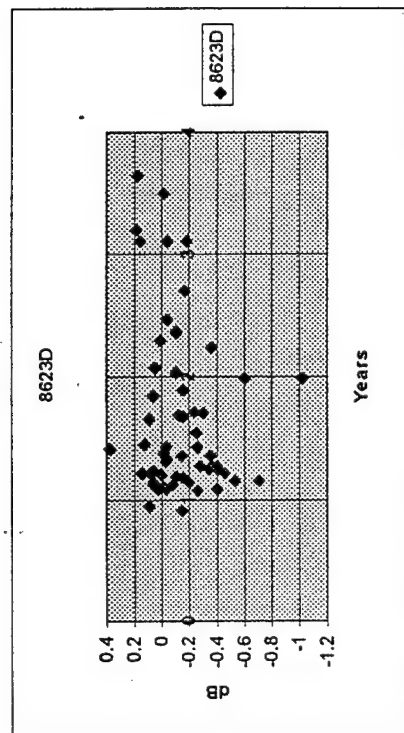
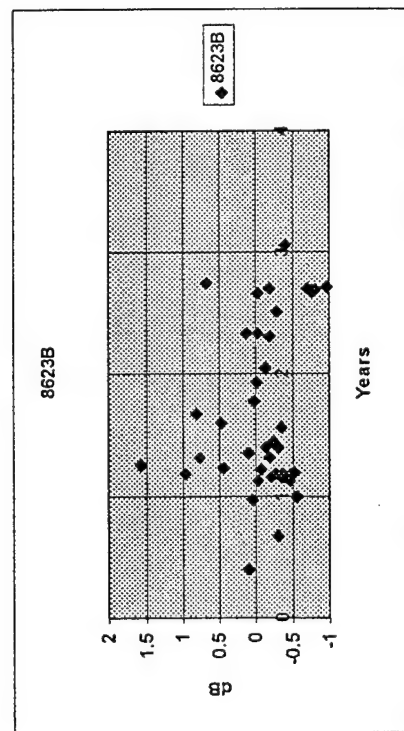
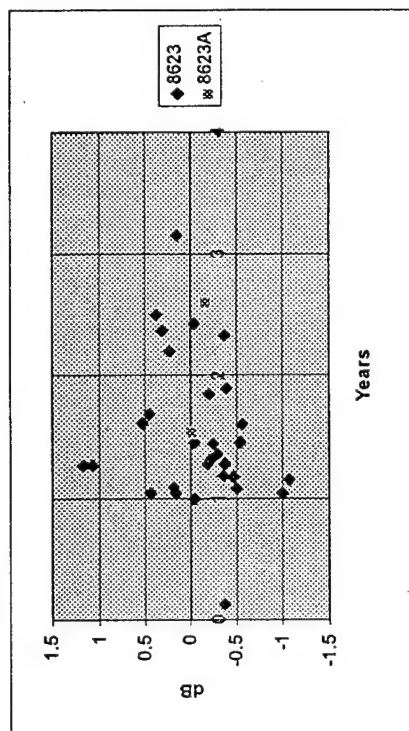


## Narda 8623 Probe Drift

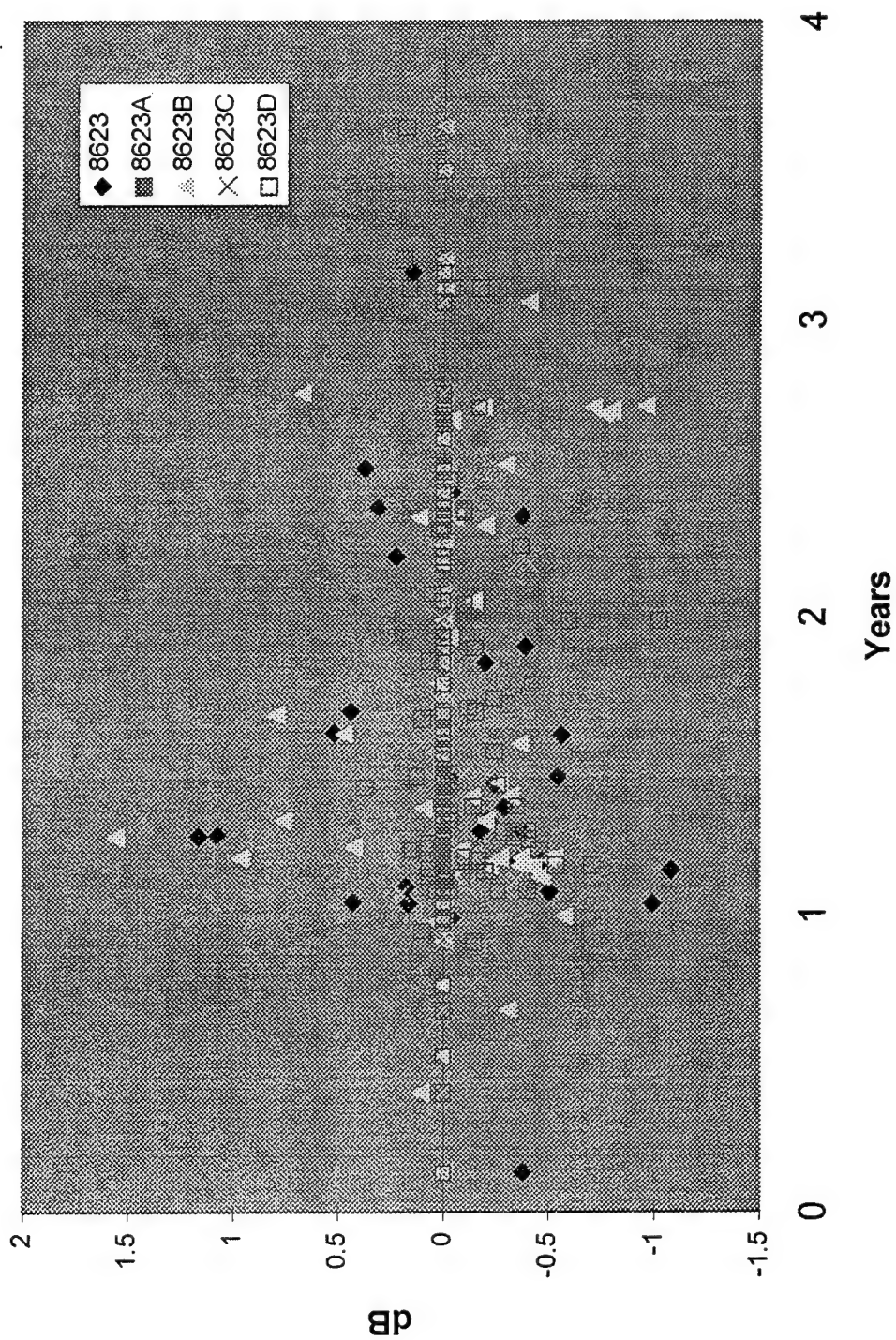




# Narda 8623 Probe Drift



## Narda 8623 Probe Drift



# Overview of UWB Free-Field Measurement and Signal Recording Techniques

Dr. Donald E. Voss, Voss Scientific, Albuquerque, New Mexico

## ABSTRACT

The free-field measurement of radiated UWB signal's time history envelope and frequency spectrum poses unique challenges because of limited capability of appropriate off-the-shelf recording instrumentation, cabling, and sensors. For example, accurate signal shape recording requires (1) multi-GHz bandpass recording of the first few ns of the signal's leading edge; (2) GHz bandpass recording of the long time portion of the signal, often extending 10s to 100s of ns after the early time portion; and (3) determining shot-to-shot reproducibility of the entire waveform shape and frequency content for repetition rates extending as high as many kHz. Because no single digitizer can simultaneously meet these requirements, we have for years used a solution based on use of complementary capability, multiple digitizers operated in parallel under computer control to record sensor output. Automated software then allows full waveform reconstruction within 10s of seconds of the actual test. Another difficulty is the inherent frequency-dependent loss of coaxial cables, which essentially always significantly distorts UWB signals at practical-lengths, i.e. > few meters; no practical multi-GHz fiber-optic link exists to eliminate the problem. Based on cable-characterization at multi-GHz frequencies and Fourier deconvolution, we describe cable compensation techniques used by many researchers to mitigate this problem. These and other issues and practical solutions, applicable to both the free-field measurement as well as the more general UWB signal recording problem, are discussed.

## 1. Introduction.

The goal of free-field ultra-wideband (UWB) measurements is the determination of the full time history envelope of the electric and/or magnetic field(s) at the physical location of the sensor. From this recorded time history envelope, or waveform, summary parameters such as risetime, peak field, frequency spectral content, etc., can be straightforwardly calculated; these summary parameters are often termed "figures-of-merit." This paper provides an overview of the free-field measurement process; however, simply by conceptually replacing the free-field sensor with any of the broader classes of surface current or voltage sensors, the techniques described are fully applicable to measurement/recording of these signals. We note that the nature of many high power UWB sources is that their output envelope shape is not fully reproducible from pulse-to-pulse within multi-pulse bursts; this is particularly true with oil or gas switch-based devices. Our goal is thus broadened to going beyond merely characterizing one pulse within a burst, to measuring the time history envelope of all (or at least a representative sample) of pulses within a burst. This reproducibility measurement is critical for accurate EM dosimetry.

Characterizing the free-field UWB electromagnetic (EM) environment requires a number of major hardware and software components, as shown schematically in Figure 1 below. These include the sensor/transducer; high bandwidth, low loss coaxial cable; signal recording instrumentation; and the computer used for data analysis and control. Each major component of the measurement process is described in detail in the balance of the paper.

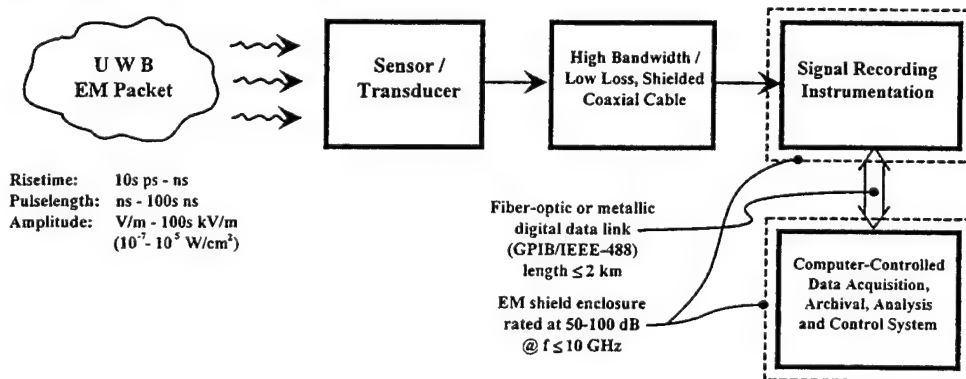


Figure 1. Major components in UWB signal characterization include sensor, cable, digitizers, and software.

## 2. Sensor Selection

Sensors selection for free-field measurements should meet requirements for (1) adequate bandwidth to record the UWB signal's leading edge and any other fast features; (2) adequate sensitivity to drive recording instrumentation so that digitization bit-noise is negligible; (3) power handling capability sufficient to avoid arcing or other non-linear behavior at the highest peak electric fields expected; and (4) known, linear sensor response to the incident EM field, or its time derivative. Either electric field (E) or magnetic field (B) sensors are appropriate for far-field free-field measurements, as knowledge of either E or B is sufficient to infer the other under far field conditions. In free-field measurements that are not in the far-field of a radiating antenna (i.e., the radiating near field), separate measurements of both E and B may be required, since E and B are not necessarily linearly related.

Since space considerations prevent a full discussion of the various sensors available, we discuss the advantages of a particular free-field sensor configuration which has worked well at the Air Force Phillips Laboratory for many years. The Asymptotic Conical Dipole (ACD) class of differentiating electric-field sensors (termed "D-dot" sensors) have been shown rigorously to have maximum bandwidth for a given sensitivity, and thus provide an optimum solution to the competing issues of (1) and (2) above; their response is rigorously linear, and their equivalent area is a-priori known to an accuracy of 1%, meeting criteria (4) above. Our workhorse sensor consists of the following: an ACD type sensor (typically 6-GHz bandwidth/60-ps intrinsic risetime, 3-cm<sup>2</sup> equivalent area, manufactured by either EG&G or Prodyn) used with a 10-GHz balun (Prodyn) to reject common mode signals, and interconnected with a pair of 10-cm length .141 semirigid cables matched to <10 ps transit time. A pair of matched 6-dB broadband attenuators are installed at the 2 inputs to the balun; these improve VSWR and reduce anomalies generated by reflections from the balun's input back to the ACD sensor. This sensor configuration, for typical sub-ns (~150 ps) risetime UWB signals, can operate at peak fields to ~560 kV/m without arcing; the same sensor configuration has good sensitivity, providing a measurable ~ 1/2 division of deflection (0.25 V peak) for a directly driven SCD5000 or 7250 digitizer at ~ 560 V/m (including typical cable loss) incident field. If required, the low end sensitivity can be improved by either or both of the following: using a 10 cm<sup>2</sup> equivalent area D-dot sensor instead of 3 cm<sup>2</sup>, at the cost of reducing bandwidth to ~ 3 GHz (~120 ps intrinsic risetime); and/or inserting 1 (or 2) off-the-shelf 20-dB gain amplifiers (bandwidths extending to > 20 GHz) from B&H Electronics. Use of both amplifier and sensor modifications improves minimum measurable UWB signal to ~ 6 V/m for 150 ps risetime.

## 3. Cables

Because no commercial multi-GHz bandwidth, wide dynamic range, highly linear analog fiber-optic transmitter/receiver exists, it is necessary to route UWB sensor/transducer outputs through conventional coaxial cable to signal recording instrumentation, as shown schematically in Figure 1. Choice of cable is very important at multi-GHz frequencies corresponding to UWB signals as fast as 50-psec risetime. Insertion loss and phase distortion both increase with frequency and a poor cable choice may make the recovery of high frequency/fast risetime signal components via software compensation impossible. While larger diameter cables improve amplitude but not phase distortion, unfortunately the cutoff frequency for undesirable cable overmoding decreases with increasing diameter. Ideally, the spectral signal content should be negligible above 90% of cable cutoff frequencies, corresponding to approximately 5 and 9 GHz for commonly available 7/8 and 1/2 inch foamflex, respectively.

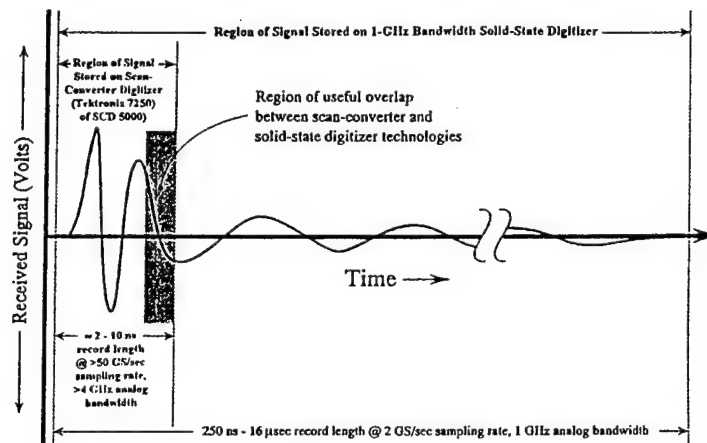


Figure 2. Accurate recording of a typical UWB signal using two complementary digitizers with overlapping records.

We have found that the 1/2 inch diameter foam-flex cable (Andrews or Cablewave) is a good choice, since it is solid-jacketed and thus fully shielded, is lower loss than similar sized polyethylene or teflon type cables, has an acceptably high cutoff frequency for 1st overmode (10 GHz), is reasonably flexible, and is readily available at modest cost. Prior to diagnosing a UWB experiment/test, the magnitude and phase of the insertion loss of all cables and attenuators in a signal line should be measured and archived from 45 MHz to >10 GHz using an HP 8510 vector network analyzer or equivalent. Using standard Fourier transform techniques and frequency domain correction, this calibration data is used to correct the digitized signal for frequency dependent cable distortion effects with software.

#### 4. Signal Recording Instrumentation

A solution to the difficult UWB signal recording problem is shown in Figure 2. The recording goal is to store the entire UWB waveform, which may extend to a few hundred ns in time, at full fidelity (i.e. bandwidth) for every shot of a multi-shot burst. Limitations on state-of-the-art digitization hardware prevent this goal from being fully realized. Note that sampling scopes are fundamentally unsuitable because they require many shots to acquire a single waveform, and thus assume rather than verify/determine signal reproducibility. A 4-GHz analog bandwidth, long record length solid state digitizer would be ideal; it doesn't presently exist, however, and little progress in advancing the single-shot analog bandwidths of solid-state digitizers beyond 1-GHz is anticipated in the near term.

An advanced hardware complement has been assembled to address this need. The SVA (System Verification Apparatus) has been used successfully by the Air Force Phillips Laboratory since 1992, and is based on the fact that essentially all the high frequency content of typical radiated UWB waveforms occurs in the first few ns. The remaining portion of the waveform has frequency content that can be accurately captured by standard long-record length, 1-GHz bandwidth solid-state digitizers such as the Tektronix DSA602 or equivalent. There are only 2 commercially available digitizers that have the required analog bandwidth (i.e. > 4 GHz) for storing the first 5-10 ns of advanced UWB signals, and both are based on scan converter technology which limits record lengths; these are the 4.5 GHz bandwidth Tektronix SCD5000 and the 6 GHz Tek 7250. As shown in Figure 2, our procedure is to split the incoming signal into 2 pieces, record the leading edge on a 7250, and the entire waveform on a 1 GHz-bandwidth solid state digitizer such as the DSA602. Both digitizers have deep local storage and so can store many shots from a burst. These corresponding two waveforms are then spliced together, using automated routines, to form one waveform having both the fast risetime characteristics of the short time window and the long time aspects of the slower sweep digitizer. Computer controlled logic-based triggering, which accounts for the fact that the different digitizers rearm at different rates and trigger at different effective bandwidths, must also be implemented to assure that this 2-digitizer splicing is accurately carried out throughout a many shot burst.

#### 5. Computer Controlled Data Acquisition, Archival, Analysis, and Control System

Although a computer is necessary to control and automate the UWB data reduction process, it does not necessarily have to be co-located with the instrumentation complement. As shown schematically in Figure 1, the computer can be remote; commercial fiber-optic digital data links allow up to 2-km extensions of the GPIB/IEEE-488 data link. There are several advantages of operating this way: (1) the container which shields the instrumentation from the UWB EM energy can be much smaller and portable, since it no longer needs to accommodate personnel; (2) the smaller container/shield room which houses the signal recording instrumentation can therefore be much closer to the sensor itself - this allows shorter cables to be used and thus cable-induced signal distortion, a major effect in UWB recording, to be reduced; and (3) personnel can operate the experiment remotely from electromagnetically safer surroundings - the need for shielding of the control computer can thus often be eliminated completely. In the case of the Air Force Phillips Lab's SVA, all instrumentation is enclosed in a single rack 100-dB shield box, with remote GPIB computer control of all digitizers, attenuators, trigger discriminators, and counters.

Ideally the control computer performs the complete data acquisition and reduction operation. This includes setting up the digitizers, triggering, and attenuators; storing the configuration in the database; archiving the data in retrievable form; performing cable compensations, splicing waveforms, and carrying out sensor data reduction operations (i.e. integrating ACD sensor output waveforms to generate electric field vs. time waveforms); and printing report quality hard copy. As implemented in the SVA, specific data reduction processes applicable to a wide variety of sensors are available, including differentiating B-dot or D-dot free-field sensors, self integrating E sensors, voltage, current, etc. Fully reduced hardcopy data defining the EM environment is available to researchers within 10s of seconds after a UWB burst, providing immediate feedback for planning the next set of experiments.





# DEVELOPMENT OF DIRECT MEANS FOR MEASURING ANKLE CURRENTS IN RF FIELDS

V. ANDERSON and K.H. JOYNER  
Telecom Research Laboratories  
P.O. Box 249 Clayton, Vic 3168  
Australia

**ABSTRACT.** *A direct method of measuring the electrical current induced in the ankles of a subject exposed to radiofrequency (RF) radiation has been developed using a RF current probe coupled to a battery operated DC voltmeter by a RF detector. This system was trialled using the same subject in bare feet and wearing rubber soled shoes at frequencies ranging between 0.7 and 87.5 MHz, standing on different ground planes. The device was also used to survey a high powered HF broadcast site. It was concluded that the current probe offered several advantages over the traditional method of measuring ankle currents using a resistive plate.*

## 1. INTRODUCTION

Many international standards governing safe exposure to RF radiation now incorporate maximum allowable limits (typically up to 100 mA per leg) for the amount of body to ground current induced in exposed persons. These limits are designed to restrict excessive heating in the ankles arising from high local current flow. Consequently, it has become necessary to develop reliable methods for measuring ankle currents.

## 2. METHOD

Traditionally, a resistive plate has been used [1]. This device functions as a voltage divider which is inserted between the subject and the ground. In its simplest form it consists of two metal plates separated by a non conducting dielectric and electrically connected by a low impedance resistor. Body to ground currents are calculated by dividing the RF voltage drop across the metal plates by the impedance of the device and are assumed to be equivalent to ankle currents.

Alternatively, the authors have chosen to develop a method of measuring ankle currents directly using a RF current probe (Eaton 94606-1). The current probe is basically a toroidal voltage transformer (inside diameter = 12.7 cm) that is clamped around the ankle and suspended in place by a harness worn by the subject. Current flowing in the primary circuit of the leg is induced in the secondary coils of the probe. The output of the probe is rectified by a RF detector which is impedance matched to the probe (50 ohm) and connected directly to the probe output terminal to minimise external RF pickup. The detected output voltage is measured by a battery operated DC voltmeter connected by a short double shielded cable. The device is thus self contained and electrically fully floating with minimal external RF pickup.

The system was calibrated as a whole by correlating a known ( $\pm 0.5$ dB) RF current passing through the aperture of the current probe with the observed output on the DC voltmeter. The current probe has a variable frequency response and was calibrated over a range of frequencies. The current was delivered along a transmission line that was impedance matched as far as possible to 50 ohm along its length using time delay reflectometry. The transmission line was terminated in a 50 ohm power head and meter with an S11 return loss of between 30 to 40 dB. The transmitted power from the line to the probe output terminal peaked at an S21 of -18.4 dB indicating minimal disruption to the line current.

A resistive plate as described above was also constructed for comparison with the current probe [2]. The footprint of the plate measured 20 x 30 cm and had an equivalent impedance of 9.9 ohm in parallel with 195pF capacitance up to 100 MHz. The RF voltage was measured at the mid-side of the plate by a calibrated ( $\pm 0.5$ dB) high impedance detector connected to a battery operated DC voltmeter.

The two devices were tested under identical exposure conditions using a 1.82 m tall male of light frame and average build. A variety of RF sources were used including: (1) a 215 m tall 100 kW MF broadcast mast at 0.7 MHz; (2) the Radio Australia 200 kW broadside co-linear arrays operating from 6.1 to 21.7 MHz; and (3) helical whips and quarter wave monopoles operating from 27.1 to 87.5 MHz. All measurements were taken in the far field of the antennas by the  $\lambda/2\pi$  criterion, though the measurements at the MF mast and the HF arrays were within the radiating near field by the  $2D^2/\lambda$  criterion due to the large size,  $D$ , of the radiating elements. The vertical component of the electric field was characterised at each measurement location using an Instruments for Industry EFS-1 polarised E field meter. E-field readings were recorded from 20 to 180 cm above ground at 20 cm intervals and averaged over that height. Most measurements were taken on imperfect grassy ground of varying wetness. Measurements for the whips and monopoles were also taken over a metal wire mesh mat extending from the subject to the antenna.

### 3. RESULTS

The specific induced current (SIC) is defined as the ankle current through both feet divided by the averaged vertical E-field [3]. Probe measurements on the right leg were found to be equivalent to left leg measurements when the subject faced the antenna and the total SIC was obtained thereafter by doubling the right leg reading. The effect of body orientation relative to the radiating source (i.e., facing towards, away or side on to the source) was also examined. For a well defined source origin such as in the far field of the 27.1 and 40.7 MHz monopoles there was little variation ( $\pm 3\%$ ). In the radiating near field of the large HF antenna arrays (6.1 to 21.7 MHz) there was more considerably more variability (up to  $\pm 23\%$ ).

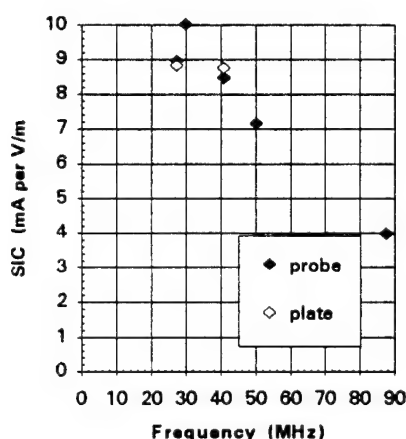


Fig.1 SIC vs frequency for bare feet on wire mesh.

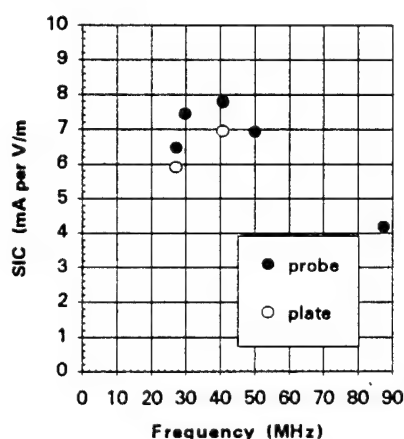


Fig.2 SIC vs frequency for rubber sole shoes on wire mesh.

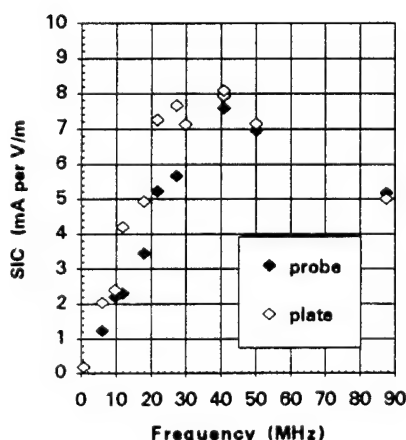


Fig.3 SIC vs frequency for bare feet on grass.

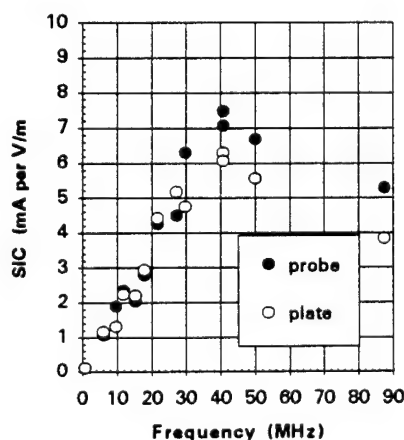


Fig.4 SIC vs frequency for rubber sole shoes on grass.

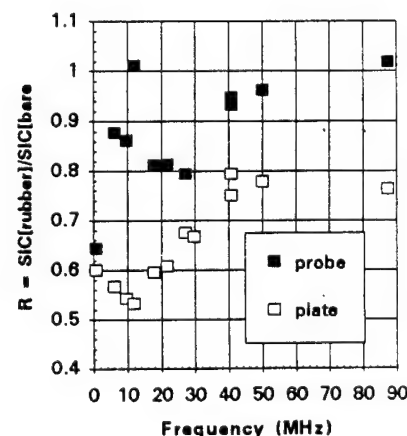


Fig.5 Current reduction ratio,  $R$ , for measurements on grass



Measurements taken on a metal ground with the subject in bare feet (Fig. 1) showed good agreement between plate and probe measurements and plate measurements reported elsewhere [1] when allowing for height differences between subjects ( $I_{\text{ankle}} \propto \text{height}^2$ ). Both devices indicated a relative decline in SIC when the subject wore rubber soled shoes (Fig. 2), particularly the plate.

The more comprehensive SIC vs frequency plots in Figs 3 and 4 for measurements standing on grass show the typical linear rise of SIC with frequency up to whole body resonance, with a post resonance decay as observed by others [3] [4]. Again the plate measurements indicate a greater decline in the footwear measurements relative to those in bare feet. Another difference between the plate and probe measurements is an apparent frequency shift with the plate indicating the onset of resonance below the probe. These differences are more readily apparent in Fig. 5 which plots the ratio of footwear/bare feet SIC when standing on grass.

Because of the low insertion loss of the probe, the authors believe the differences between the plate and probe measurements are due to artefacts introduced by base loading of the subject by the plate. This was borne out by separate and simultaneous measurements with the plate and probe which indicated no impact of the probe on plate measurements, but a significant enhancement of the plate on probe measurements. As well as introducing a series impedance and changing contact the impedance between subject and ground, the plate may also alter the coupling to ground analogous to the base plate on a vertical quarter wave monopole. It is believed that the plate does not register displacement currents that bypass the device in fringing fields from the feet and ankles to ground.

Both devices have also been used for ankle current surveys of high powered HF antenna arrays. Measurements were typically taken on rough uneven ground or long grass where the ground had to be cleared for even siting of the plate. In contrast, with the DC voltmeter tied to the foot it was possible to make continuous measurements with the probe as the subject walked around. Furthermore, unlike the probe, the plate was prone to a small amount of electrical pickup when placed close to the source in the near field. This effect was dramatically observed on a commercial plate device which registered up to 160 mA with no one standing on it.

#### 4. CONCLUSION

Relative to the resistive plate the authors believe that the direct method of measurement with a current probe provides a less intrusive method of measurement. It also provides the possibility of allowing continual monitoring as the subject walks around which can be a useful feature in survey work. A list of desirable features in a commercially developed probe device would include: low weight and appropriate size for ankle diameter, good sensitivity (down to 1 mA), immunity from RF pickup, data logging capability and broadband response.

#### 5. ACKNOWLEDGMENTS

The authors would like to thank Tony Cole, Barry Gilbert, Tony Fleming and Ian Macfarlane for helpful discussions in the preparation this document. The permission of the Director of Research, Telecom Research Laboratories to publish the above paper is hereby acknowledged.

#### 6. REFERENCES

- [1] Gandhi O.P., Chatterjee I., Wu D., D'Andrea J.A. & Sakamoto K. (Jan 1985) "Very low frequency (VLF) hazard study", USAF school of aerospace medicine, Report No. USAFSAM-TR-84.
- [2] Lubinas V. & Joyner K.H. (1991) "Measurement of induced current flows in the ankles of humans exposed to radiofrequency fields" Telecom Research Laboratories, Australia, Report 8000
- [3] Gandhi, O.M., Chen, J.Y., and Riaz, A. "Currents induced in a human being for plane-wave exposure conditions 0-50 MHz and for RF sealers", IEEE Trans. BME-35, 1988, pp. 757-767.
- [4] Blackwell, R.P., Allen, S.G., and Unsworth, C., "Electric field strengths and induced body currents close to monopole antennas", Radiological Protection Bulletin, no. 30, March, 1991, pp. 14-17.



## HATFIELD &amp; DAWSON

JAMES B. HATFIELD, PE  
BENJAMIN F. DAWSON III, PE  
THOMAS M. ECKELS, PE

CONSULTING ELECTRICAL ENGINEERS  
4226 SIXTH AVE. N.W.  
SEATTLE, WASHINGTON 98107

PAUL W. LEONARD, PE  
L.S. CHRISTIANE ENSLOW  
STEPHEN S. LOCKWOOD, PE

TELEPHONE  
(206) 783-9151  
FACSIMILE  
(206) 789-9834

MAURY L. HATFIELD, PE  
CONSULTANT  
Box 1326  
ALICE SPRINGS, NT 5950  
AUSTRALIA

## SOME OBSERVATIONS ON THE MEASUREMENT OF INDUCED AND CONTACT RF CURRENTS

By James B. Hatfield

**ANSI C95.1-1992 *Standard for Safety Levels with Respect to Human Exposure to Radio Frequency Electromagnetic Fields, 3 kHz to 300 GHz*** specifies the measurement of induced and grasping contact RF currents through an equivalent human impedance. Certain problems have arisen regarding the measurement and prediction of both types of body current.

Attention has been given, by broadcast engineering and trade organizations, to the burdensome nature of measuring induced currents around broadcast facilities. This is more easily resolved for domestic Medium Wave (MW) antenna environments where maximum antenna input powers are 50 Kilo Watts. The problem is more complex for HF and VHF antenna sites. Attempts have been made to relate measured induced human body currents to measured ambient fields. Herein are shown specific measurements relating ambient fields near FM broadcast antennas and induced currents as measured with the NARDA induced current meter. The dramatic effect of electric field polarization is also demonstrated.

A series of contact current measurements were made around MF and HF antenna systems using the NARDA contact current meter and also using a calibrated thermocouple ammeter to measure the current through an actual person. The range of agreement and disagreement between the two measurement techniques is shown herein. The discrepancies are also discussed. It is concluded that great care must be taken when contact currents are measured.

### SUMMARY

Contact and induced body current measurements are included as a part of the new ANSI C95.1-1992 ***Standard for Safety Levels with Respect to Human Exposure to Radio Frequency Electromagnetic Fields, 3 kHz to 300 GHz***. These measurements will also be imposed by licensees of the FCC when the Commission adopts C95.1-1992. There currently is one commercially available contact current meter, the Narda 8870. This meter measures the current through a human equivalent impedance specified by ANSI C95.1-1992 (Figure A6) as a function of frequency. The NARDA 8870 meter does not cover the portion of the VHF band (88 - 108 MHz) that includes high power (100 KW) FM commercial broadcast facilities. Both Holaday and

NARDA manufacture induced current meters that include VHF commercial FM frequencies. These meters measure the current exiting the feet of a person, but human equivalent antennas are available.

### CONTACT CURRENTS

Contact current measurements were made at a medium wave (10 KW, 1500 KHz) AM broadcast antenna site and at an HF (9 MHz) antenna site using the NARDA 8870 contact current meter. Measurements of contact currents through a human were at the same locations using an RF thermocouple Ammeter (Weston mod. 733, 250 m.A. full scale). The ammeter was calibrated, as customary, at 60 Hz. The meter is specified as having a "frequency effect less than 2% up to 65 (MHz)..." Figure One shows the 1500 KHz contact current measurements. Actual grasping contact current was measured through two human subjects. It can be seen that the subjects conduct less than half of the contact current indicated by the 8870 meter.

Figure Two shows contact current measurements taken on the guy wires of a 9373 KHz HF antenna with 25 KW input power. In this case the readings taken with the NARDA are generally lower than the readings of actual contact current through a person (this writer). The ground in the area of the antennas and the guy wires was grassy in nature. Heavy objects, such as a person, make better contact with the earth than the grounding plate of the 8870 contact current meter. The contact current through a person could therefore be expected to be higher than the current measured by the 8870. In fact, the contact current indicated by the 8870 meter increased as the downward pressure on the grounding plate was increased. The agreement shown in Figure Two between the contact currents measured by the two methods, with a few exceptions, is quite good.

### VHF INDUCED CURRENTS

The NARDA 8850 induced current meter was used to make measurements near the antennas of two VHF commercial FM broadcast antennas. Spatially averaged electric field equivalent plane wave power density measurements were also made, with a Holaday HI 3001 meter using the "Green" probe, for comparison purposes. The induced currents were made at locations beneath the two antennas where the measured fields were the highest. Induced currents were measured flowing through three subjects, one female and two males. Figure Three shows the

results of the measurements, the subjects are labeled by number while the two bars on the right show the Measured Power Density (MPD) as a percentage of the Maximum Permissible Exposures (MPE) allowed by C95.1-1992, Fig. 1, for the two antennas. The effective radiated powers for the two circularly polarized antennas are the same (100 KW). It can be observed that the antenna closest to the ground has the highest measured field while, at the same time, inducing lower currents in the test subjects.

Induced currents are a function of vertically polarized electric fields while the electric fields were measured with an isotropic probe. The predominant field, due to reflections, near ground is horizontally polarized. This means that isotropic measurements of mainly horizontally polarized electric fields do not track the measured induced currents that are mainly a function of the vertically polarized component of the incident electric field.

### CONCLUSIONS

One must be very careful when measuring contact currents to be sure that they accurately depict the currents that would flow through a person under the same circumstances. Meter ground plate contact with earth can have a strong impact upon the accuracy of such measurements. When measurements are made with a commercial meter, using an equivalent human impedance as a load, it may be wise to measure the actual human contact current when near the MPE limits.

Meters commonly used to survey antenna sites for power density MPE compliance usually employ isotropic measurement probes. Measurements made with these meters do not accurately predict the likelihood of induced current MPE exceedance. It may be possible, however, to relate measured contact currents to measured vertically polarized electric fields.

FIGURE ONE

# 1500KHZ M.W. ANTENNA CONTACT CURRENTS

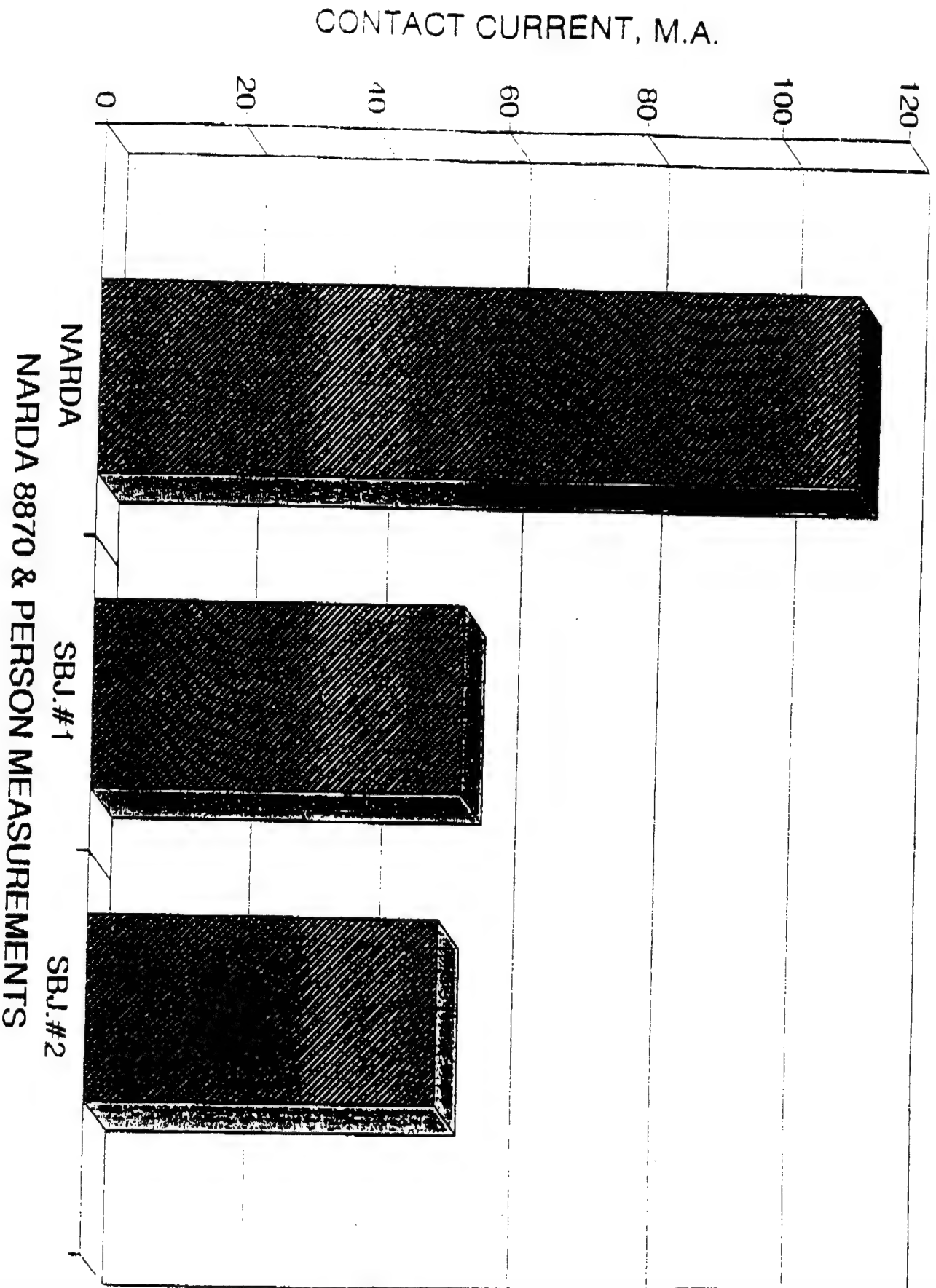
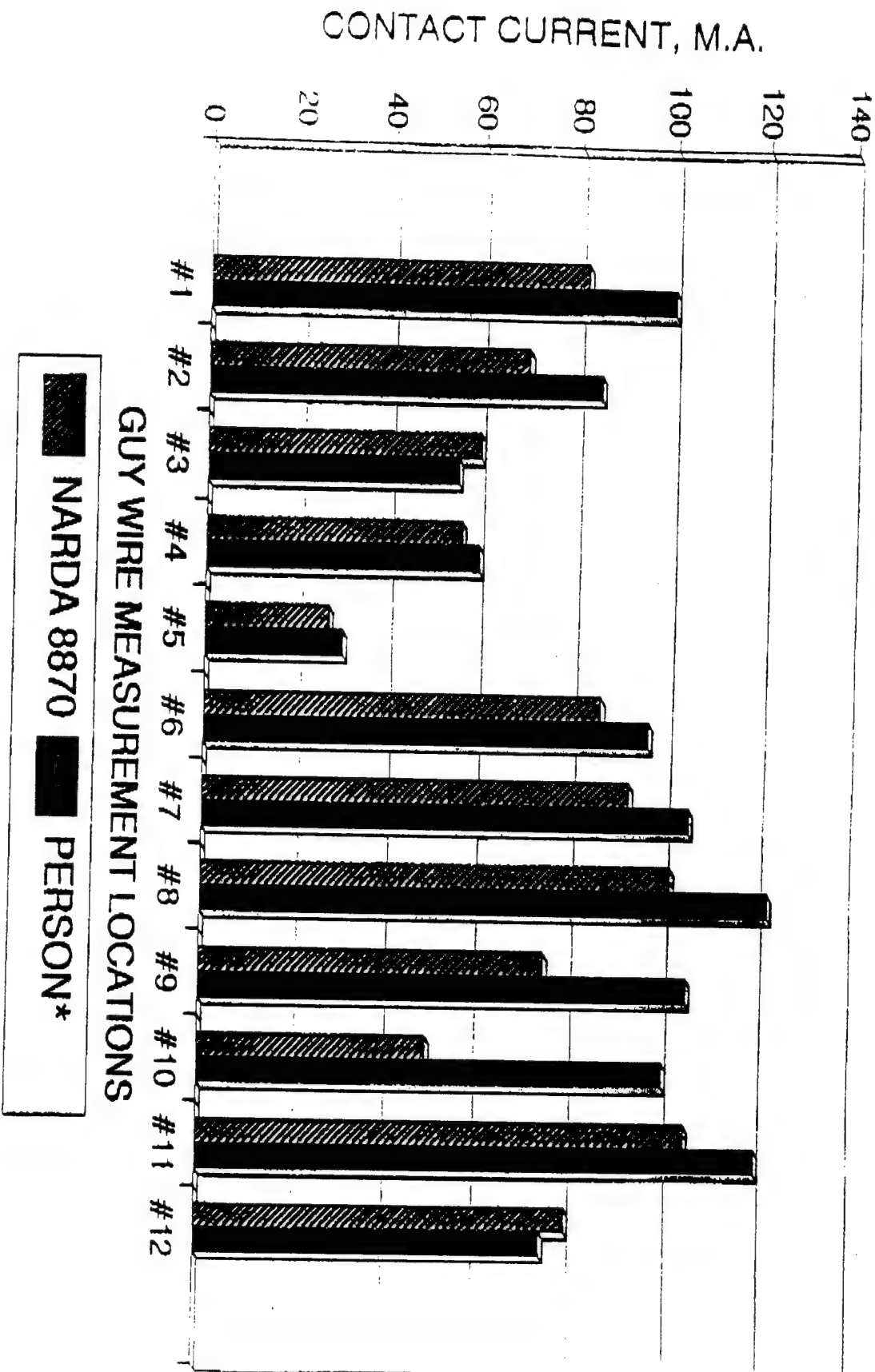


FIGURE TWO

# CONTACT CURRENT MEASUREMENTS HF ANTENNA GUY WIRES AT 9373 KHZ



\* GRASPING CURRENT THROUGH PERSON USING WESTON MOD. 733  
250 M.A. FULL SCALE THERMOCOUPLE RF AMMETER.

# INDUCED CURRENTS & MEAS. POWER DENSITIES AS % MPE







Symposium on Current Issues in RF and UWB  
Measurements.

Brooks Air Force Base, San Antonio  
February 13-16, 1995

## MEASUREMENTS OF INDUCED BODY CURRENTS AT HF/MF BROADCASTING STATION AND RESULTS OF LABORATORY TESTS

Kari Jokela, Lauri Puranen, Lasse Ylianttila, Ari Lukkarinen

Finnish Centre for Radiation and Nuclear Safety  
P.O. Box 14, FIN-00881 Helsinki, Finland

### ABSTRACT

Measurements of electric fields and induced body currents were carried out at Pori HF/MF broadcasting station and in the laboratory in the frequency range from about 1 to 30 MHz. Different optically coupled dipole antennas were used for the measurements of electric fields. The induced body currents were measured at ankles with plate type meters and ferrite-core current transformers. The current distribution over the whole body was measured with a specially designed large air-core and non-resistive current transformer. The results showed that the plate-type meter measures the ankle current correctly only when the feet are in good capacitive or galvanic contact with the ground. The ferrite-core transformers can be used for both the ankle and neck current measurements without any requirements for the grounding. The large air-core transformer measures correctly the distribution of the body current from the head to the feet up to about 40 MHz. The whole body average SAR can be estimated from the current distribution. The measurements at the broadcasting station showed that at MF (963 kHz) the distance when the 200 mA limit for the current through both feet is exceeded is less than 14 m for a monopole antenna transmitting 600 kW power. In the case of a typical curtain type HF dipole array, transmitting 500 kW at 21.55 MHz, this distance is about 50 m.



Symposium on Current Issues in RF and UWB  
Measurements.

Brooks Air Force Base, San Antonio  
February 13-16, 1995

## MEASUREMENTS OF INDUCED BODY CURRENTS AT HF/MF BROADCASTING STATION AND RESULTS OF LABORATORY TESTS

Kari Jokela, Lauri Puranen, Lasse Ylianttila, Ari Lukkarinen

Finnish Centre for Radiation and Nuclear Safety  
P.O. Box 14, FIN-00881 Helsinki, Finland

### 1. INTRODUCTION

At HF and MF frequencies (0.3 to 30 MHz) the external electric fields induce currents flowing along the body and limbs<sup>1,2,3</sup>. These currents cause directly heating of the body and are thus better related to the biological effects than the external electric field. Magnetic fields cause circulating currents which, however, are significantly smaller than the electrically induced currents in the case of wave impedance levels encountered typically at high power HF and MF stations.

In this paper we will report results of the electric field and induced body current measurements carried out at Pori HF/MF broadcasting station<sup>3</sup> and in the Non-Ionizing Radiation Laboratory of Finnish Centre for Radiation and Nuclear Safety (STUK). The frequency range extends ca. from 1 MHz to 30 MHz. The measurement instruments were designed by our laboratory except some commercial meters mentioned separately.

### 2. INSTRUMENTATION

The disturbance caused by weakly conducting signal leads is a serious problem in many commercial meters. To avoid this problem the electric fields were measured with an active dipole meter where the measured signal is transmitted through an optical link or the display is attached to the dipole. The need to measure separately all three orthogonal field components is not a serious drawback because it is the vertical component of the electric field that couples most strongly to the standing body. In the MF range an optically coupled dipole of 30 cm length was used<sup>4</sup> while at the HF range "visually" coupled passive and active dipole meters were used. In the active dipole the batteries have been imbedded in one branch of the dipole and the detector circuit as well as the liquid crystal display in the other branch. The total length of the dipole is 18 cm and the 3 dB bandwidth extends from 0.5 MHz to 90 MHz.

Three different type meters were used for the induced current measurements: parallel-plate meters for the feet, ferrite-core current transformer for the legs and a large air-core current transformer fitting around the whole body. The original parallel-plate meter GC-2 (size 29 x 29 cm<sup>2</sup>) was

purchased from prof. Gandhi. In the modified version designated by STUK-FC9 interference shielding and detecting properties were improved. Also, the commercial NARDA 8850 induced foot current meter was at our disposal in some measurements carried out jointly with Mr. Eicher from the Swiss Telecom.

Induced leg current meter consisted of a large ferrite core current transformer Tegam Model 94606 and a specially designed small battery operated RF millivoltmeter attached directly to the output connector of the transformer. The aperture diameter of the transformer is 12.7 cm; hence the current distribution in the neck as well as in the upper and lower legs up to the knee can be measured. The measured 3 dB frequency range of the system extends from 0.45 to 65 MHz.

The large body current transformer consists of a circular tube of 25 mm thickness with a slit around the inner periphery. A non-resistive coaxial conductor with 25 equally spaced circular loops of 17 mm diameter were placed inside the tube. The open ends of the conductor were fed through a hole in the tube wall forming the symmetrical output. 200 to 50 ohms or 50 to 50 ohms balun transformers were inserted between the current transformer and RF millivoltmeter having an asymmetrical coaxial input. The aperture diameter of the current transformer was 40 cm. Theoretical simulations with a circuit simulator and laboratory tests showed that the upper limit frequency of the transformer extends about up to 40 MHz; at higher frequencies the output voltage becomes increasingly sensitive to the distribution of the current in the aperture due to the propagation delay (transmission line effects) from different loops. The transfer impedance at 27 MHz is 0.21 ohms when using the 200 to 50 ohms balun.

Some of the most interesting findings gained during the field and laboratory measurements on the suitability of electric field and induced current measurements for RF hazard assessments are next briefly summarized:

Parallel-plate meters and current transformers around the ankle give consistent results (within  $\pm 15\%$ ) when the feet are well grounded, which is the worst case exposure situation. The grounding is sufficient when the test subject stands barefoot on a ca.  $1 \times 1 \text{ m}^2$  metallic plate; in the case of smaller plate it must be connected to a metallic rod pushed several tens of centimeters to the ground. In the ungrounded case only the current transformer gives correct results for the currents flowing in the ankles. The plate meter changes ankle currents and about half of the displacement current flows from the upper plate to the free space bypassing the current measuring resistor between the plates.

In the grounded conditions the standing human body couples to the vertical component of the field and the current is in relatively good agreement with the theoretical current computed by using the the empirically derived formula<sup>2</sup>

$$I_{sc} = K_0 h^2 f E \quad (1)$$

where

$K_0 = 0.108 \text{ nA}/(\text{m}^2 \text{ Hz Vm}^{-1})$ ,  $h$  = height of the individual [m]  
 $f$  = frequency [Hz],  $E$  = electric field strength [ $\text{Vm}^{-1}$ ].

Various types of amplitude modulations are used in HF broadcastings (AM, SSB, DCC) and the field may consist of several frequencies. If the detector of the field strength or current meter does not indicate true rms values, the audio modulation and interference in multifrequency fields<sup>5</sup> cause errors which easily may exceed 2 dB. This error cannot be eliminated with electronic or numerical linearity correction based on CW calibration. Hence, true rms detectors are preferred but an acceptable choice would be a linear envelope detector followed by an averaging circuit or a detector showing the peak

value of the measured signal. In any case, it is strongly recommended to check the calibration of the meter by comparing the readings obtained with the modulation to be used in the field to the reading given by CW at the same rms power level.

The calibration of the current meters is not an easy task; one must be sure that the current flowing through the well-known reference resistor is actually the current flowing through the measurement resistor (plate meter) or aperture (current transformer). We first calibrated the plate and ferrite leg transformer by injecting a known current to them; the large air core transformer was calibrated on the spot by comparing the indicated ankle current with the current value given by the plate and ferrite current transformer meters. The estimated accuracy of induced current measurements including calibration uncertainty and various systematic error sources may easily exceed  $\pm 15\%$ , which consists of calibration uncertainty and various systematic errors specific to the measurement conditions in question. Intercomparisons of different current meters and their calibrations between RF dosimetry laboratories would give valuable information on the actual uncertainty of the induced current measurements.

### 3. MEASUREMENTS AT PORI HF/MF BROADCASTING STATION

Measurements were carried out in the vicinity of the MF antenna and a large curtain type HF antenna. In the MF case the antenna tower forms a base-fed vertical monopole of 185 m height. The frequency and transmitted carrier power are 963 kHz and 600 kW, respectively. The HF antennas operate at different frequencies but the transmitted carrier power is 500 kW. During our measurements the frequency was 21.55 MHz.

Figures 1 and 2 show the measured vertical electric fields and for the HF antennas also the total field (equal to the vertical fields for MF antenna). Additionally, effective electric fields were computed from the measured foot current by solving E from the current formula (eq. 1). The effective fields are close to the vertical electric field components as stated previously.

The foot currents given both for the MF and HF antenna as a function of distance is given in Fig. 3 together with the new limit recommended by IEEE. It is of interest to note that the distance when the IEEE limit is exceeded is about 50 m for the HF antenna but less than 14 m for the MF antenna. In the latter case the practical safety distance is determined by high electric fields causing unpleasant RF shocks when ungrounded metallic objects are touched. The risk of RF shocks becomes significant when the electric field strength exceeds 200 V/m. The present occupational limits being typically 614 V/m at 1 MHz may be too high in actual working conditions.

### 4. MEASUREMENTS OF THE WHOLE BODY CURRENT

A relatively homogeneous test field was generated in a spacious hall in our office building by using a quarter-wave monopole antenna on a floor covered by aluminum sheets. The frequency and transmitted power were 27 MHz and 200 W, respectively. The distribution of the body current was measured for a test person (height 178 cm, weight 70 kg) standing barefooted on the aluminum sheets (grounded) or separated from the sheets with an insulating platform of 28 cm thick (insulated).

The measured electric fields and induced body currents as a function of height are shown in Fig. 4. It can be seen that in the insulated case the maximum current in the trunk is about half of the current in the ankles of a grounded person. The corresponding current factors averaged for 44 adult test persons (25 males, 19 females) are 0.036 and 0.081 nA/(m<sup>2</sup>HzVm<sup>-1</sup>). Hence, the measured current

factor at ankles for an average grounded person is 25 % smaller than the value used in Eq. 1.

It is possible to transform the measured current distribution to the whole body average SAR by applying the effective cross-sectional area method<sup>2</sup> to the whole body instead of lower legs. For the insulated and grounded test person the SAR:s were 0.11 and 0.56 W/kg, respectively. These values are in good agreement with 0.079 W/kg and 0.45 W/kg computed by Gandhi et al. with the FDTD method for an average person standing in a homogeneous 27 MHz electric field<sup>1</sup>.

## REFERENCES

1. Chen, J.Y.; Gandhi, O.P. RF currents induced in an anatomically-based model of human for plane-wave exposures (20-100 MHz). *Health Phys.* 57:89-98; 1989.
2. Gandhi, O.P.; Chen, J-Y.; Riazi, A. Currents induced in a human being for plane-wave exposure conditions 0-50 MHz and for RF sealers. *IEEE Trans. on Biomedical Engineering* 33:757-767; 1986.
3. Jokela, K.J.; Puranen, L.P., Gandhi, O.P. Radio frequency currents induced in the human body for medium-frequency/high-frequency broadcast antennas. *Health Phys.* 66:237-244; 1994.
4. Jokela, K.J.; Aaltonen, J., Lukkarinen, A. Measurements of electromagnetic emissions from video display terminals at the frequency range from 30 Hz to 1 MHz. *Health Phys.* 57:79-88; 1989.
5. Puranen, L.; Jokela, K.J. Simultaneous measurements of RF electric and magnetic near fields - Theoretical considerations. *IEEE Trans. on Instr. and Meas.* 42:1001-1008; 1993.

# FIGURES

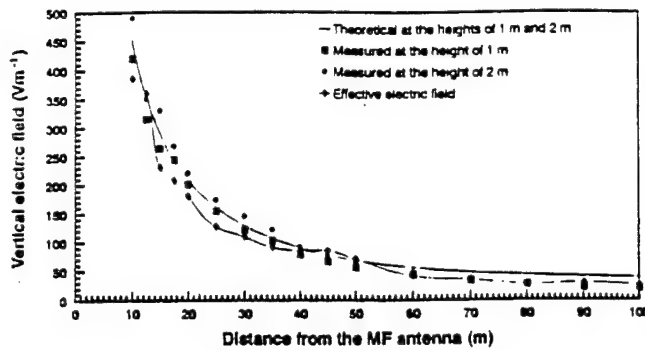


Fig. 1. Measured and theoretical electric fields as a function of distance from the MF antenna.

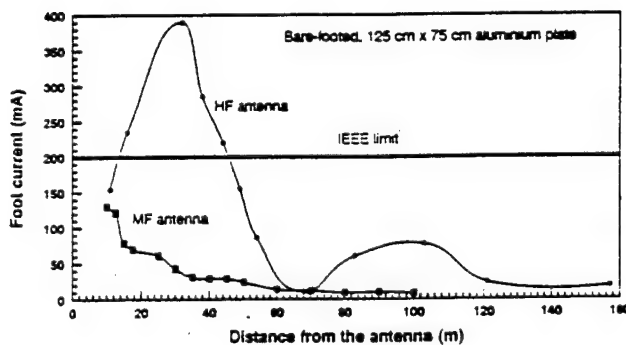


Fig. 3 Measured foot currents (both feet) as a function of distance from the antenna.

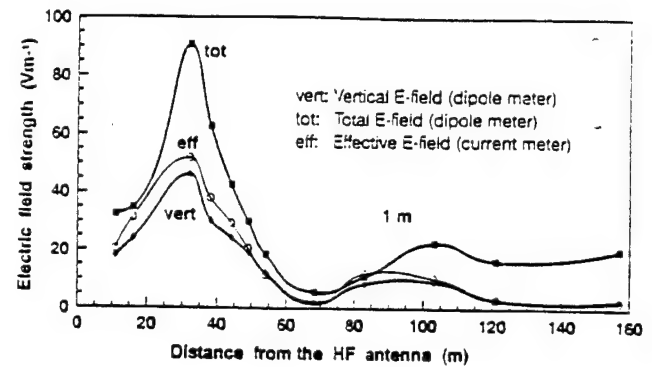


Fig. 2. Measured total and vertical electric fields as a function of distance from the HF antenna.

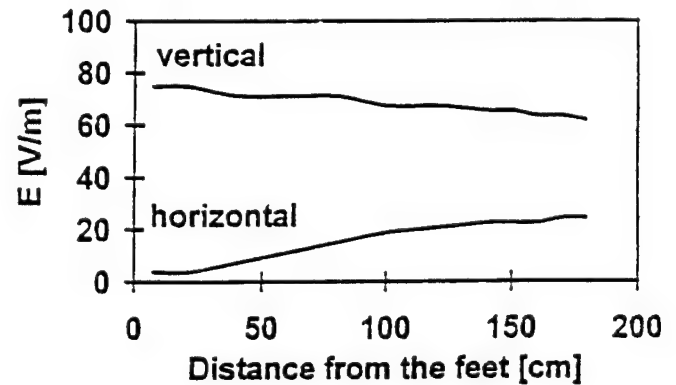
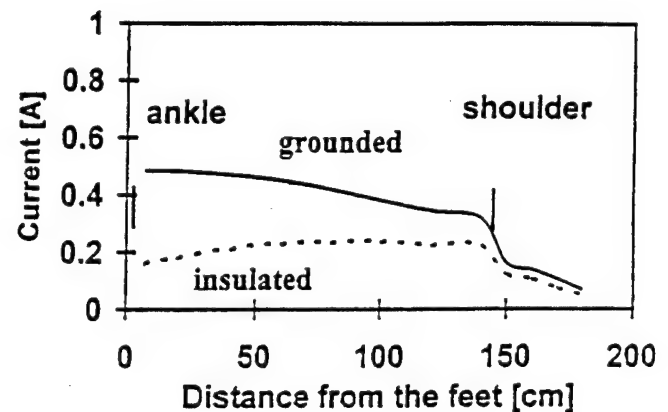


Fig. 4. Electric fields and induced body currents measured at a distance of 2 m from a monopole.

Abstract and Summary  
Presented February 14, 1995  
Symposium on Current Issues in RFR  
and UWB Measurements and Safety  
San Antonio, TX

## Measurements for OSHA Compliant RF Protection Programs

Robert A. Curtis, Director  
US DOL/OSHA Health Response Team

### ABSTRACT

*OSHA recognizes that its most effective activities, including inspections, are those which encourage employers to implement their own comprehensive safety and health program. For work sites involving potentially hazardous radiofrequency radiation, OSHA compliance officer should evaluate the RF protection component of the overall program. This presentation will discuss the measurements which are necessary for the support of expected elements of an RF Protection Program. These include measurements to evaluate the effectiveness of RF controls; to ensure proper maintenance of RF radiating equipment; to develop work practices to minimize exposures; to obtain information to be used in training workers regarding their potential hazards and how they are controlled; to identify "RF Hazard" zones and other areas requiring signs and training; to determine the need for medical surveillance; as an alternative or enhancement of Lockout/Tagout procedures; to evaluate the effectiveness of RF personal protective equipment; and as a periodic audit of the effectiveness of the RF Protection Program. Based on numerous RF surveys conducted by the author, it is concluded that effective measurement of RF hazards depends primarily on an employer's understanding and commitment to these Program elements, and not on sophisticated RF survey equipment or measurement procedures.*

### SUMMARY

To minimize the risk of adverse health effects, radiofrequency (RF) fields as well as induced and contact currents must be in compliance with applicable guidelines (e.g., ICNIRP, ANSI, ACGIH). Reduction in RF exposures can be accomplished through the implementation of appropriate administrative, work practice and engineering controls. These various controls are the elements of an RF Protection Program, and part of an employer's comprehensive safety and health program. The following outlines the principal elements of an RF Protection Program and examples of the RF measurements necessary to implement the program elements.

**Element 1: Utilization of RF source equipment which meet applicable RF and other safety standards when new and during the time of use, including after any modifications.**

- Manufacturers of RF source equipment are responsible for making equipment that complies with applicable standards, and for providing information on the hazards of operating and servicing the equipment. The information must be sufficient to alert the end-user of potential hazards and necessary controls applicable to using the equipment. Manufacturers are therefore required to make detailed RF emission measurements of their products. Appropriate RF survey results should be provided to the end-user for comparison purposes.
- For many low-power products, such as cellular phones, no additional measurements are required by the end-user.
- For other products, the users should conduct RF "screening" measurements of equipment emissions after installation, major maintenance, and any modifications which could effect RF emissions. Significant deviations from previous measurements should be resolved.

**Element 2: RF hazard identification and periodic surveillance by a competent person who can effectively assess RF exposures.**

- Screening measurements are normally sufficient to identify potentially hazardous RF areas which will require some control strategy, such as to determine where a fence should be located. More complex measurements are necessary if the employer intends to allow exposures to employees approaching RF standards. For example, detailed measurements are necessary if whole-body and/or time-weighted averaging of exposures is necessary to bring exposures into compliance.
- RF fields can induce currents in nearby conducting objects, such as a metal barrier or fence used to restrict access to RF hazard areas. These must be evaluated to ensure they do not constitute RF shock and burn hazards. Although detail measurements can be made, the "measurement" of startling/annoying RF spark discharge can usually be made by a quick touch.

**Element 3: Identification and Control of RF Hazard Areas.**

- Controlling exposure time and the distance between the RF source and the operator are important in maintaining workers' exposures below recommended levels. When necessary due to excessive leakage, "RF hazard areas" must be



identified to alert workers of areas that are not to be occupied during RF application. The location of the hazard areas must be based on exposure measurements made during maximum field generation and duty factor (i.e., ratio of RF "on" time during any 6 minute period, assuming intermittent exposure).

- Access to RF hazard areas should be controlled with standard Lockout/Tagout procedures (ref. 29 CFR 1910.147) to ensure workers are not occupying these areas during the application of RF energy. It may be possible to use continuous monitors and/or personal monitors in lieu of, or to supplement, more traditional Lockout/Tagout procedures which lockout the RF power source.
- The RF hazard areas shall be clearly marked with appropriate signs, barricades, floor markings, etc. such that any worker who has access to the facility will be alerted not to occupy the hazardous locations. Signs shall be of standard design and shape (ref. ANSI C95.1), and of sufficient size to be recognizable and readable from a safe distance.
- Screening measurements can be used to determine where to locate signs to alert workers approaching an RF hazard area, including the appropriate warning message on the sign (e.g., Notice, Caution, Danger).
- The evacuation of hazard areas prior to RF application must be strictly enforced. For example, a procedure which requires an RF sealer operator to first load the sealer, step back 2 meters to get outside the RF hazard area prior to activating the RF energy, and then walk back to unload the sealer will be difficult to enforce. The additional time required and increased operator fatigue will discourage operators from following such procedures, particularly for workers who are paid on a piecework production basis.

**Element 4: Implementation of controls to reduce RF exposures to levels in compliance with applicable guidelines (e.g., ANSI, ICNIRP), including the establishment of safe work practice procedures.**

- Reliance on averaging is normally not recommended when establishing basic control strategies because it obligates the employer to conduct "measurement" of employee activity to ensure the averaging is applicable, such as timing an employee's access inside an area which can not be occupied for 6 minutes without exceeding the allowable time-weighted exposure. Where possible, controls should be establish under the assumption that standards are not time-weighted, i.e., assume the standards are ceiling limits which are not to be exceeded.
- Measurements are necessary during the development of work practices to ensure

the practices are effective in preventing excessive exposures. Detailed measurements are required if exposures are approaching guideline limits as discussed above.

- Appropriate work practices must be followed during the repair and maintenance of RF equipment. Occasionally, cabinet panels must be removed by service personnel to allow access for maintenance. Failure to replace a panel properly may result in excessive RF leakage. RF screening measurements can be used to determine which panels can be removed during operation (assuming other hazards, such as electrical shock, are controlled), and to ensure the shielding is reinstalled properly.
- Detailed measurements must be made by the manufacturers' of RF personal protective equipment (PPE) to show its effectiveness and limitations. Limited measurements are necessary by the user to ensure the PPE is applicable and effective for the specific worksite conditions.

**Element 5: RF safety and health training to ensure that all employees understand the RF hazards to which they may be exposed and the means by which the hazards are controlled.**

- Measurement of worker exposures is necessary so that this information can be provided as part of employee hazard training. The scope of training, including reviews of potential biological effects, will be dependent on measured exposure levels.

**Element 6: Employee involvement in the structure and operation of the program and in decisions that affect their safety and health, to make full use of their insight and to encourage their understanding and commitment to the safe work practices established.**

- RF screening measurements should be made in the presence of employees to facilitate understanding and confidence in the program.

**Element 7: Implementation of an appropriate medical surveillance program.**

- RF measurements are necessary to determine the need and scope of medical surveillance. For example, medical surveillance may consist of a means to report the occurrence of RF burns, implanted medical devices (e.g., copper IUD), or the sensation of non-routine heating as a means of identifying potential problem areas. A medical exam may be appropriate for "accidental" exposures defined as an

exposure above some measured trigger level.

- Although not required for compliance with existing standards, RF exposure data is necessary to enhance epidemiology studies of RF biological effects.

**Element 8: Periodic (e.g., annual) reviews of the effectiveness of the program so that deficiencies can be identified and resolved.**

- Periodic RF screening measurements are necessary to ensure conditions have not changed and that the RF Protection Program continues to be effective in preventing excessive RF exposures.

**Element 9: Assignment of responsibilities, including the necessary authority and resources to implement and enforce all aspects of the RF protection program.**

- Although this element does not directly require RF measurements, it is included for completeness of the list of RF Program elements. Without the commitment to the Program, as demonstrated by the assignment of necessary responsibility, authority and resources, the previous elements will not be effective.

As described above, a variety of RF measurements are necessary for an effective RF Protection Program. Usually RF screening measurements are adequate unless control strategies allow exposures approaching RF limits. Detailed RF measurements are required of manufacturers of RF products (e.g., RF transmitters, PPE, RF meters) to document their effectiveness and limitations. The effectiveness of the RF Protection Program depends primarily on an employer's understanding and commitment to the listed Program elements, rather than on sophisticated RF survey equipment or measurement procedures.



# DEVELOPMENT, CHARACTERISTICS AND USE OF AIR-CORE RF CURRENT TRANSFORMERS FOR MEASURING INDUCED BODY CURRENTS

Mark J. Hagmann and George Cabrera  
Department of Electrical and Computer Engineering  
Florida International University, Miami, FL 33199  
Phone (305) 348-3017, FAX (305) 348-3707  
Internet HAGMANN@ENG.FIU.EDU

## Abstract

We have developed minimally perturbing probes for non-invasively measuring the currents induced in various parts of the human body by electromagnetic fields. Each probe has a non-ferromagnetic resistive toroidal coil that passes around the leg or other body member in which the current is to be determined. Eliminating the ferrous core has the advantages of 1) permitting greater aperture size at a specified frequency, 2) reducing errors due to perturbation by the probe, 3) an exact calibration ( $\mu = \mu_0$ ), 4) simplifying probe fabrication, and 5) lowering the weight. However, the sensitivity is much lower than that of ferrous current probes. The upper frequency limit for our non-ferrous probes occurs when the aperture diameter is approximately one-fifth of a wavelength (product of aperture diameter x frequency = 6000 cm MHz). Thus, non-ferrous current probes may be used at frequencies up to 150 MHz in the human torso, 600 MHz in the ankle, 750 MHz in the wrist, and 2.5 GHz in the finger. Our probes were interfaced with fiber-optics links for data acquisition in order to measure the waveforms of currents induced in human subjects by EMP simulators. However, if coaxial cable is used to connect the probes to readout devices it is necessary to use a self-contained preamplifier in order to limit the errors due to cable pickup. We have also made a self-contained current meter for measuring induced body currents at frequencies as high as 600 MHz, with a sensitivity of 8 mA. The non-ferrous probe used in this meter has an aperture diameter of 10 cm which permits measurements in the human ankle or wrist, and it opens as a clamp-on meter. The circuit in this meter uses a RF mixer as a variable attenuator in order to increase the dynamic range, two Monolithic Microwave Integrated Circuits (MMIC) for preamplification, a final broadband amplifier to raise the output compression point, a Schottky diode detector, a sample and hold circuit for the option of retaining the maximum reading, and a liquid crystal digital panel meter.

## DEVELOPMENT, CHARACTERISTICS AND USE OF AIR-CORE RF CURRENT TRANSFORMERS FOR MEASURING INDUCED BODY CURRENTS

Mark J. Hagmann and George Cabrera

Clamp-on AC ammeters are commonly used to measure electrical current without interrupting a circuit, and high-frequency current probes are used for the same purpose in RF applications as well as in EMP simulations [1],[2]. These commercial instruments typically use a ferromagnetic core to couple the magnetic flux produced by a current to a coil, and the voltage induced in this coil is measured in order to evaluate the current. Ferrous current probes have been used to non-invasively measure currents induced in humans in EMP simulations [3] and with fixed-frequency sources [4]

It has been shown [5],[6] that a uniformly wound non-ferrous toroidal coil will also act as a transformer, and the output voltage is independent of the distribution of current within the aperture and not influenced by currents outside the aperture. The voltage induced on the coil is given by  $V = M \, dI/dt$ , where  $M$  is the mutual inductance and  $dI/dt$  is the time rate of change of the current. The mutual inductance is given by  $(\mu_0 N A / c) \, dI/dt$ , where  $N$  is the total number of turns, and  $A$  and  $c$  are the cross-sectional area and length of the toroid, respectively. It is necessary to surround the toroid with an electrostatic shield in order to limit capacitive coupling. Furthermore, resistive loading is used to limit the effects of resonances.

Non-ferrous current probes have a number of advantages relative to the ferrous probes.

- 1) The maximum aperture diameter for a non-ferrous probe may be several times greater than that for a ferrous current probe designed to be used at the same frequency [5]. This difference is attributed to the increased velocity of propagation on the toroid due to the lower value of relative permeability. The upper frequency limit for our non-ferrous probes occurs when the aperture diameter is approximately one-fifth of a wavelength (product of aperture diameter x frequency = 6000 cm MHz). Thus, non-ferrous current probes may be used at frequencies up to 150 MHz in the human torso, 600 MHz in the ankle, 750 MHz in the wrist, and 2.5 GHz in the finger.
- 2) It has been shown by both calculations and measurements [5],[6] that errors due to perturbation (insertion impedance) are much less for non-ferrous probes. This difference may be understood in that the added inductance is decreased due to the lower value of relative permeability.
- 3) The non-ferrous current probes are inherently more accurate because the sensitivity is proportional to the permeability of free space, a fundamental constant, instead of the permeability of the ferrous core.
- 4) The non-ferrous current probes are much simpler to construct and should be less expensive.
- 5) The non-ferrous current probes have much less weight, which makes them more practical for applications in dosimetry. However, the sensitivity is much lower than that of ferrous current probes.

A typical non-ferrous probe, which we have made and used to measure currents induced in the human thigh [6], has an aluminum shield that is a cylindrical shell with an inner diameter (aperture diameter) of 22 cm, an outer diameter of 30 cm, and a height of 5 cm. Inside the shield there is a coil with 200 turns of resistive line, having a total resistance of 33 k $\Omega$ . This

coil is evenly wound on a Plexiglas core having a diameter of 1.9 cm and a length of 82 cm. From theory, the unloaded value of the mutual inductance is  $M = 100 \text{ nH}$  for the unloaded coil. However, when each end of the resistive coil is connected to a  $50 \Omega$  load, we measure a value of  $300 \text{ pH} \pm 12\%$  for frequencies from 1 to 250 MHz, which is consistent with calculations allowing for the loading. This corresponds to a transfer impedance (ratio of the output voltage to the current) of  $1.90 \text{ m}\Omega \pm 12\%$  over the same frequency range. By comparison, the model 94606-2 ferrous current probe (Eaton Corporation, now produced by Tegam), which has an unusually large aperture for a ferrous probe (13 cm diameter, accommodating a human ankle), has a transfer impedance of  $1.0 \Omega \pm 20\%$  for frequencies from 300 kHz to 70 MHz, with appreciable oscillations over 100 MHz and appreciable roll-off below 100 kHz. These values confirm that the non-ferrous current probes may be several times larger in diameter than a ferrous current probe designed to be used at the same frequency. However, they also confirm that the non-ferrous probes have much lower sensitivity.

Others have also used non-ferrous current probes. For example, I-dot probes (so named because the output is proportional to  $dI/dt$ ) have been used to measure the currents induced in inanimate objects during EMP simulations [7],[8]. The Rogowski coil [9] should also be mentioned because it is a type of current probe that has been made either with [10] or without [11] a ferrous core.

The non-ferrous probe, already described, which we made to measure currents induced in the human thigh, was used with human subjects in the EMP simulators at both the ALECS and EMPRESS I facilities [6]. The probes were interfaced with the fiber-optics links used for data acquisition at both facilities, so that no conducting cables were connected to the probes. We found that our current probes have excellent RFI immunity under these conditions. When there was no conducting element in the aperture, there was no measurable signal when the probes were subjected to pulses with a peak electric field of 60 kV/m. However, in other tests made at NAMRL and Brooks AFB, we have found that, when coaxial cable is used to connect the probes to readout devices, it is necessary to use a self-contained preamplifier in order to limit the errors due to cable pickup. The preamplifier [12], which uses a single MAR-6 (Mini-Circuits, Brooklyn, New York) as a MMIC (Microwave Monolithic Integrated Circuit) provides a gain of 20 dB. The internal structure of the MAR series of MMIC amplifiers are Darlington-connected transistor pairs, each with resistive feedback and resistive biasing. A miniaturized 1:1 balun is used to match the balanced output of the toroidal coil to the unbalanced preamplifier circuit.

We have also made a self-contained current meter [12] for measuring induced body currents at frequencies as high as 600 MHz, with a sensitivity of 8 mA. The non-ferrous probe used in this meter has an aperture diameter of 10 cm which permits measurements in the human ankle or wrist, and it opens as a clamp-on meter. After working with circuits using biased and unbiased Schottky diodes, we concluded that greater accuracy and stability may be obtained by amplifying the signal and then detecting it with an unbiased Schottky diode in the linear region. The challenge in this approach came from the fact that considerable amplification is required to bring a small input signal from the probe (typically -40 dBm) to levels as high as 0 dBm at

which the Schottky diode is linear. Compensation circuits, which were used with others [4], were not appropriate because of the low sensitivity of non-ferrous current probes. The circuit in this meter uses a RF mixer as a variable attenuator (SBL-1, Mini-Circuits) in order to increase the dynamic range, two cascaded MAR-6 MMIC for preamplification, a final broadband amplifier based on a MWA-120 to raise the output compression point, a Schottky diode detector, a sample and hold circuit for the option of retaining the maximum reading, and a liquid crystal digital panel meter.

## ACKNOWLEDGEMENTS

This research was sponsored in part by the USAF School of Aerospace Medicine, NIOSH, and the Division of Sponsored Research and Training at Florida International University.

## BIBLIOGRAPHY

1. E. K. Miller, *Time-Domain Measurements in Electromagnetics* (New York, Van Nostrand Reinhold, 1986) pp. 283-286.
2. L. W. Ricketts, J. E. Bridges and J. Miletta, *EMP Radiation and Protective Techniques* (New York, John Wiley, 1976) p. 231.
3. K.-L. Grønhaug, *Measurements and Calculations of Current Induced in a Human Body by EMP Illumination* (FFI/NOTAT-86/4008, Norwegian Defence Research Establishment, 1986).
4. R. P. Balckwell, "The Personal Current Meter—A Novel Ankle-Worn Device for the Measurement of RF Body Current in a Mobile Subject," *J. Radio. Prot.* (UK), Vol. 10, pp. 109-114, June 1990.
5. M. J. Hagmann and T. M. Babij, "Noninvasive Measurement of Current in the Human Body for Electromagnetic Dosimetry," *IEEE Tran. Biomed. Eng.*, Vol. 40, pp. 418-423, May 1993.
6. M. J. Hagmann, "Human Dosimetry in EMP Exposures with Minimally-Perturbing Current Probes," in *EMP Human Health Effects Science Review Panel Proceedings* (Springfield, VA, National Technical Information Service, 1993), pp. 59-78.
7. C. E. Baum, E. L. Breen, J. C. Giles, J. O'Neill and G. D. Sower, "Sensors for Electromagnetic Pulse Measurements Both Inside and Away from Nuclear Source Regions," *IEEE Trans. Ant. Prop.*, Vol. 26, pp. 22-35, January 1978.
8. G. D. Sower, *I-Dot Probes for Pulsed Power Monitors* (Albuquerque, NM, EG&G).
9. A. G. Klein, "On Demonstrations of Ampere's Law," *Am. J. Phys.*, Vol. 61, p. 1045, November 1993.
10. A. G. Klein, "Demonstration of Ampere's Circuitual Law using a Rogowski Coil," *Am. J. Phys.*, Vol. 43, pp. 368-370, January 1975.
11. H. F. Meiners, ed., *Physics Demonstration Experiments* (New York, AAPT/Ronald, 1970), Vol. II, pp. 925-926.
12. G. Cabrera, *Broadband RF Current Detector* (Florida International University, MSEE Thesis, 1994).



# CALCULATED AND MEASURED CURRENTS INDUCED IN THE HUMAN BODY FOR VHF PLANE-WAVE, EMP, AND UWB EXPOSURES

Om P. Gandhi and Jin-Yuan Chen  
Department of Electrical Engineering  
University of Utah  
Salt Lake City, Utah 84112

## Abstract

Numerical methods with increasingly sophisticated anatomically based models and realistic modeling of the incident fields have been used to calculate induced electric fields, current densities, and SAR distributions for far-field and near-field exposure conditions, and for NEMP and UWB exposures. We will describe the induced current distributions for a 1.31-cm-resolution, anatomically based model of the human body for plane-wave exposures for frequencies 27-130 MHz and for one each of representative NEMP and UWB EMP. We will also describe some instruments such as the stand-on foot current meters for CW and EMP exposures, a contact current meter, and an RF stored energy meter, and compare the measured data with calculated foot currents for a number of exposure conditions.

## Introduction

We have used the finite-difference time-domain (FDTD) method to calculate internal **E** and **H** fields, induced current densities, and specific absorption rates (SAR) for anatomically based models of the human body for plane-wave exposures for frequencies 20-915 MHz [1, 2]. As previously described [1, 2], the models of the human body were obtained from the anatomical sectional diagrams available in the book, *A Cross Section Anatomy* [3]. Three different heterogeneous models with resolutions of 0.655, 1.31, and 2.62 cm were obtained from the anatomical data, each with a height of 175.54 and a weight of 69.6 kg. Volume-averaged dielectric properties ( $\epsilon_r$ ,  $\sigma$ ) were prescribed for each of the subvolumes or cells of the model representing the human body. The coarser model with a resolution of 2.62 cm has been used for calculations at lower frequencies 20-100 MHz, and a higher-resolution model (cell size of 1.31 cm) has been used for calculations at higher frequencies [2] and for exposure to vertically polarized electromagnetic pulses (EMPs) of durations of 50 ns to hundreds of nanoseconds that are characteristic of NEMP [4].

Because of the need to extend dosimetric calculations to higher frequencies of several gigahertz and for near-field devices such as handheld wireless communication systems, etc., we have developed a new high-resolution model based on MRI scans of an adult male volunteer [5, 6]. This model has a resolution of  $1.875 \times 1.875 \times 3$  mm and has, to date, been used to calculate SARs and induced current densities and electric fields for EM fields of cellular telephones at 835 and 1900 MHz [7] and for nonuniform magnetic fields of a hair dryer and a hair clipper [8]. In the future, this millimeter-resolution model ought to be used to obtain the currents induced in the human legs with a higher degree of precision than the past models for plane-wave exposures in the VHF band.

## Currents and SARs for VHF Plane-Wave Exposures

Taken from references 1 and 2, the currents induced in the human body are shown in Fig. 1 for an incident, vertically polarized, plane-wave electric field of 1 V/m at a few

representative frequencies for isolated and grounded models. Shown in Fig. 2 are the calculated SAR distributions for the same frequencies as for Fig. 1. It is interesting to note that the highest SARs are calculated for the ankle section for the grounded condition of the model to frequencies as high as 130 MHz, even though the currents passing through the feet are not as high for frequencies in excess of 100-110 MHz.

A comparison is made in Fig. 3 of the foot currents calculated for a grounded model to those that were measured for human subjects [9]. Somewhat lower currents were obtained from the model calculations than were measured experimentally. This may be due to the fact that relatively crude models with a cell size of 2.62 cm (each ankle section was represented by only a few cells) were used for the model calculations at that time [1]. Further work with higher-resolution models may help resolve this discrepancy.

### Induced Currents and Specific Absorptions for NEMPs

We have used the FDTD method to calculate the currents induced and specific absorptions (SA) for a couple of vertically polarized EMPs provided to us on a floppy disk by the Air Force and the Navy [4]. For the negatively polarized EMP shown in Fig. 4a, modeled by the pulse shape given in Fig. 4b, the calculated time-domain variations of the currents passing through the sections through the ankles and the knees are shown in Figs. 4c and 4d, respectively.

In Table I we compare the calculated and measured values of peak currents passing through the various sections of the body for an incident EMP peak amplitude of 55.4 KV/m. The measured data is for a 167.6-cm-tall female with shoes, while the calculated values are for a shoe-wearing, 175.54-cm-tall model of the human body with a resolution of 2.62 cm. As given in [4], the shoe was modeled by a layer of dielectric constant  $\epsilon_r = 4.2$  of thickness, 2.62 cm under the feet of the model. Measurements were taken by Wayne Hammer of the Naval Surface Warfare Center, White Oak, Maryland, using calibrated ferrite-loaded loop current probes. Even though the peak current was not calculated for the highest current section through the thighs, agreement between the calculated and measured peak currents for the other sections is quite good. The whole-body SA for the EMP of Fig. 4a is calculated to be 0.43 mJ/kg.

### Currents Induced in the Human Body for UWB Pulses

Ultrawideband pulses are marked by instantaneous bandwidths on the order of a few gigahertz. We therefore modified the FDTD code so that the frequency dependence of the dielectric properties ( $\epsilon_r$ ,  $\sigma$ ) of the various tissues could be accounted for in the numerical calculations [10]. Even though the frequency-dependent FDTD ((FD)<sup>2</sup>TD) code allows any rational function formulation of the complex permittivity  $\epsilon^*(\omega)$  defined by  $(\epsilon_r - j\sigma/\omega \epsilon_0)$ , Debye equations with two relaxation constants were found to be quite adequate to obtain good fits to the experimental data for  $\epsilon_r$ ,  $\sigma$  of the various tissues [10]. The (FD)<sup>2</sup>TD method was used to calculate the currents induced in the human model with a resolution of 1.31 cm for two different UWB pulses prescribed on floppy disks by the Air Force and the Army. The UWB prescribed by the Air Force is shown in Fig. 5a. Its Fourier spectrum is given in Fig. 5b and the calculated time-domain variations of the calculated currents through a couple of representative sections of the body are given in Figs. 5c and 5d, respectively [11]. The calculated peak currents for the various sections of the body for shoe-wearing grounded and ungrounded conditions of the model are shown in Fig. 6. The calculated peak currents are on the order of 1.1 to 3.2 mA per V/m of peak incident fields.

The total energy absorbed by the body exposed to the single pulse of Fig. 5a is calculated to be 2.0 and 1.91 pJ for isolated and shoe-wearing grounded conditions, respectively.

### Meters for Assessment of Induced Currents and Stored Energy

Limits on foot currents and contact currents have been included in the ANSI/IEEE C95.1-1992 [12] to reduce the internal SARs and the potential for RF shocks and burns. It has also been recognized that transient discharge of stored energy from insulated or poorly grounded objects or from an ungrounded subject to a grounded metallic object may result in startle reactions and burns. We have developed the following prototype meters for assessment of hazards for frequencies to 30-100 MHz [13].

1. A stand-on foot current meter for the frequency range 3 kHz to 110 MHz capable of measuring up to 2000 mA. With a frequency response that is relatively flat (within  $\pm 0.5$  dB) above 100 kHz and increasing linearly with frequency below 100 kHz, as called for in ANSI/IEEE C95.1-1992 RF safety guidelines, this meter is capable of assessing the hazard due to induced body currents for single- or mixed-frequency EM fields.
2. A contact current meter (0-300 mA) with internal impedance equivalent to that of the human body for a variety of contact conditions such as smaller-area finger contact and larger-area grasping contact for various conditions such as grounded and shoe-wearing, respectively [14]. This meter is rated for the frequency band 3 kHz to 30 MHz, and has a relatively flat frequency response above 100 kHz and a sensitivity that increases linearly with frequency below 100 kHz, as called for in the ANSI/IEEE safety limits on contact currents [12].
3. A stored RF energy meter capable of measuring open-circuit voltages (0-5000 V) and short-circuit currents (0-1000 mA) for frequencies up to 30 MHz.

### A Stand-On Induced Current Measuring Device for EMP

As previously described, we have used the FDTD method to calculate the currents induced for the various parts of the body for exposure to EMPs of duration 50 ns to several hundred ns that are characteristic of nuclear EMPs (NEMPs) [4]. The currents passing through a couple of representative sections of the body are shown in Figs. 4c and d, respectively. The entire duration of the induced current is typically less than 100-200 ns with the bulk of the current in the first 30-50 ns of the EMP. Under joint Navy and Air Force sponsorship, we have designed and fabricated a stand-on device with a bilayer sensor of dimensions  $29 \times 29$  cm to measure the current passing through the feet of a person [15]. This digital display meter using sample and hold circuits and two digital displays is capable of displaying the following quantities:

1. The peak current passing through the feet (typically 40-200 A for incident vertically polarized E fields on the order of 10-50 kV/m).
2. The integrated charge  $\int I dt$  passing through the body up to 20  $\mu C$ .

Since the absorbed energy may often be of interest, the second digital display showing the integrated charge could instead be adapted to display the absorbed energy which is proportional to  $\int I^2 dt$ .

We have field-tested this stand-on device at two EMP installations using human volunteers [16]. Highly repetitive data were obtained for identical EMPs. A slight initial variability in the peak current and integrated charge was observed and ascribed to the different pressures (and, hence, variability of impedance to ground) exerted from run to run by the different subjects. This variability vanished when a larger  $60 \times 60 \text{ cm}^2$  aluminum plate was used underneath the device. Because of easy portability and simplicity of operation, this device may be useful for personnel-induced peak currents, integrated charge, and also, perhaps, the absorbed energy for exposure to EMP. The device could also be made so that the bilayer would be divided in two parts, each of which would be inserted in the shoes worn by the personnel.

## REFERENCES

1. J. Y. Chen and O. P. Gandhi, "RF Currents Induced in an Anatomically Based Model of a Human for Plane-Wave Exposures (20-100 MHz)," *Health Physics*, Vol. 57, pp. 89-98, 1989.
2. O. P. Gandhi, Y. G. Gu, J. Y. Chen, and H. I. Bassen, "Specific Absorption Rates and Induced Current Distributions in an Anatomically Based Human Model for Plane-Wave Exposures (to 915 MHz)," *Health Physics*, Vol. 63, pp. 281-290, 1992.
3. A. C. Eycleshymer and D. M. Schoemaker, *A Cross-Section Anatomy*, D. Appleton and Company, New York, 1970.
4. J. Y. Chen and O. P. Gandhi, "Currents Induced in an Anatomically Based Model of a Human for Exposure to Vertically Polarized Electromagnetic Pulses," *IEEE Transactions on Microwave Theory and Techniques*, Vol. 39, pp. 31-39, 1991.
5. J. N. Lee and O. P. Gandhi, "Models of the Human Body: A Historical Perspective," paper presented at the Radio Frequency Radiation Dosimetry Workshop, Brooks Air Force Base, Texas, December 8-9, 1992; to appear in the *Proceedings of the Workshop*.
6. O. P. Gandhi (invited paper), "Some Numerical Methods for Dosimetry: Extremely Low Frequencies to Microwave Frequencies," *Radio Science*, Vol. 30, January/February 1995.
7. O. P. Gandhi, J. Y. Chen, and D. Wu, "Electromagnetic Absorption in the Human Head for Mobile Telephones at 835 and 1900 MHz," *Proceedings of the International Symposium on Electromagnetic Compatibility (EMC '94 Roma)*, Vol. I, pp. 1-5, September 13-16, 1994.
8. D. Wu, O. P. Gandhi, and J. Y. Chen, "Electric Field and Current Density Distributions Induced in a **Millimeter-Resolution** Model of the Human Head and Neck by Magnetic Fields of a Hair Dryer and an Electric Shaver," paper presented at the Sixteenth Annual Meeting of the Bioelectromagnetics Society, Copenhagen, Denmark, June 12-17, 1994; to be submitted for publication.
9. O. P. Gandhi, J. Y. Chen, and A. Riazi, "Currents Induced in a Human Being for Plane-Wave Exposure Conditions 0-50 MHz and for RF Sealers," *IEEE Transactions on Biomedical Engineering*, Vol. 33, pp. 757-767, 1986.
10. C. M. Furse, J. Y. Chen, and O. P. Gandhi, "The Use of the Frequency-Dependent Finite-Difference Time-Domain Method for Induced Current and SAR Calculations for a Heterogeneous Model of the Human Body," *IEEE Transactions on Electromagnetic Compatibility*, Vol. 36, pp. 128-133, 1994.
11. O. P. Gandhi and C. M. Furse, "Currents Induced in the Human Body for Exposure to Ultrawideband Pulses," Technical Report AL-TR-1992-0156, Radio Frequency Radiation Division, Armstrong Laboratory (AFMC), Brooks Air Force Base, Texas, 1992.

12. ANSI/IEEE C95.1-1992, "Standard for Safety Levels with Respect to Human Exposure to Radio Frequency Electromagnetic Fields, 3 kHz to 300 GHz," published by the Institute of Electrical and Electronics Engineers, 345 East 47th Street, New York, New York, 10017.
13. O. P. Gandhi and J. Y. Chen, "Meters for Assessment of Induced Body and Contact Currents and Stored Energy in Electromagnetic Fields," *Abstracts of the Twelfth Annual Meeting of the Bioelectromagnetics Society*, San Antonio, Texas, June 10-14, 1990, pp. 35-36.
14. I. Chatterjee, D. Wu, and O. P. Gandhi, "Human Body Impedance and Threshold Currents for Perception and Pain for Contact Hazard Analysis in the VLF-MF Band," *IEEE Transactions on Biomedical Engineering*, Vol. BME-33, pp. 486-494, 1986.
15. O. P. Gandhi and J. Y. Chen, "Electromagnetic Pulse-Induced Current Measurement Device," Final Report on Contract F 33615-87-D-0609, Task 26, submitted to the USAF School of Aerospace Medicine (RZP), Human Systems Division (AFSC), Brooks Air Force Base, Texas, March 7, 1991.
16. O. P. Gandhi, J. Y. Chen, W. D. Hurt, and D. N. Erwin, "Field Tests of a Stand-On EMP-Induced Current Measurement Device," *Abstracts of the First World Congress for Electricity and Magnetism in Biology and Medicine*, Lake Buena Vista, Florida, June 14-19, 1992, p. 51.

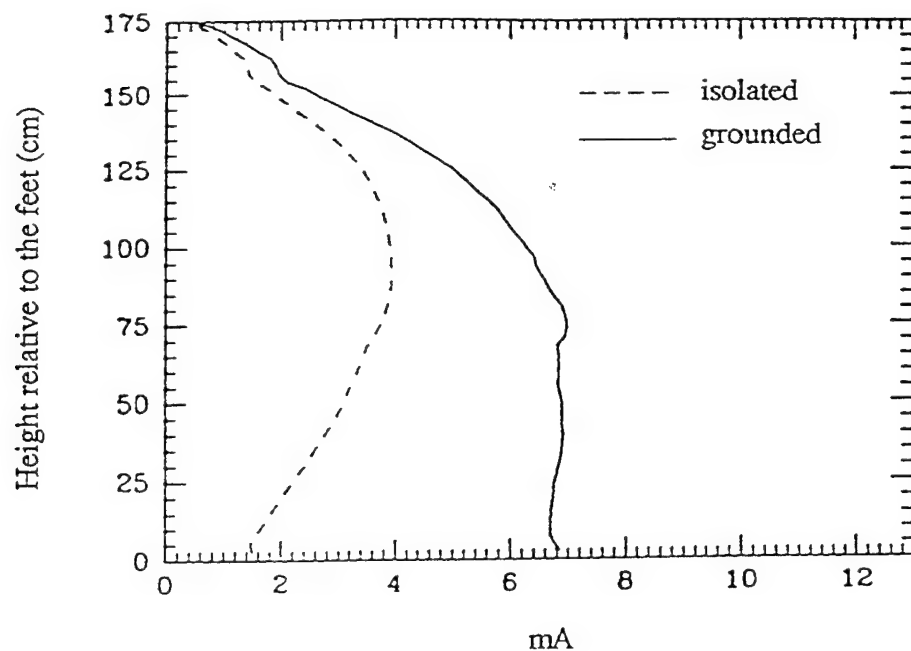
Table I. Comparison of measured and calculated values  
(Peak E  $\approx$  55.4 kV/m).

Section of Body	Peak Current	
	Measured*	Calculated
	A	A
Both ankles	220	192
Both knees	244	235
Both thighs	284	---
Neck	100	81

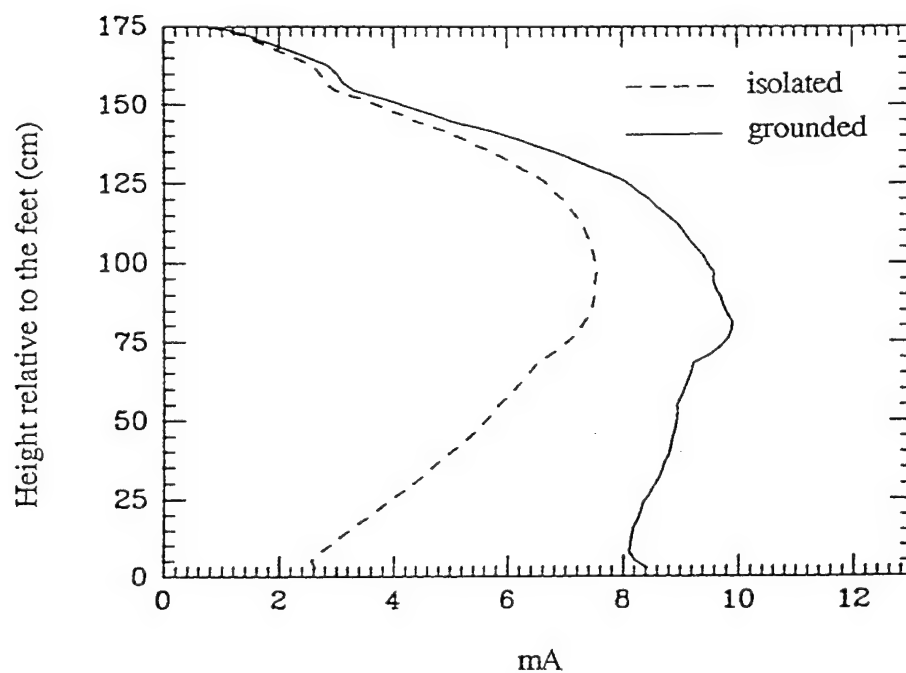
Measured values are for a 5 ft, 6 in. female with shoes.

Time duration for half cycle of current is  $\sim$ 17 ns for both measured and calculated currents.

\* Data courtesy of Wayne Hammer, Naval Surface Warfare Center, White Oak, Maryland.



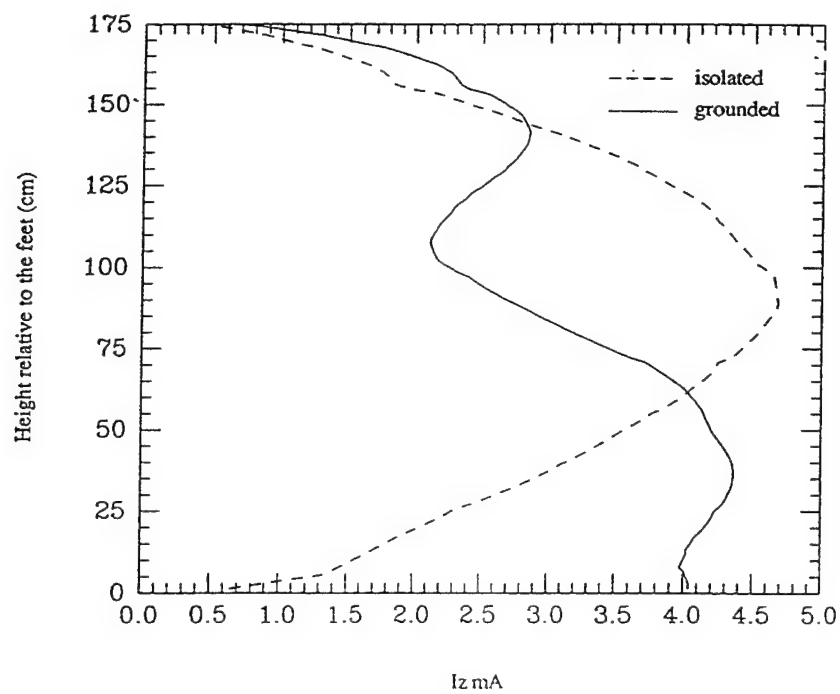
a. 27 MHz



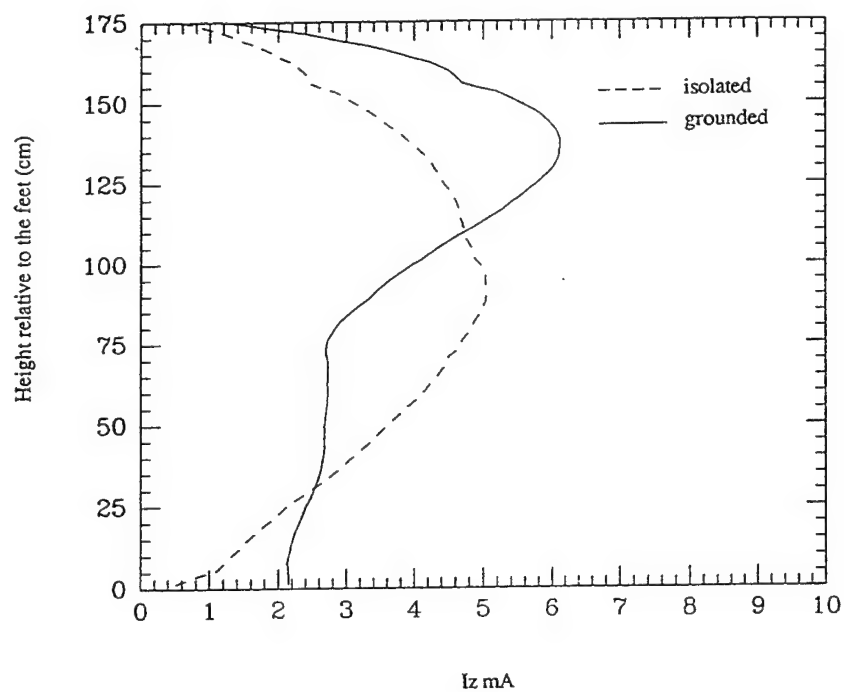
b. 45 MHz

Fig. 1. Induced vertically directed RF current distributions for a grounded and isolated human model for frequencies 27-130 MHz. The currents are for vertically polarized plane waves for an incident rms E field of 1 V/m.



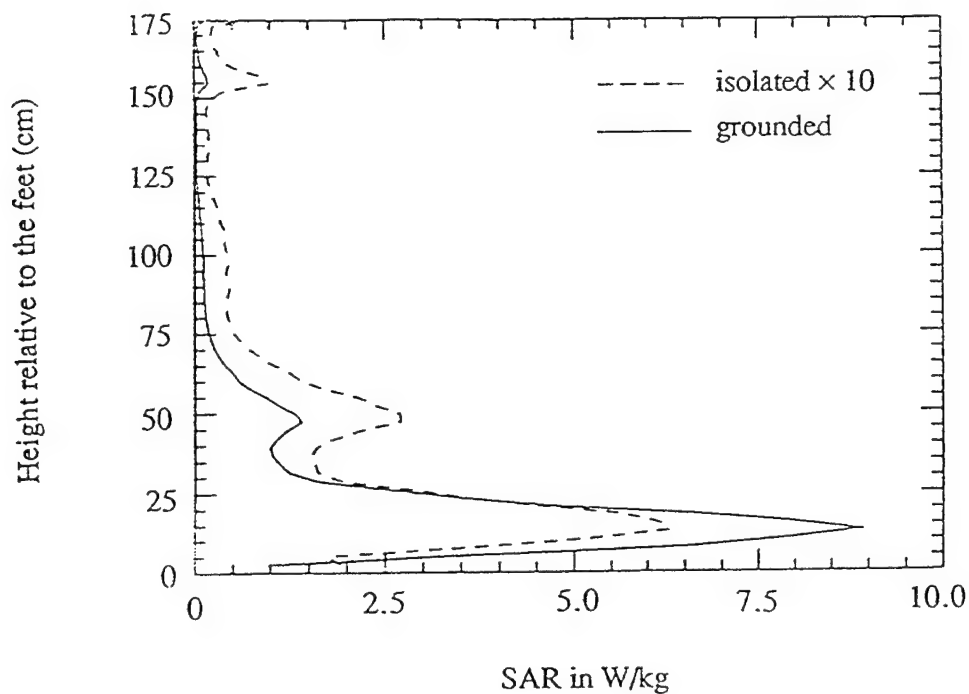


c. 100 MHz

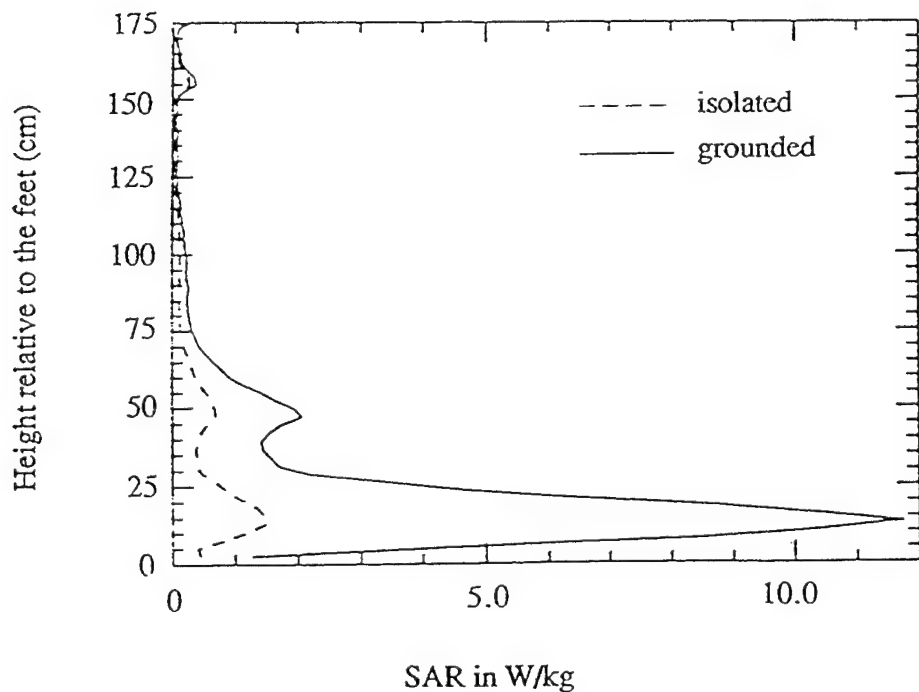


d. 130 MHz

Fig. 1 (continued)

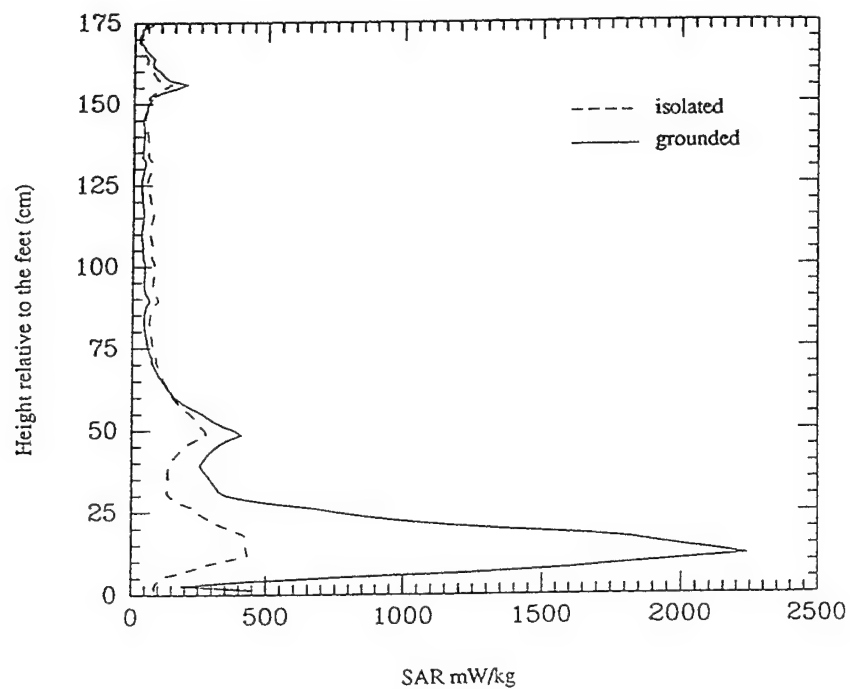


a. 27 MHz

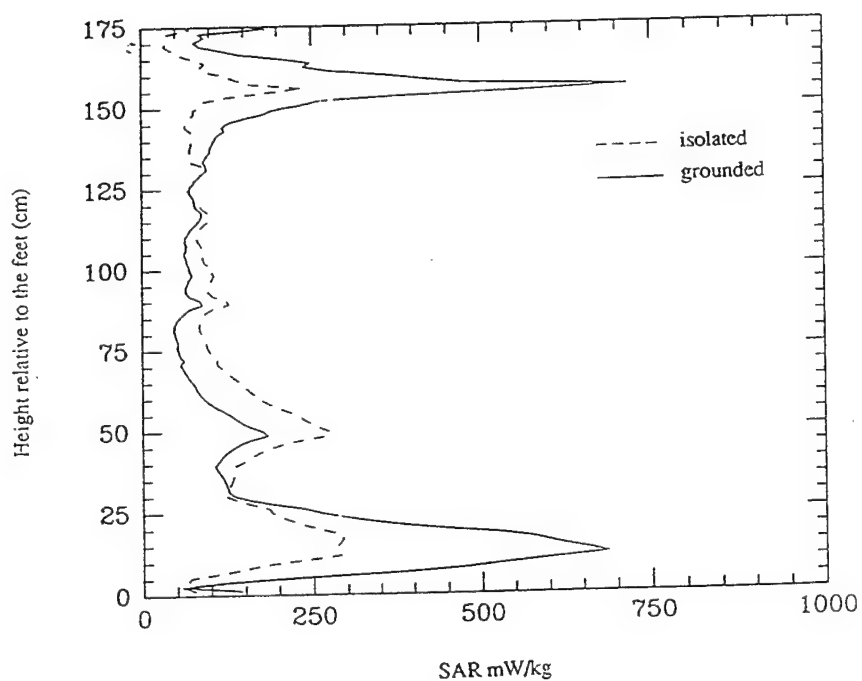


b. 45 MHz

Fig. 2. Layer-averaged SAR distributions for a grounded and isolated man model for frequencies 27-130 MHz. The SARs are for vertically polarized plane waves of  $1 \text{ mW/cm}^2$  ( $E = 61.4 \text{ V/m}$ ). A model with cell size  $\delta = 2.62 \text{ cm}$  is used for 27 and 45 MHz, while a finer resolution  $\delta = 1.31 \text{ cm}$  is used for higher frequencies.



c. 100 MHz



d. 130 MHz

Fig. 2 (continued)

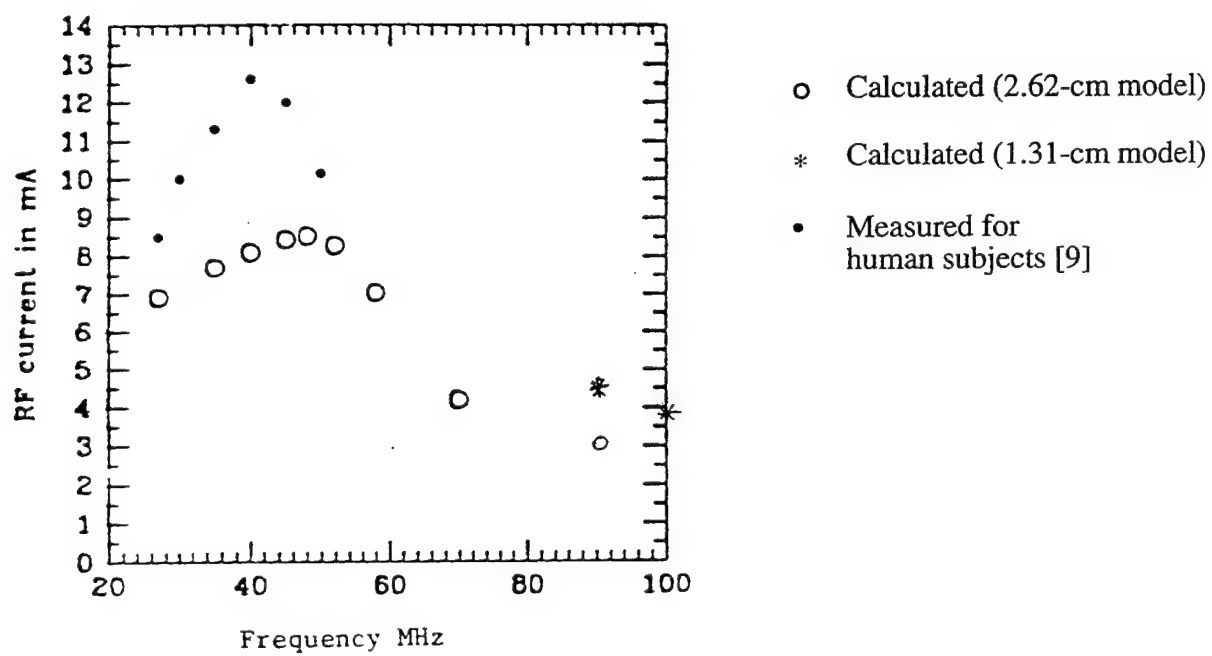
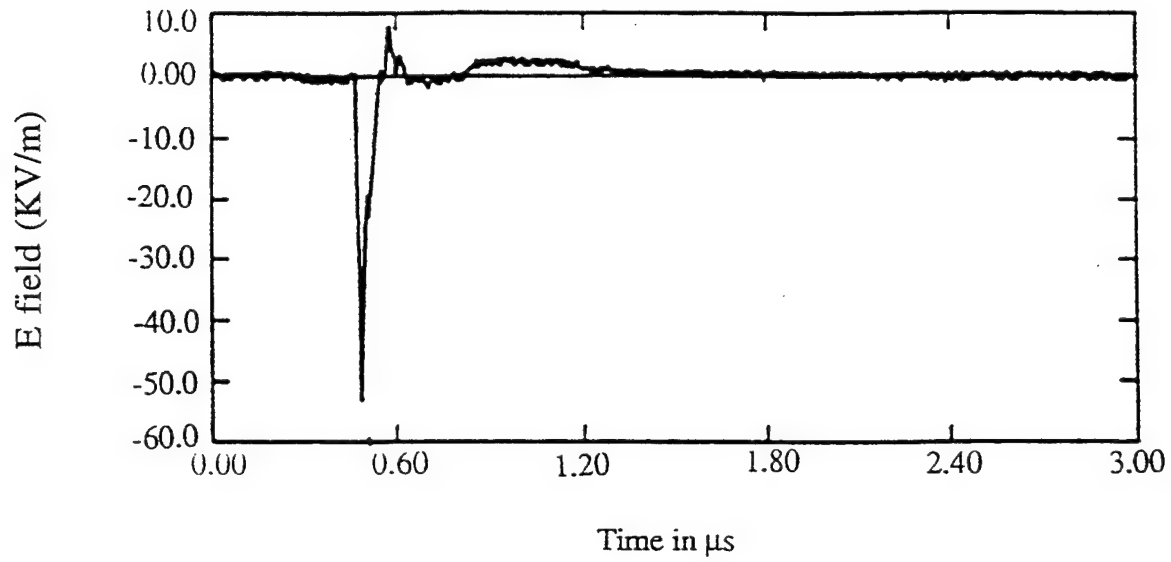


Fig. 3. RF foot currents for a grounded subject exposed to a vertically polarized plane wave.

a. The measured pulse shape.



b. The simulated pulse plotted on an expanded time scale.

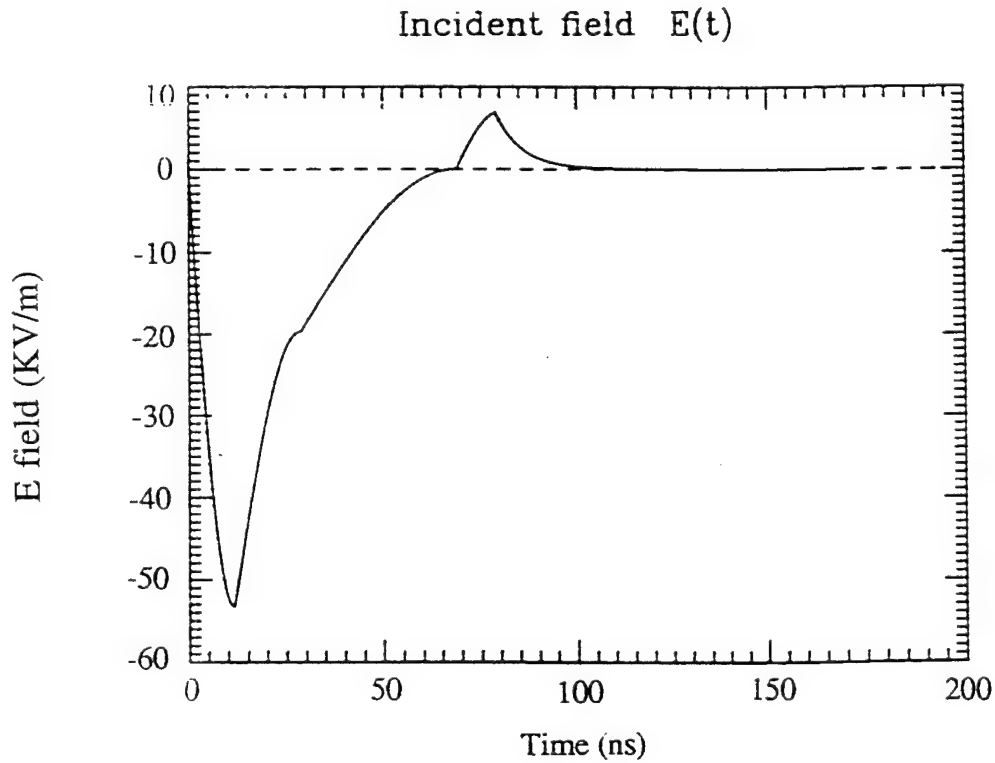
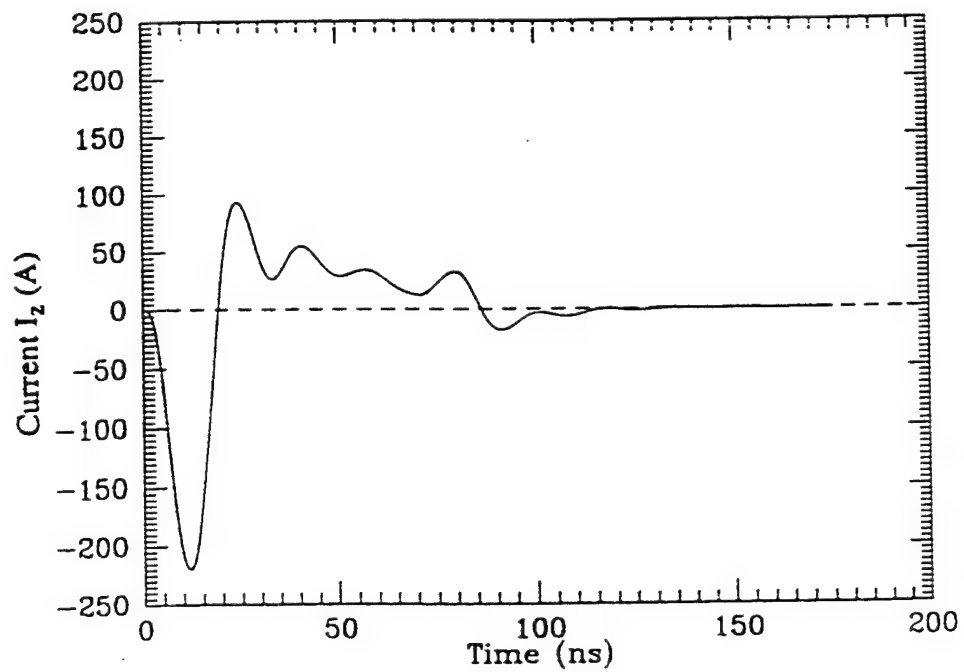


Fig. 4. Currents induced for a representative EMP with a peak incident amplitude of -53,330 V/m.

c. Current for the section through the knees.



d. Current for the section through the ankle.

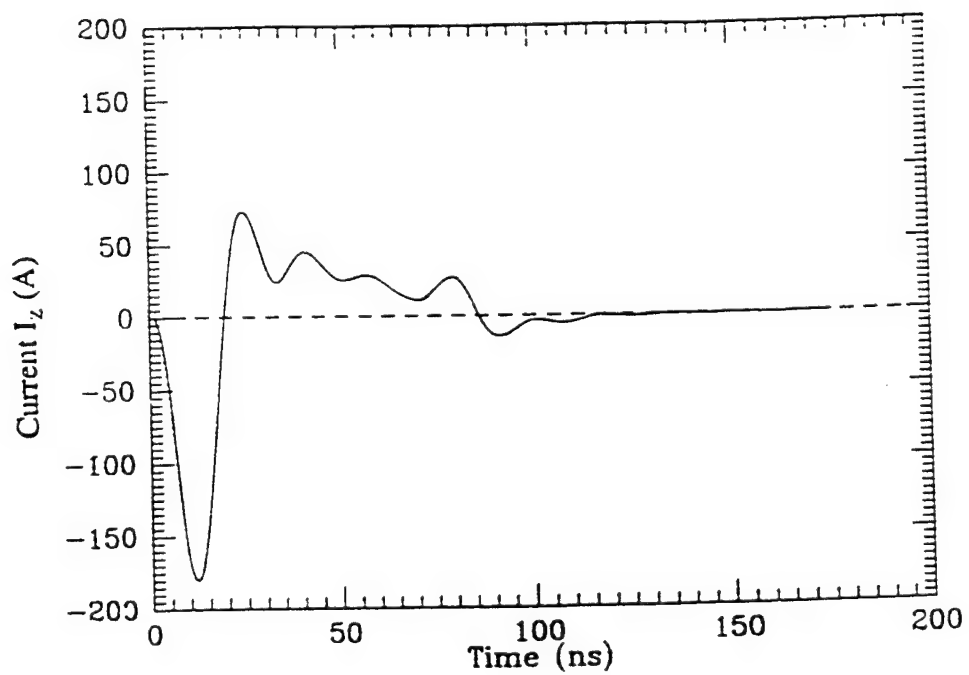
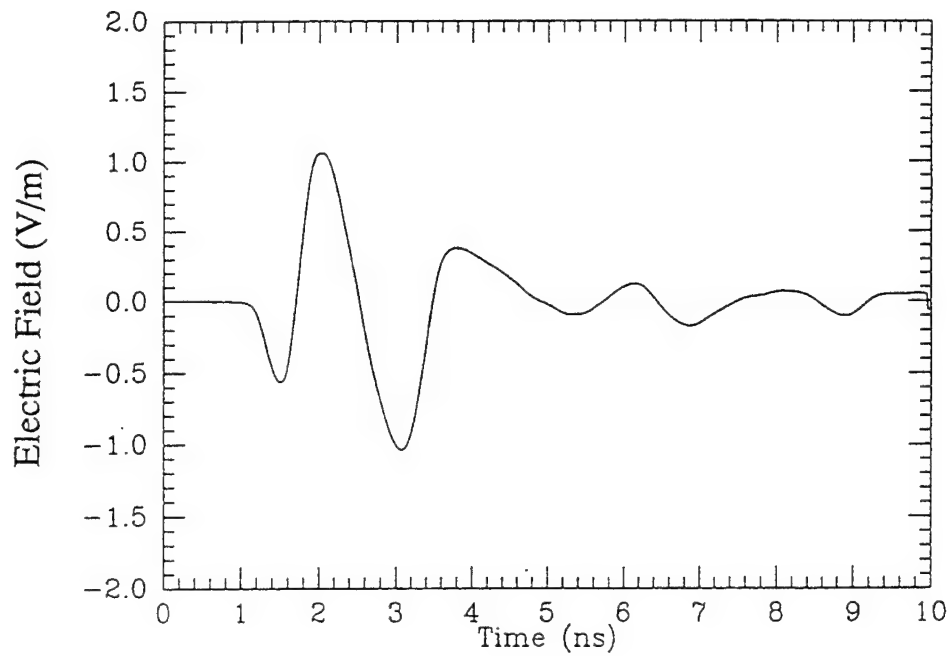


Fig. 4. (continued).

a. The measured domain variation of the UWB pulse.



b. Fourier spectrum of the UWB pulse.

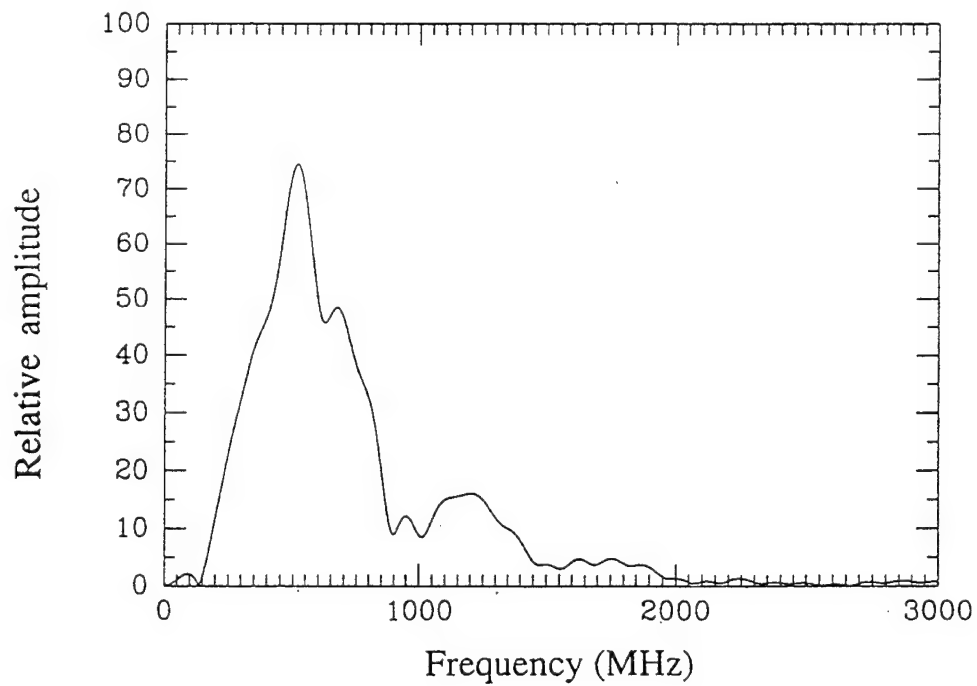
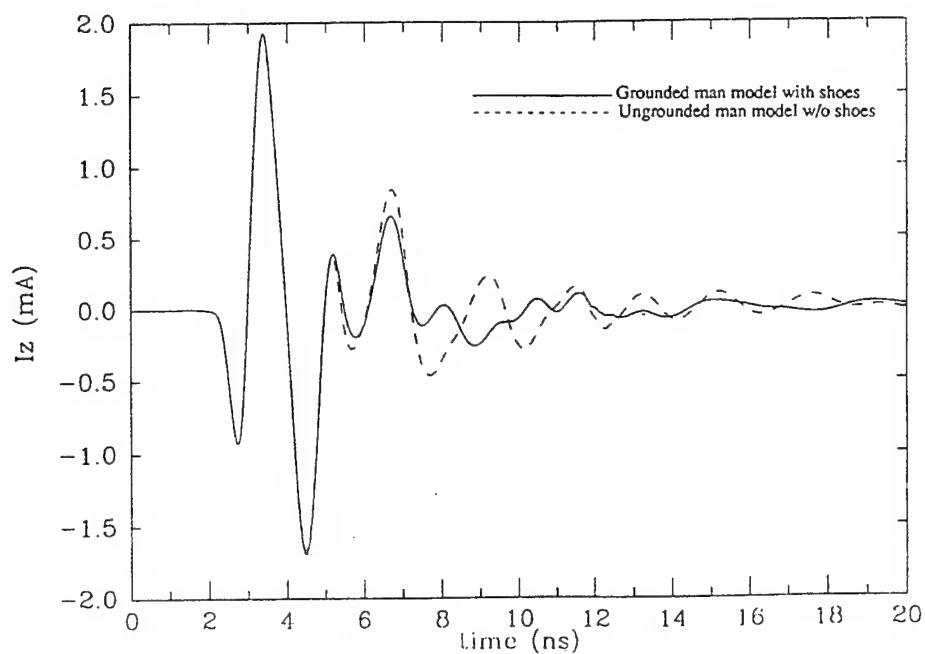


Fig. 5. Currents induced for a representative UWB pulse with a peak incident amplitude of 1.1 V/m.

c. Current for the section through the knees.



d. Current for the section through the heart.

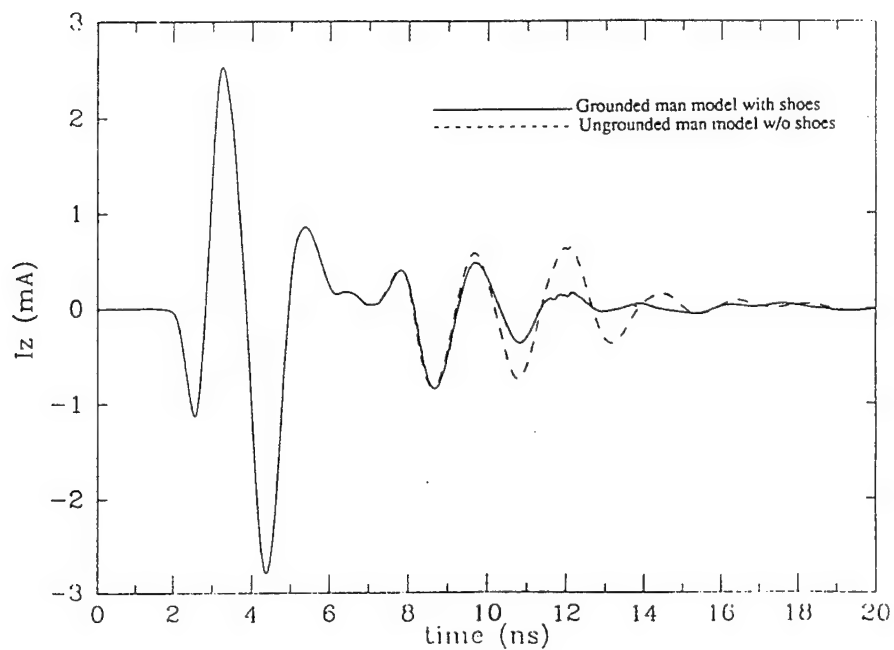


Fig. 5 (continued)



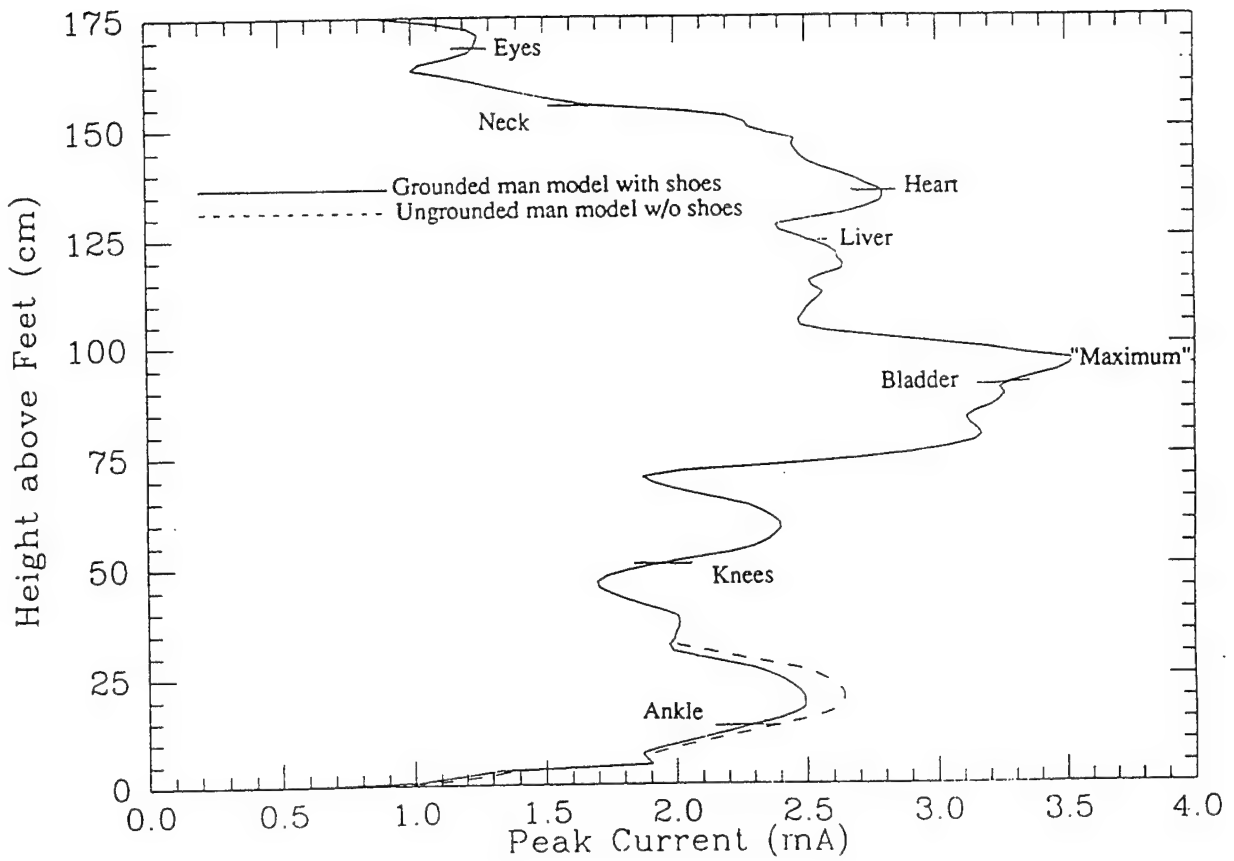


Fig. 6. Peak currents induced for the various sections of the body for shoe-wearing grounded and ungrounded conditions of the model.



## **COMPARISON OF FERROUS AND NON-FERROUS INDUCTIVE PROBES WITH STAND-ON PROBES FOR MEASURING INDUCED CURRENTS**

**John A. Pasour and Mark J. Hagmann\***

**Mission Research Corporation**

**8560 Cinderbed Rd., Newington, VA 22122**

**(703) 339-6500**

### **ABSTRACT**

Mission Research Corporation (MRC) is developing a set of inductive current probes to measure induced body currents and has performed two series of tests at Brooks AFB to test various versions of these probes. The tests were performed at frequencies from 60 to 200 MHz, with both human subjects and simple test objects (metal rods and saline-solution-filled PVC pipe). The performance of the MRC probes was compared with commercial ferrous inductive probes (Eaton and Bergoz), non-ferrous inductive probes from Dr. Mark Hagmann of Florida International University, and with stand-on probes from Holaday and Narda. Both ferrous and non-ferrous MRC probes were tested, in some cases using a specially-designed electronic circuit that is attached directly to the probe to provide a digital readout of the current. The inductive probes generally agreed rather well with each other, but there were large differences with the stand-on probes. The inductive probes as a group were also much less affected by RFI effects than the stand-on probes. We will briefly describe the MRC probes, present the calibration curves that we have obtained in our laboratory, and report the results of the Brooks tests.

\* Permanent Address: Dept. of Electrical and Computer Engineering, Florida International University, University Park, Miami, FL 33199

# COMPARISON OF FERROUS AND NON-FERROUS INDUCTIVE PROBES WITH STAND-ON PROBES FOR MEASURING INDUCED CURRENTS

John A. Pasour and Mark J. Hagmann

## SUMMARY

We have performed induced current measurements in an anechoic chamber at Brooks AFB. The general configuration used throughout these tests is shown schematically in Fig. 1. An RF amplifier was used to drive a dipole antenna mounted in front of a corner reflector. A human subject or a test object, either a 180-cm-long  $\times$  7.5-cm-diameter saline-filled PVC pipe or a 120-cm-long  $\times$  2.2-cm-diam. steel rod, (each oriented vertically) was placed  $\sim$ 3 meters from the apex of the corner reflector. Measurements were made either on a 4  $\times$  8 foot ground plane, on a 4  $\times$  8 foot sheet of plywood with no ground plane, or directly on the chamber floor. Various current probes, including stand-on or platform types (Narda 8850 and Holaday 3701), ferrous inductive probes (Eaton 94606 and two MRC prototypes), and non-ferrous inductive probes (FIU and MRC), were used in various combinations to measure the current induced in the test objects. The incident and reflected power were measured using a Bird power meter placed in the coaxial line between the amplifier and antenna. The power density in the chamber was measured with no test object in place using Narda RF field probes (both electric and magnetic field sensors were employed). All of the measurements were made using a CW input signal, which was typically switched on for  $\sim$ 10 seconds while readings were made. The current transformer probes were monitored directly on a calibrated oscilloscope, via shielded coaxial cables.

The MRC probes used in these tests are all wound in a similar fashion, illustrated in Fig. 2, but the cores and shields vary. The basic winding is split into two halves, joined at the output connector, which is located near the center of the open probe (at the hinge when a rigid shield is used). Resistive shunt loading, a terminating resistor, and, in some cases, a shunt capacitor are used to provide flat frequency response. Only a few turns (4 to 8) are used on each half of the probe. Typical calibration curves for a ferrous (3.5-inch opening) and non-ferrous (5-inch opening) version of the probe are also shown in Fig. 2.

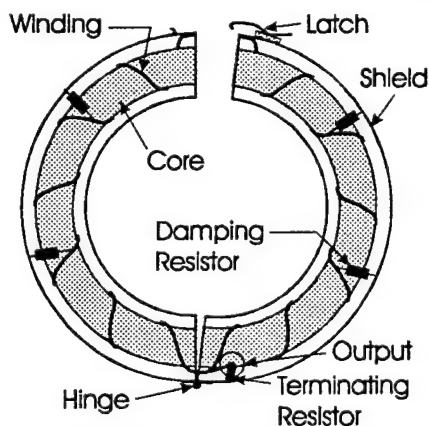


Figure 2. Schematic diagram of MRC probe and frequency response of two versions.

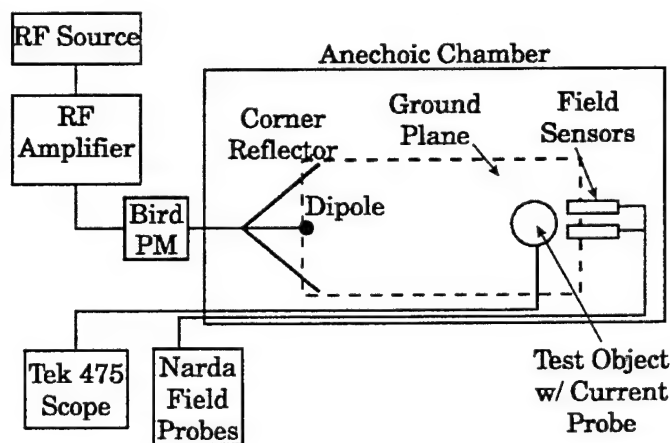
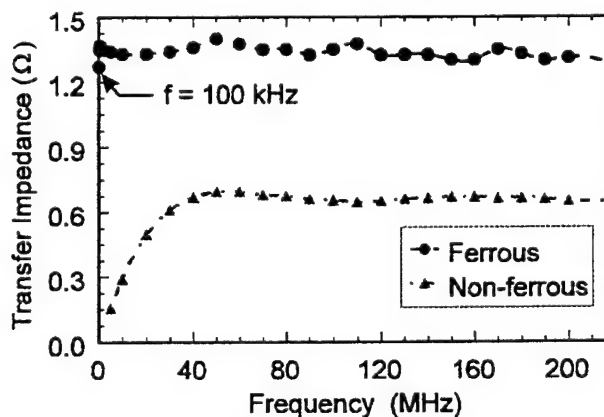


Figure 1. Configuration used for tests.



Typical responses of the various probes are shown in Figs. 3 and 4. The data points are all normalized to an incident electric field of 61 V/m (corresponding to a far-field power density of 1 mW/cm<sup>2</sup>), although the actual field was lower by a factor of 2 to 5. Also, the data points have been slightly shifted horizontally to avoid overlap. All measurements were made at 60, 100, 150, or 200 MHz. The plotted values in Fig. 4 are the RMS, single-leg currents, so the actual platform probe readings have been divided by two. The Narda probe was not used with the inanimate test objects because of its design (foot pads separated by the meter electronics), but the Holaday probe was. Its readings at 60 MHz were 2.9 times larger than the inductive probes, with both the metal rod and the saline-filled tube. At 100 MHz, the Holaday probe readings were 6.5 times larger with the metal rod and 4.3 times larger with the saline-filled tube.

The error bars arise from several sources. The MRC and Eaton data points represent an average of multiple probes. Two Eaton probes of the same model were used along with three different types of MRC probes (two ferrous and one non-ferrous). Because there were few discernable systematic differences in the response of these probes, they are plotted as a single data point. However, this does result in larger error bars than if individual probe data are plotted. The repeatability for any individual probe was very good (<5% variation) if exactly the same conditions were repeated. However, small changes in orientation could produce larger variations. With the inductive probes, a variation of ~10% was found as the positioning (e.g., centering) of the probe on the leg was varied. The response of both platform probes was quite dependent on their orientation relative to the antenna, and the error bars shown are dominated by this effect. The Narda probe was also quite sensitive to loading symmetry (i.e., if one foot was lifted off the probe, the reading would be much different than if the other were lifted off). This effect is not shown in the graphed measurements, which were made with both feet on the probe.

The probes were checked for RFI in the absence of a test object by placing them either directly on the ground plane or suspended 5–10 cm above it, essentially in the

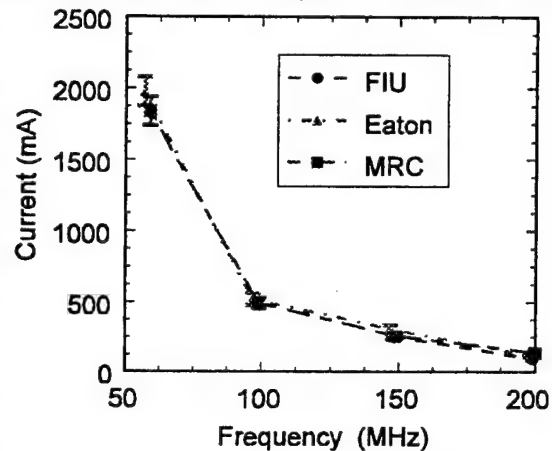


Figure 3. Current induced in metal rod.

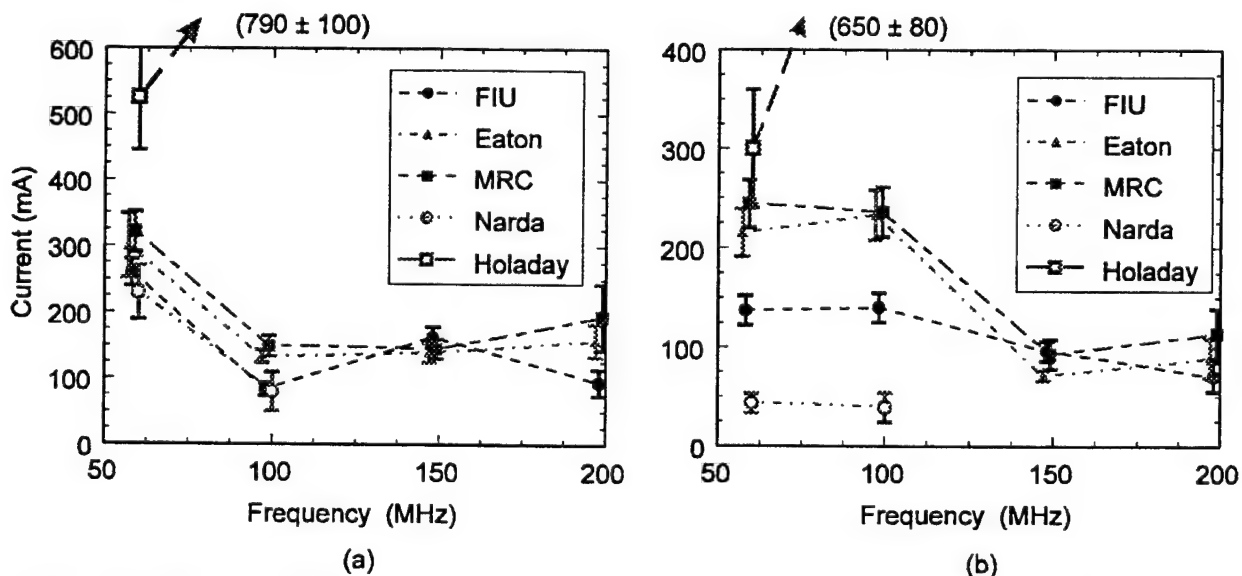


Figure 4. Single-leg RMS current measurements of human subject, normalized to 61 V/m. (a) With ground plane. (b) Without ground plane (directly on floor of chamber).

same position they occupied in normal tests. These null results, again normalized to an incident field of 61 V/m, are shown in Fig. 5. The null response of the inductive probes was typically  $\leq 10\%$  of their reading when placed on a human subject. The stand-on probes were much more susceptible to RFI, presumably because of their capacitive nature (essentially parallel plate). The Narda probe was less susceptible to RFI than the Holaday probe so long as a ground plane (GP) was used. However, with no ground plane, its response with a test object was a factor of 5–10 lower than that of the other probes, and at 100 MHz its RFI response was very large (50–200% of the reading with a human). The Holaday probe gave much higher readings than the other probes; but subtracting the large RFI signal from the measurement (as has sometimes been done by other researchers) also was not feasible, because the response was sometimes larger with no test object than with one.

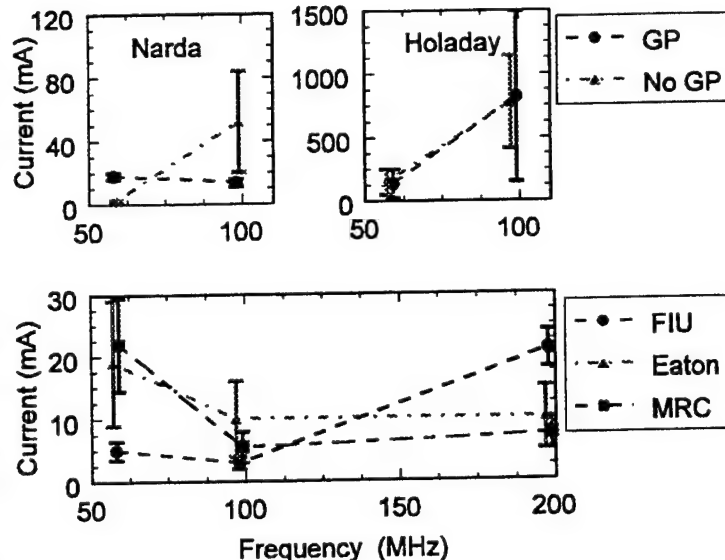


Figure 5. Null probe readings in a 61 V/m field.

Measurements were also made to look for perturbations caused by the various probes. No significant difference ( $<5\%$ ) was observed in the platform probe readings when an inductive probe was placed around one or both ankles. When the inductive probe was connected to a grounded-shield cable, the platform probe reading was reduced slightly ( $\leq 10\%$ ). Similarly, when two or more inductive probes were placed around the same leg and each connected to cables, the reading of the lower probe decreased by about 10–25%. This reduction was not observed unless the upper probe was connected to a cable, and no difference could be observed in the effects of ferrous versus non-ferrous probes. At 100 MHz, the inductive probes typically read lower by  $\sim 10$ –20% when the subject was standing on the platform probes than when he was standing directly on the floor. This effect was not observed at 60 MHz.

In summary, we found that the various inductive probes were in relatively good agreement. The disagreements that were observed were probably due to several factors, including phase variations from one probe to another relative to the induced cable signal, different calibration techniques, etc. There were no systematic differences in ferrous vs. non-ferrous probes, but ferrous probes obviously have an advantage at low frequencies ( $\leq 10$  MHz). The platform probes behaved better at lower frequencies, but they were completely unusable much above 100 MHz. Even at 100 MHz, which is within the specified operating range of each probe, serious problems were identified. The inductive probes seemed to work well even at the highest frequency tested, 200 MHz, but there will clearly be limits to their use at even higher frequencies. First, transit time effects become pronounced when the signal transit time in the winding is comparable to the RF period, making the probes sensitive to the position of the current-carrying member. Also, the inductive probes respond to the displacement current of the incident RF field, which is proportional to frequency. Both these effects tend to limit the diameter of inductive probes that can be used at frequencies much higher than used in these tests, at least so long as operation is required over a broad range of frequencies.

This work was supported by Brooks AFB under an SBIR Phase II contract (No. F41624-92-C-9005). The authors thank Mr. William Hurt of Brooks AFB for coordinating the tests and Capt. Sherrie Sorensen and her engineering staff for their superb technical support during the tests.

## SAR MEASUREMENTS IN THE FIELD AND PRACTICAL CONSTRAINTS

Richard G. Olsen

### ABSTRACT

Since the promulgation of ANSI C95.1-1982, the need for on-site SAR measurements has continued to grow. Real-world exposure conditions such as on towers or aboard ships cannot be adequately modeled for the theoretical prediction of average or localized SAR in workers; therefore, simple reliance on tabulated permissible exposure limits (PELs) is improper. In 1983, personnel from the Naval Aerospace Medical Research Laboratory began using a full-size, sewn-bag human model to assess both localized and whole-body SAR in Navy workers at many locations including the topside decks of ships and various industrial irradiation locations. The results of these SAR measurements have provided much insight into the nature of real-world occupational RFR exposure and have provided the Navy with data to support a realistic basis for worker protection consistent with mission accomplishment. Field-usable SAR assessment tools remain at a low stage of development, but they show promise for further refinement as interest in this technology grows.

## SAR MEASUREMENTS IN THE FIELD AND PRACTICAL CONSTRAINTS

Richard G. Olsen

### INTRODUCTION AND HISTORY

Specific Absorption Rate (SAR), as a metric in bioelectromagnetics, has been used for only about twenty years; before that, some investigators attempted to describe the radiofrequency energy deposited in various biological systems as a "dosing rate" or "absorbed power density," etc. Other investigators simply ignored the need to assess internal fields and reported fields in the surrounding region. In 1975, after an open and thorough discussion of the needs of the researchers and others, SAR became an accepted (even required) quantity in the description of irradiation experiments in bioelectromagnetics.

Unfortunately, the determination of SAR cannot be made with simple hand-held probes that are routinely used to measure E-fields and H-fields. As the rate of in-tissue energy deposition, SAR must be calculated from internal radiometric or thermometric measurements. The physical difficulty of embedding miniature field probes or thermal probes into biological preparations has given rise to extensive theoretical analyses of a large number of standard irradiation configurations for dose determination. Sadly, the simplifying assumptions that were, many times, required in the rigorous application of mathematics produced results of marginal usefulness when applied to real-world irradiation situations. Theoretical predictions and/or handbook values of SAR were, in general, a good starting point, but nearly every researcher pursued some sort of actual SAR measurements before concluding a given study.

In 1982, SAR became the criterion on which ANSI C95.1-1982 was based. Maximum local and whole-body average SARs were specified, and questions immediately arose regarding workplace SAR for many common jobs such as RF heat sealer operators, radio station and tower workers, and topside shipboard workers. The frequency spectrum causing concern was not the microwave spectrum as in past years but the spectrum of the "Gandhi gully" (3-300 MHz), a prominent feature of the 1982 standard that accounted for human resonance absorption. In most instances, no demonstrable harm to workers was evident, but locally high field intensities could be measured at some locations near the workers. Strict comparison to (theoretically derived) permissible exposure limits (PELs) raised a red flag to survey personnel and/or industrial hygienists; therefore, many workplace locations were erroneously branded as hazardous. During the next few years, when the "hazardous" situations were investigated, it was usually found that strict comparison to published PELs was not valid since the PELs came from the assumption of worst-case, far-field irradiation. But the actual workplace situation was typically a near-field, highly non-uniform irradiation zone and much



different than worst-case conditions. Considerable confusion usually occurred at this point for many occupational situations.

In the Navy, much topside shipboard space was marked as restricted, even some locations that were required to be occupied during operations. Relief was needed from the overly restrictive application of the PELs. Fortunately, the ANSI guideline contained an exclusion to allow field intensities to exceed the PELs provided that SAR measurements showed compliance with the criterion. On-site SAR measurements, however crude and/or approximate, were needed to ease topside deck restrictions on Navy ships.

#### DEVELOPMENT OF FIELD-USABLE SAR MEASUREMENT TOOLS

Two large problems loomed ahead. What to measure SAR with, and what to measure SAR in. Both localized and whole-body SARs were needed for a typical worker on the job. Measurement technology needed to be taken from the laboratory to a variety sites, some outdoors.

Localized SAR. Fortunately, the Vitek thermal probe was available but was limited as a "single-channel" instrument; furthermore, it turned out to be highly insensitive at chilly outdoor temperatures near or below 10° C. The first models of the Luxtron fluoro optic thermal probe were also single-channel and drifted wildly over time.

A full-size human model, encased in a heavy foam mold, had been produced at the Naval Aerospace Medical Research Laboratory (NAMRL) for laboratory use in microwave dosimetry studies. It was not portable but had been successfully used to produce consistent SAR results for several years. One day, I was admiring the strength of a multi-layer plastic bag in which some heavy material had just been delivered; the idea struck me that a bag of similarly constructed plastic might be strong enough to hold 70 kg of muscle-equivalent material in the form of an adult human. After much trial and error, a highly practical irradiation model evolved. The green-bag model was first presented as a dosimetric tool at the 1985 BEMS meeting in Atlanta. It has since seen use aboard many Navy ships and several shore stations on two continents.

About this time, the Vitek thermal probe disappeared from the commercial market. The high-resistance, carbon-teflon technology was sold to a medical electronics firm who incorporated the non-perturbing thermal sensors into a hyperthermic cancer treatment irradiation system. Probe tips would continue to be available from the new owners of the technology, but no more "Vitek" boxes would be built.

Better Luxtron probes were beginning to emerge and were multichannel devices. Luxtron sensors, however, were very fragile, and the heavy electronic systems were definitely designed for laboratory rather than field use. I contacted Dr. Ron Bowman, the original maker of Vitek instrument, and asked about the possibility of resurrecting the simple, non-perturbing probe of the past. He told me that recent progress in single-chip, high-impedance voltmeter technology had produced a highly stable circuit that could work easily and simply with the high-resistance elements of the his former thermal probe. He assisted me in locating all of the necessary components, and in 1988 we were able to construct a battery-operated prototype device. Using the recently perfected full-size human model exposed to near-field irradiation, we conducted a side-by-side dosimetric comparison between the new probe and an aging Vitek probe aboard a Navy aircraft carrier. The results showed the prototype to be much more sensitive than the Vitek, especially below 20° C. The reason for the prototype's increased sensitivity at cool temperatures was error the Vitek's internal linearization circuitry. High-resistance thermistors have a steeper characteristic for cooler temperatures and should show a higher resolution. The Vitek's internal circuitry tended to over-compensate for this effect; whereas, the prototype device took advantage of the effect and could reliably resolve thermal differences of as little as 0.021° C below 20° C. In 1989, Dr. Bowman and I published the SAR comparison results in BIOELECTROMAGNETICS and included most of the construction details concerning the prototype thermometer.

Whole-body SAR. For the field measurement of average whole-body SAR, coffin-sized gradient-layer calorimeters were configured inside a transportable enclosure. Two full-sized human models were then thermally equilibrated inside the calorimeters. Thereafter, the models were removed, one was irradiated while the other remained nearby, and then both were returned to the calorimeters as quickly as possible. This system became the basis for a Navy patent (U. S. Patent No. 4,813,789) in 1989. With it, we have measured SAR aboard two classes of Navy ships and at Kirtland Air Force Base, but the system remains sufficiently labor intensive to preclude it's widespread use or commercial production.

#### PRACTICAL CONSTRAINTS

Compared to sophisticated, multi-tissue, bone-containing laboratory models, the sewn-bag, muscle-equivalent "green man" is rather crude. Fine structure such as feet and hands have not yet been added. Procedures involving the phantoms are arduous and require a crew of several strong individuals. Outdoor measurements cannot be conducted in bad or very cold weather. The technology is, however, available for further development. If interest in on-site SAR measurement continues to increase, future refinements will naturally occur.

14. Olsen, R.G.; Griner, T.A.; Van Matre, B.J.: Measurement of RF Current and Localized SAR Near a Shipboard RF Heat Sealer. In: The First World Congress for Electricity and Magnetism in Biology and Medicine, June 14-19, 1992, paper P-303, page 151, Lake Buena Vista, FL (1992).
15. Joyner, K.H.: Measurement of Induced Current Flows in the Ankles of Humans Exposed to Radiofrequency Fields, Report #8000. Telecom Research Laboratories, Australian Telecommunications Corporation, Clayton, Victoria, Australia (1991).
16. Allen, S.G.; Blackwell, R.P.; Chadwick, P.J.; Dimbylow, P.J.; Unsworth, C.: Body Currents from HF/VHF Antennas and RF Heat Sealers. In: Bioelectromagnetics Twelfth Annual Meeting, June 10-14, 1990, paper P-9, page 78, San Antonio, TX (1990).
17. Ruggera, P.S.; Schaubert, D.H.: Concepts and Approaches for Minimizing Excessive Exposure to Electromagnetic Radiation for RF Sealers. Rockville, MD: Food and Drug Administration. DHHS Publication No. (FDA) 82-8192 (1982).
18. Grajewski, B.; Cox, C.; Schrader, S.M.; Murray, W.E.; Edwards, R.M.; Turner, T.W.; Smith, J.M.; Shekar, S.S.; Evenson, D.P.; Simon, S.D.; Conover, D.L.: Semen Quality Study of Radiofrequency Heat Sealer Operators. National Institute for Occupational Safety and Health, Division of Biomedical and Behavioral Science, Cincinnati, Ohio, Final Report (1991).
19. Conover, D.L.; Edwards, R.M.; Shaw, P.B.; Snyder, D.L.; Lotz, W.G.: The Effect of Operator Hand Position and Workstation Furniture on Foot Current for Radio Frequency Heater Operators. Appl. Occup. Environ. Hyg. 9(4):256-261 (1994).
20. Conover, D.L.; Murray, W.E.; Edwards, R.M.; Werren, D.M.: The Effects of Operator Posture and Workplace Variables on Foot Current for RF Heater Operators. In: Bioelectromagnetics Twelfth Annual Meeting, June 10-14, 1990, paper C-1-6, page 32, San Antonio, TX (1990).
21. Gandhi, O.P.: RF Currents and SARs in an Anatomically-Based Model of Man for Leakage Fields of a Parallel-Plate Dielectric Heater, Final Report. National Institute for Occupational Safety and Health, Division of Biomedical and Behavioral Science, Physical Agents Effects Branch, Cincinnati, Ohio, 38 pages (1988).
22. Gandhi, O.P.; Chen, J.Y.: SAR and Induced Current Distributions for Operator Exposure to RF Dielectric Sealers, Final Report. National Institute for Occupational Safety and Health, Division of Biomedical and Behavioral Science, Physical Agents Effects Branch, Cincinnati, Ohio, 51 pages (1989).

# brooks4.ms



# Automated Dosimetric Scanning System for Mobile Communications

Klaus Meier and Niels Kuster

Swiss Federal Institute of Technology (ETH), CH-8092 Zurich, Switzerland

**Abstract** - In this paper a newly developed, robot-based system is presented which allows automated E-field scanning in tissue simulating solutions. The distinguishing characteristics of the system are its high sensitivity and its broad dynamic range ( $1 \mu\text{W/g}$  to  $100 \text{ mW/g}$ ) over the entire frequency range (10 MHz to over 3 GHz) used for mobile communications. The reproducibility of the dosimetric evaluations has been shown to be considerably better than  $\pm 5\%$ . This has been accomplished by the use of an improved isotropic E-field probe connected to amplifiers with extremely low noise and drift characteristics in conjunction with digital processing of the data. Special emphasis has been placed on system reliability, user-friendliness and graphical visualization of the data, as well as on its applicability for compliance tests with current safety limits. The suitability of the simple phantom which was used to simulate the human body, as well as results from tests on various commercially available cellular telephones are briefly discussed here.

## Introduction

The basic restrictions stipulated by current EMF safety standards are defined in terms of the maximally tolerable absorbed power per unit tissue mass ( $\text{mW/g}$ ), known as the Specific Absorption Rate (SAR). The spatial peak SAR is limited to  $2 \text{ mW/g}$  averaged over 10g tissue (CENELEC [1]),  $1.6 \text{ mW/g}$  averaged over 1g, respectively (ANSI/IEEE [2]).

Maximally permissible exposure (MPE) values were derived in order to obtain an easy to measure reference for the maximally induced field strength. However, the MPE values strongly over-estimate the exposure in the nearfield which leads to violations by most transmitters.

Exclusion clauses for particular devices are questionable since they should ensure full compliance with the basic restrictions even when the devices are being used under the worst possible operational conditions. In order to gain public confidence all operating conditions must be considered. However, such an exclusion clause covering "worst case" conditions would be too restrictive, i.e., would forestall technology development. Type approval by dosimetric tests, as recommended by the German Agency for Radiation Protection [3] and FCC [4] seems to be the most suitable approach for industry as well as for the public interest.

Because of possible far-reaching economic consequences, the testing procedure must meet the highest possible standards regarding accuracy, reproducibility, standardization and availability during the design process of new devices.

A critical issue is the position of the device being tested. In case compliance must be demonstrated for the use of the device under all operational conditions [3], it is not sufficient to test the device by measurement or computation in one particular position, but the "worst case" situation must be determined from among a great variety of parameters such as the position of the device, use by left or right handers, variations of head shape and the position of the hand holding the device.

Several groups have begun to develop computer simulation techniques for compliance tests. This approach was chosen because the inhomogeneities of the head were seen as the crucial factors for absorption. However, the studies [5], [6] suggested that the design of the radios (antenna, packaging, front end) have a stronger impact than anatomical properties. Based on these results an experimental approach was chosen, which should enable simpler, more cost-effective and reliable compliance tests than from numerical techniques. In addition, this approach allows the testing of randomly selected samples of a product, which is often required for compliance tests.

## Dosimetric Assessment System

As it is well known, SAR can be determined by measuring either the electric field ( $E$ ) or the temperature rise ( $\partial T/\partial t$ ) inside the exposed tissue. One of the major difficulties encountered in dosimetric compliance tests by measurement is that at best weak a priori predictions can be made about the site of maximum

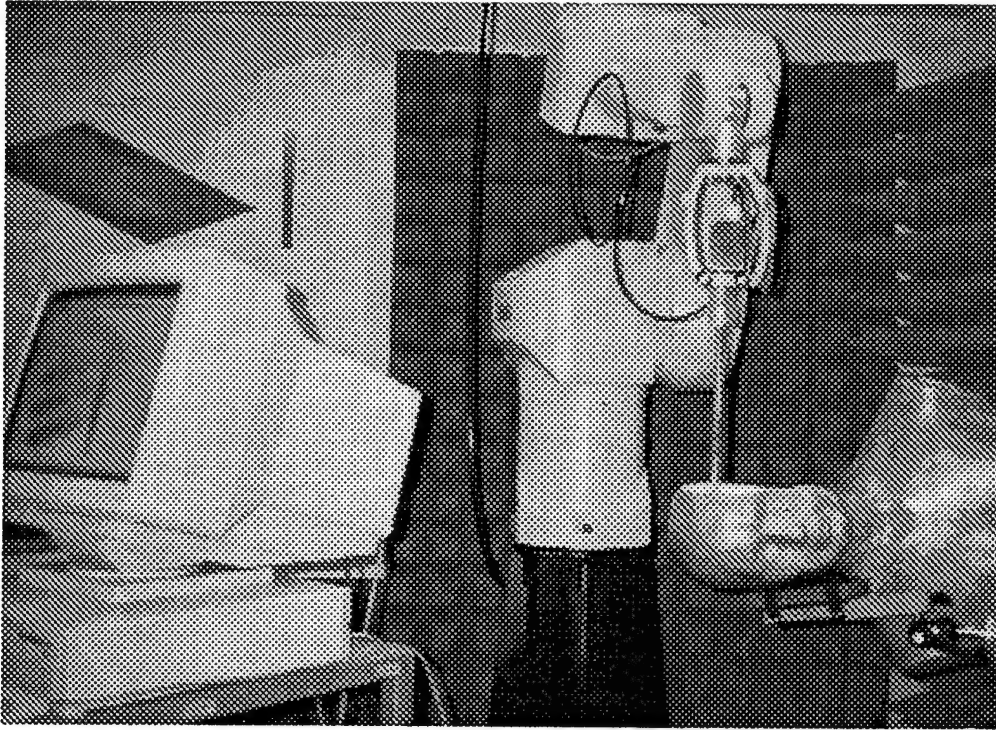


Figure 1: Laboratory set-up including robot, probe, data acquisition electronics, phantom and PC.

absorption for a given device. Furthermore, the higher the frequency, the more localized this maxima is. In order to nonetheless reliably determine the maxima, measurements must be carried out within a relatively large body volume on a fine three-dimensional lattice. In practice, this makes it necessary to work with shell models filled with tissue-simulating liquids. Thus the inhomogeneous human body has to be approximated by a largely homogeneous phantom. How this affects the spatial peak SAR values will be discussed below.

In the setup shown in Figure 1, the SAR distribution is determined by measuring the electric field with miniaturized E-Field probes. Measuring the temperature rise in the simulated tissue does not provide sufficient sensitivity for compliance testing of consumer products nor is it sufficiently time-efficient. However, this technique is used for the validation of the system as well as for the calibration of the probes. The developed system, which is described in detail in [7], includes the following components.

- The measurement procedure is based on a newly developed, isotropic nearfield-probe. The sensitivity, bandwidth, and immunity to disturbances of which could be considerably improved compared to known designs. The bandwidth ranges from 10 MHz to at least 3 GHz, the sensitivity is better than  $1 \mu\text{W/g}$  and the overall diameter of the probe (casing included) is only 8 mm (length of the dipole is 3 mm). The dynamic range covers values up to 100 mW/g.
- These improved probe characteristics (total internal resistance of the probe: 5 – 8 M $\Omega$ ) were obtained at the expense of increased demands on the signal amplifier and the data processing. Extremely low noise and low drift differential amplifiers were necessary. Approximately 2600 complete field measurements per second are transmitted by an optical link to a PC for data processing. The antenna inputs are frequently short circuited with pulse relays to compensate for voltage offsets. For measurements in very low and sub- $\mu\text{W}$ -range current drifts can be compensated as well. All the electronic hardware (including batteries) is housed in a small box (68 x 57 x 46 mm<sup>3</sup>) and is software-controlled.
- The probe is equipped with an integrated, non-metallic optical sensor. This sensor was developed so that the probe's position relative to any surface is automatically determined ( $\pm 0.2\text{mm}$ ), instead of having to provide the system with information on the geometry of the surface beforehand. This simplifies measurements and shortens preparation and measurement times.



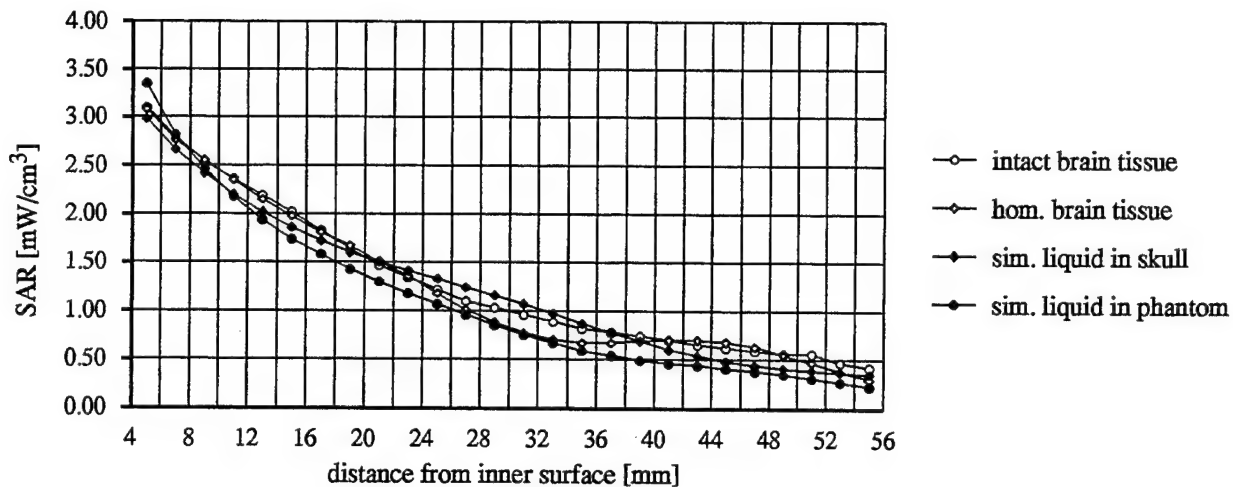


Figure 2: Difference between inhomogeneous real brain, homogenized real brain and simulating solution on the absorption mechanism. Input power of the dipole antenna was 1 W and the frequency 900 MHz.

- A 6-axis precision robot (Stäubli RX90) is used to automatically position the probe along a spatial measurement lattice within the shell phantom.
- The measurement is entirely controlled by the PC: 1.) control of robot; 2.) evaluation of surface sensor; 3.) control and monitoring of the measurement electronics (error detection); 4.) digital filtering of highly noisy signals; 5.) evaluation and data visualization.

The dynamic range, frequency range and isotropy relative to the probe axis were determined using a TEM cell (ifi, CC110), while isotropy relative to the probe plane was measured in the liquid. The conversion factor between air and tissue-simulating liquids was assessed by comparing computed and measured data.

### Measurement Strategies

For compliance tests the following test strategies have been implemented: Firstly, measurements are taken in a coarse-mesh lattice which covers the entire device. More detailed measurements are then made, using a finer, cube-like lattice (with 175 lattice sites). This cube-like lattice is located so as to enclose the maxima obtained from the previous measurement. The SAR values for given tissue masses (e.g. 10g and 1g) are now calculated by means of three-dimensional polynomial integration, using these more detailed measurements.

The German Radiation Protection Agency requires that safety limits must be met under all possible operational conditions [3]. Since the absorption strongly depends on the position of the mobile device in respect to the head, a "worst case" must be found for each model. The number of measurements which are necessary to find such a "worst case" exposure can be greatly reduced by measurements on a flat phantom which provides valuable information on the distribution of HF-current on the device, which in turn determines the SAR (see [5]). Thus, the "worst case" exposition can be found with a small number of measurements.

### Validation

The whole measurement procedure has been extensively validated. The E-field measurements have been compared to computer simulations and to the SAR values found by measuring the increase in liquid temperature at particular points at high power levels. A large number of temperature measurements were carried out for two simulating solutions. The frequency was varied as was the distance of the dipole from the surface of the phantom. An agreement between the electric field measurements, the temperature measurements and the computer simulations of  $< \pm 20\%$  is decisively better than error estimations had let us to expect.

### Homogeneous versus Inhomogeneous Shell Phantoms

The degree to which this approach is suited in assessing the real absorption in a human head has been repeatedly called into question, since neither the complex structure of the skull, nor the inhomogeneity of the skull, nor the hand holding the device were simulated. Therefore, the approach was experimentally verified, although the theoretical studies [5] have already shown that the absorption mechanism in water based tissue is very similar and differences caused by inhomogeneities become negligible in comparison to other factors such as the position of the radiating structure or the construction of the device.

A dry human skull was first filled with inhomogeneous bovine brain tissue, then with homogenized brain and in a third measurement with a tissue simulating liquid. Finally, using a similar setup, the fiber-glass shell-phantom was used. The different phantoms were exposed to a dipole in the typical "worst case" position, i.e., the dipole feedpoint was placed directly above the ear. The resulting SAR-values showed a considerable degree of correspondence (Figure 2). The differences between the measurements were well within  $\pm 10\%$ . These results confirm that under "worst case" circumstances neither the complex anatomical structure of the head nor the inhomogeneity of the interior of the head have any significant impact on the absorption. In a further experiment the influence of the hand was studied. Various models of cellular telephones were used. The hand holding the device was at different locations on the device and the maximal, spatial SAR was measured using the measurement strategies which were mentioned above. The results showed that the difference between a handheld and a free standing device is between  $+1\%$  und  $-15\%$  ( $f = 900\text{MHz}$ ).

### Measurement Results on Various Cellular Telephones

Several different cellular phones from various manufacturers were dosimetrically characterized (transmitting frequency band: 890 - 915 MHz, normalized to an output power of one Watt).

During an initial series of tests, the phones were held in the "standard position", i.e. with earpiece on ear, body of phone on cheek and microphone near mouth. In this position the antenna protrudes out behind the ear and has about the greatest possible distance from the surface of the head.

In everyday use, however, a phone can be held in various ways. This leads to the initially mentioned "worst case" question. It is necessary to examine the extent to which the "worst case" load depends on the position of the device relative to the head. An attempt was made to determine the "worst case" under operational conditions using information that was obtained from previous measurements (with the plane phantoms). This "worst case" was mostly found to occur when the transmitting structure, at the location of the highest HF-currents, touched the head. Actual "touching" was prevented by using a 3 mm thick spacer made of styrofoam. The measurement results are summarized in Figure 3.

### Conclusions

The developed measurement system is a flexible, automated, time-efficient tool to assess SAR distributions in tissue simulating solutions. It is especially suited for compliance testing of handheld or body mounted devices with specific safety standards. Tests have shown an excellent reproducibility of the integrated peak SAR values of well within  $\pm 5\%$  even when changing the initial coarse grid. The specifications can be summarized as follows:

sensitivity in air:	1 V/m to 900 V/m
sensitivity in tissue simulating solutions:	1 $\mu\text{W/g}$ to 100 mW/g
linearity:	$< \pm 0.2 \text{ dB}$
deviation from isotropy in tissue:	$< \pm 0.3 \text{ dB}$ normal to probe axis $< \pm 0.8 \text{ dB}$ in all planes, all polarisations (10 MHz to $> 2.5 \text{ GHz}$ , triangular probe)
variation with frequency:	$< \pm 0.2 \text{ dB}^a$ (10 MHz to $> 2.5 \text{ GHz}$ )
spatial resolution of SAR measurements:	$< 0.125 \text{ cm}^3$
reproducibility of probe positioning:	$< \pm 0.2 \text{ mm}$

<sup>a</sup>value within the specified frequency limits

Although the main emphasis is now on the prevailing phantom issue several improvements are anticipated. E.g., measurements on arbitrary volume grids which are now restricted to "rectangular" grids in



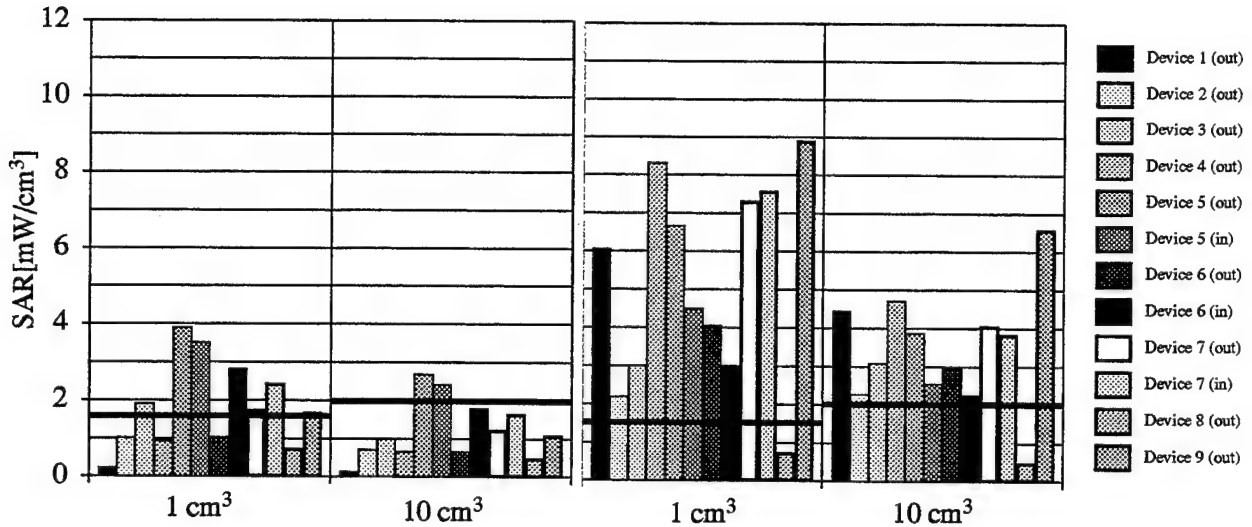


Figure 3: Spatial peak SAR values caused by different mobile phones used in the "standard position" (left) and under "worst case" conditions (right). Measured in anatomically correct shell phantoms filled with a liquids ( $\epsilon_r = 42$ ,  $\sigma = 1.2$  mho/m) simulating brain-like tissue. The black horizontal bars indicate the current maximum limits of ANSI/IEEE (1.6 mW/g) and DIN/VDE (20mW/10g). "in" = retracted antenna; "out" = extended antenna.

the horizontal plane (xy-plane) or the extension of the system for general near field measurements used in antenna design, EMI, EMC.

## References

- [1] CENELEC CLC/SC111B, *Draft European Prestandard (prENV 50166-2, Human Exposure to Electromagnetic Fields High-Frequency : 10 kHz - 300 GHz*. Brussels: CENELEC, 1993. Draft, September, 1994.
- [2] ANSI/IEEE C95.1-1991, *IEEE Standard for Safety Levels with Respect to Human Exposure to Radio Frequency Electromagnetic Fields, 3 kHz to 300 GHz*. Inc., New York, NY 10017: The Institute of Electrical and Electronics Engineers, 1992.
- [3] Strahlenschutzkommission, "Empfehlung der Strahlenschutzkommission verabschiedet auf der 107. Sitzung am 12./13. Dezember 1991," in *Schutz vor elektromagnetischer Strahlung beim Mobilfunk* (SSK, ed.), pp. 3-18, Gustav Fischer Verlag, 1992.
- [4] Federal Communication Commission, "Amendment of the commission's rules to establish new personal communication services," Tech. Rep. FCC 94-144, FCC, Washington, D.C. 20554, 1994.
- [5] N. Kuster and Q. Balzano, "Energy absorption mechanism by biological bodies in the near field of dipole antennas above 300 MHz," *IEEE Transactions Vehicular Technology*, vol. 41, pp. 17-23, Feb. 1992.
- [6] N. Kuster, "Multiple multipole method applied to an exposure safety study," in *ACES Special Issue on Bioelectromagnetic Computations* (A. Fleming and K.H.Joyner, eds.), vol. 7, pp. 43-60, Applied Computational Electromagnetics Society, No. 2, 1992.
- [7] T. Schmid, O. Egger, and N. Kuster, "Automated scanning system for dosimetric assessment," *IEEE Transactions on Microwave Theory and Techniques*, 1995. submitted.



# PRACTICAL ASPECTS OF APPLYING TIME-AVERAGING TO DETERMINATION OF COMPLIANCE WITH RFR EXPOSURE STANDARDS.

Rick Woolnough<sup>1</sup>

## SUMMARY

### *INTRODUCTION*

My name is Rick Woolnough and I am the RADHAZ/Laser Safety Specialist for British Aerospace Defence Ltd. Military Aircraft Division's Warton Unit. In this role I provide a technical consultancy to the Warton Unit Radiation Safety Officer(Non-Ionising) and the Warton Unit Laser Safety Officer who is responsible for the control of non-ionising and laser radiation hazards within the organisation.

This assignment is broken down into a number of smaller sections as shown in Figure 1- "Contents".

### *THE DOSIMETRIC STANDARD*

Traditionally, when carrying out measurements and assessments of RF radiation hazards (RADHAZ) the main emphasis has been to carry out measurements of power with respect to time for a known frequency. This may inadequately deal with frequency variations, which for ultra-wideband signals may have a significant impact upon the maximum permissible exposure (M.P.E.) levels.

What we must always be aware of is that all emitted signals operate in a three dimensional domain and a simple waveform is shown in Figure 2. These domains are: the time domain, the amplitude domain, and the frequency domain. Modern standards operate to cover these 3 domains and an example of this is the IEEE C95.1:1991 standard [1] as summarised in Figure 3.

Therefore as we can see this leads to a number of different levels of assessment which can be made as detailed as necessary to ensure that there is a balance between the costs of the RADHAZ assessment and the limitations to operations. With Ultra-wideband and complex waveforms the spread of the three domains can be quite extensive and therefore difficult to assess.

---

<sup>1</sup> RADHAZ/Laser Safety Specialist, British Aerospace Defence Ltd., Military Aircraft Division, Warton Aerodrome Preston PR4 1AX. Telephone: +44 1772 854590. Facsimile: +44 1772 855227.  
E-mail: rick.woolnough@bae.euromail.com

## ***THEORETICAL ASSESSMENTS***

### ***Introduction***

The traditional method of evaluating exposure conditions is based upon either measuring or calculating the levels of either field strength or power density at a given point. There are a number of significant problems associated with both techniques when carrying out an analysis of modern modulated radio- and radar-frequency waveforms.

Modulations which may be encountered in modern systems include: Intentional modulations e.g. Amplitude, Frequency, Pulse, Pulse Compression, noise and Ultra-wide-band Modulations, and unintentional modulations such as ringing, transmitter frequency pulling and component generated noise. The analysis of the multiplicity of these modulations which can be found in the Military Scenario and typical industrial/airfield environments [2] may not lend itself to traditional measurement techniques.

It is also highly likely that unless a centralised resource for the organisation is used, highly sophisticated analysis techniques and facilities may not be available and therefore a staged approach to evaluation is essential. It is here that a risk assessment should be carried out. The risk assessment should consist of a very simple calculation to establish if the emitter poses a potential hazard and, if it does, a review of how the risk could be reduced or the potential hazard removed. If the installation as proposed (or already located) causes operational limitations it should be further risk assessed to see if the operational limitations are such that further work is required. It may be found that at this stage a more detailed theoretical assessment or practical measurements may remove the limitations or reduce them to an acceptable measure. During this process it should also be discussed whether the further work should be done 'in-house' or by an external consultant or specialist agency.

### ***Methods of Assessment***

The most basic form of theoretical assessment is the simple calculation of far field power density interpolated into a circle which does not take into account pointing angle, as shown in Figure 4. This gives a conservative assessment of the conditions provided that a safety margin to take into account the survey errors, such as those given in the 'Measurement errors' section below, is included in the assessment.

This can be taken further by including near field effects to calculate what would be the maximum excursions of the near-field envelope and to include the fields caused by the maximum sidelobe(s). This assessment may include beam pointing angle and, for rotating sources, may include time averaging due to beam rotation as shown in Figures 5a (which shows a circle due to the worst case sidelobe together with the main beam's -3dB beamwidth points extrapolated to the on boresight gain) and 5b (which shows the main beam and worst sidelobe modelled [in this case the backlobe] and the other sidelobes all contained within a lower magnitude circle defined by the second largest sidelobe level).

Having eventually assessed all of the emitters individually these must be combined to give the survey map. It must be remembered to add the fields from different emitters operating both in-band and out of band (where necessary) as a small field from an emitter may have a significant effect on the hazard distance of another emitter, as shown in Figure 6. This is particularly true where some emitters may have a low M.P.E. or a very short averaging time. It is, however, very difficult to theoretically assess the effect of buildings and ground conditions and it must always be remembered that meteorological effects may be significant.

## ***MEASUREMENT TECHNIQUE PROBLEMS***

Significant errors are possible when carrying out RF measurement surveys. There are a large number of error sources which have to be considered when carrying out a field survey. We shall view these in turn. As an aid we will use Figure 6.

### ***Conditional Effects***

The weather may cause significant errors when carrying out field surveys. Rain will cause attenuation of some frequencies and also may increase perturbations due to buildings and ground effects. Dry weather also has problems associated with it. The main problems being erosion of conservatism. The electrical properties of dry materials is generally significantly different to wet materials and therefore hot spots which could not be measured in the dry may occur. Therefore whilst measurements carried out in the dry are generally most repeatable, it should be remembered when working very close to the M.P.E. that additional 'Hot-Spots' which may cause the M.P.E. to be exceeded may occur. Although exceeding the M.P.E. is moderately unlikely as it is expected that any person over-exposed in such a manner would be in the near-field of the source of perturbation and therefore partial body exposure criteria are likely to apply.

### ***Effects of Buildings***

The effects of buildings when carrying out surveys must be viewed as significant. The most significant problems are posed by metal skinned structures such as aircraft hangars and warehouses. Where these structures are found, corner reflections may give up to 15 dB of gain on the expected signal and field perturbations in the near field of these 'antennas' are significant. It must be considered also that such a corner reflector's near-field equates to  $(2D^2)/\lambda$  where  $D^2$  is either the size of the 'footprint' of the illuminating signal or the size of the edge and sides that are being illuminated. It can therefore be difficult to be out of the near-field when carrying out field surveys close to such buildings.

Edge diffraction can also have a significant effect which is very difficult to predict. The best way to minimise problems caused by this effect is to, where the risk assessment indicates that it is necessary and beneficial to remove such enhancement, fit diffraction gratings as shown in Figure 7 to buildings.

Higher fields than expected may be found inside the buildings due to such things as minimal attenuation in external structure, reflections from internal furniture, internal resonances and window frames acting as re-radiating antennas. It must also be considered whether the building is acting as a screen or if the capacity for onward re-radiation exists.

### ***Mobile Emitters***

Mobile emitters come in many forms, from the cellular phone or hand-held radio to the mobile troposcatter radio or air-traffic-control radar systems. It must be remembered that where these systems may be present the risk assessment, carried out prior to any survey, should take into account any affects that the presence of these emitters may have on the overall survey results.

### ***Topography***

The topographical layout of an area to be surveyed may lead to such things as remote areas having localised high fields and other areas, which may be within areas of high fields, may be screened from those high fields by surrounding terrain. Buildings must be considered closely as people may be working at height within or on top of those buildings.

### ***Time and Frequency Agile systems***

There are problems with the measurement of frequency-agile modulated systems. Where possible a risk assessment should be carried out on the modulation type(s) and the its mode(s) of operation to ensure that measurements are carried out in the worst case features of its modes versus the protection standard against which it is being measured.

## ***INSTRUMENT RELATED PROBLEMS***

### ***Out-of-Band Gain***

A significant problem with a number of the H-Field probes used with broad-band measurement instruments used in RF radiation measurement is that caused by out of band signals. In the simplistic scenario when all of the frequencies are within the bandwidth of the measurement device this is not a problem. However when you have to consider both in band and out of band errors there is the possibility that such out of band signals may cause the test equipment to give significantly different results due to the out of band gain of the fictional test equipment as shown in Figure 8. We can see from this slide that an out of band signal may give an alarm even though we are well below the real M.P.E. Therefore we can see that the user of a wide band of frequencies needs to be aware of the frequency spectrum of his signals.

This problem can be overcome by the use of a spectrum analyser to measure the real power density and frequency. The spectrum analyser is by no means free of significant problems in measurements. These are basically due to receiver and video bandwidth selection and the effect that these have on the response and sample time of the Spectrum Analyser. These errors can be better determined however by changing the receiver and using the widest video bandwidth to determine the shape of modulated signals (although at the risk of reducing the power accuracy and modulation shape at the lower levels due to video noise).

### ***Localised Ground Effects***

When carrying out measurements ground re-reflections of the field may give typically up to 4 dB of enhancement, as shown in Dr. D.H. Shinn's paper, therefore it is important to minimise ground effects or ensure that a sufficient number of measurements, preferably taken at a few different frequencies, in either a random or a raster type pattern are taken. A jig for these measurements is shown in Figure 9.

### ***The Use of Radiation Absorbent Material (RAM)***

RAM has been traditionally used near to measurement jigs to prevent unwanted reflections from interfering with measurements. Unfortunately the appropriate RAM to use on a field survey may only have a typical return loss of 15dB. When taking measurements near to the RAM significant field effects are found. The worst aspects of these artefacts is that if the RAM is co-mounted with the antenna then those artefacts caused by the RAM will remain with the measurement across the whole physical scan of measurements, only changing with frequency.

## ***THE USE OF SPECTRUM ANALYSERS***

### ***Introduction***

The use of spectrum analysers has briefly been mentioned under the 'Band Gain' part of the previous section. Spectrum analysers can be used to determine the real frequency, time and power domains of the signal as indicated in Figure 2. Modern spectrum analysers can feed measurements straight into a computer data-file although care must be taken when considering when to take the data and the points at which to store the data especially if the source is a scanning source or has any form of frequency agility to upset the antenna performance. The mode of operation of the system must also be assessed as included in the above section.

### ***Methods of Using the Data***

Measurements carried out in the 3 domains may be integrated and compared with the 3 domains of the appropriate standard. A significant advantage of using the system in this manner is that measurement errors associated with the operation of the spectrum analyser can be numerically catered for.

A highly sophisticated assessment may involve the following components:

1. Taking measurements to initially characterise the modulated waveform.
2. Using a characterisation jig as shown in Figure 9 to determine the sum of the errors due to such error sources as ground enhancements and ripple from buildings etc.
3. For a scanning system, making rapid data samples to characterise the polar diagram
4. Making a 'peak-hold' measurement to determine the maximum powers across the emitted frequency band. (The optimum place for taking this measurement will be the position indicated by the characterisation in 2 above).
5. Modify the output of 4 above using the real output waveform determined in 1 above.
6. Numerically adjusting the received polar diagram levels from 3 above, using the modified peak values in 5 above.
7. Compare against the 3 domain version of the relevant exposure standard.

The illustration above would be based upon a high rate of data capture and the value of the output would, like every other set of measurements be determined by the quality and care taken in setting up the measurements.

It is very likely that low order side-lobes would not be accurately measured due to their very rapid excursions but a worst case side lobe level could be determined by taking short duration 'max. hold' measurements whilst the main-beam(s) and higher order side-lobe(s) were not scanning through the measurement point. The time to start and the duration of these short duration measurement could be reasonably easily set up using triggering of the test equipment through a delay line.



## APPLICATION OF TIME-AVERAGING TECHNIQUES TO MULTIPLE WAVE-BAND SCENARIOS ABOVE 15 GHz

This is based upon IEEE C95.1 Standard for Safety Levels with Respect to Human Exposure to Radio Frequency Electromagnetic Fields, 3 kHz and is a guide for summation of multiple emitters where the frequency is above 15 GHz where the time averaging period changes. This is of interest as there is an increasing number of sources in the military and civil scenarios.

When carrying out evaluation of time averaging it can be very difficult to practically control the exposure scenario while ensuring that personnel do not exceed the M.P.E. A simplification of this would be to use an equation to sum the fields. The basis for this is that in this simplistic form it only works if all of the frequencies are on the 15-300 GHz Ramp so that the numbers easily cancel out although it would not be too difficult to convert this principle to cover the other frequencies where surface heat deposition may be additive with the 15 to 300 GHz region.

When using a reduced exposure time to constrain the time-averaged dose as a method of achieving higher field strengths without exceeding the M.P.E. the following is used to determine the maximum field strength which is acceptable:

For a time  $t_1$  which is shorter than the normal averaging time  $t_{mpe}$  the corrected acceptable power level  $P_{corr}$  which is above the acceptable power level yet will not cause over-exposure to the M.P.E. is equal to:

$$P_{corr} = P_{mpe} \times \frac{t_{mpe}}{t_1} \quad [1]$$

From IEEE C95.1:1991 - For a frequency  $f_a$

$$AveragingTime(t_a) = \frac{616000}{f_a^{1.2}} \quad [2]$$

and for a frequency  $f_n$

$$AveragingTime(t_n) = \frac{616000}{f_n^{1.2}} \quad [3]$$

If the highest frequency (and therefore the shortest exposure time) is used to define the averaging time (e.g.  $f_n$  in equation [3] is higher than  $f_a$  in equation [2]), re-arranging equation [1] to incorporate [2] and [3] above to determine the time corrected M.P.E. for  $f_a$  ( $P_{corr}$ ) using  $t_{mpe} = t_a$  and  $t_1 = t_n$  gives:

$$P_{corr} = \frac{P_n \times f_n^{1.2}}{f_a^{1.2}} \quad [4]$$

Using this with a measured power to give a ratio ( $R$ ) of the power over the M.P.E. for the averaging time at the lower frequency (as in Appendix C of IEEE C95.1) gives:



$$R = \frac{\left( \frac{P_{meas_a}}{P_{mpe} \times f_n^{1.2}} \right)}{f_a^{1.2}} \quad [5]$$

which re-arranged gives:

$$R = \frac{P_{meas_a} \times f_a^{1.2}}{P_{mpe} \times f_n^{1.2}} \quad [6]$$

adding other frequencies ('b' and 'c') to solve the sum of the ratios  $R_\Sigma$  and adding the power to M.P.E. ratio for frequency  $f_n$  gives:

$$R_\Sigma = \frac{P_{meas_a}}{P_{mpe}} + \frac{P_{meas_b}^{1.2} \times f_b^{1.2}}{P_{mpe} \times f_n^{1.2}} + \frac{P_{meas_c} \times f_c^{1.2}}{P_{mpe} \times f_n^{1.2}} \quad [7]$$

Which should be  $< 1$  to comply with the standard

Re-arranging this for an M.P.E. evaluation of (where the sum of the powers  $P_\Sigma < P_{mpe}$  (where  $P_{mpe} = 10 \text{ mW.cm}^{-2}$ )) gives:

$$P_\Sigma = \left[ \frac{1}{f_n^{1.2}} \times \left[ (P_{meas_a} \times f_a^{1.2}) + (P_{meas_b} \times f_b^{1.2}) + (P_{meas_c} \times f_c^{1.2}) \right] \right] \quad [8]$$

Therefore if the ratios of powers are known it can be determined what is the maximum power that is acceptable from a multiple frequency or wide-band source. This addition to Appendix C of C95.1 will be offered for discussion at the next meeting of IEEE SCC-28, Sub-Committee 4.

## **RADHAZ MAPS**

For a controlled environment, such as that encountered at British Aerospace's Warton (U.K.) complex - a military/civil airfield with production, test, design and office facilities - the potential benefits of a RADHAZ map are recognised. Field strength contours and hazard distances overlaid on site construction/layout maps aids the assessment of RF hazards to all four susceptible device categories - humans, electro-explosive devices, flammable atmospheres and ground/airborne electrical/electronic equipment. This enables relatively easy determination of potential hazards to new/changed susceptible devices and/or RF transmitters, and the optimal siting of new buildings with regard to existing RF transmitters.

Difficulty still remains in establishing appropriate time averaging constraints for the various emitters to be encountered in our particular environment, to enable a better definition of the multiple emitter and multi-frequency RF environment our products and personnel operate in. Some emitters are rotating systems, others ground mobiles and there are many and varied types of airborne radars and radio systems, extending in frequency from the HF band to well above 10 GHz. A potential new tool in this area is being researched in 1995 - that of RF scenario modelling. Such computer based tools as the Electronic Warfare Environment Simulator (from Data Sciences) are already used to determine power density and pulses per second on an imaginary host aircraft flying through an emitter laden scenario, suitably populated with fairly accurate ground and airborne emitter models - both in terms of RF parametrics and antenna/scan pattern.

It is believed that such tools, which are used to specify EW equipment such as radar warning receivers, may, with little modification, enable the production of RADHAZ maps an order more accurate and easily than by any other current method of RADHAZ assessment.

It is intended that one of the outputs of the research will be a link between the model and the RADHAZ map which will take into account time averaging based upon the far more realistic illumination time computed. The model works simply in that the user specifies a x,y,z for the receptor and can be interrogated vs. time, vs. frequency sub-band, or any combination thereof. This receptor can be stationary, simulating (say) a human on the first floor of a building, or mobile, e.g. aircrew flying past a set of ground transmitters. The model used includes simple weather effects and is now being upgraded to include selected terrain effects. It is likely that other such changes, aimed at increasing the level of environment model fidelity, will follow in the near future. It is probable that, assuming positive research results, the use of such EW system design tools will be of interest to both the RADHAZ and EMC communities.

## **CONCLUSIONS**

1. Theoretical assessments, augmented by appropriate risk vs. hazard assessments often negate the need for RADHAZ measurements where adequate safety margins can be determined.
2. Time averaging can be used to minimise hazard distances without increasing personnel risk of over-exposure. More accurate modelling of antenna beam and lobes minimises the volume of the hazard zone associated with a given emitter, though this is complex in practice.
3. There are many effects that complicate both theoretical assessment and practical measurements. Practical measurements will likely be required for the foreseeable future in such cases where adequate safety margins cannot be ensured.
4. Determination of any out of band signals which can significantly affect isotropic system measurement is required prior to measurements being taken with such a system. A spectrum analyser is the normal instrument for this, though it is recognised that not all may have access to such instruments.
5. Real-time spectrum analyser measurements can enable the determination of the modulation parametrics of radar/radio emitters, thereby allowing adequate assessment of any exposure time averaging needed.
6. Time averaging below 15 GHz is covered in IEEE C95.1 and a method has been proposed for assessing multiple waveband emitters above 15 GHz as an addition to that document, which will be put before IEEE SCC28, SC 4 at their next meeting.
7. Research into the use of EW RF environment models offers great promise in the prediction of multiple band, multiple emitter scenarios of the type most commonly encountered in real life.

## **ACKNOWLEDGEMENTS**

Acknowledgement is given to BAe Defence (Military Aircraft Division) for permission to present, to the USAF for the invitation to attend and to Mike Pywell, the Radiation Safety Officer (Non-Ionising) for input, comment and presenting the paper at short notice.

## **REFERENCES**

1. IEEE C95.1-1991 IEEE Standard for Safety Levels with Respect to Human Exposure to Radio Frequency Electromagnetic Fields, 3 kHz to 300 GHz.
2. Woolnough, R.C.N. and Pywell, M. The Control of Non-Ionising Radiation in an Industrial and Airfield Environment. IEE 9th Int. Conf. on EMC, Univ. of Manchester, U.K. September 1994.

## PROTECTIVE CLOTHING EVALUATIONS

Richard G. Olsen

### ABSTRACT

Protective clothing for occupational RFR exposures is receiving increased interest now that exposure guidelines limit body-to-ground and contact currents. In the past, such clothing was used primarily for microwave exposures where highly conductive suits would serve to reflect beamed microwave energy. New uses include reducing ankle and wrist SAR in workers on metal surfaces such as towers and ship decks at frequencies much lower than microwaves. Recently published results show SAR reduction down to 2 MHz. As RF technology continues to grow in areas such as cellular telephones, computer networks, and military technology, the number of workers and the number of exposure configurations requiring protective clothing will grow.

## PROTECTIVE CLOTHING EVALUATIONS

Richard G. Olsen

### INTRODUCTION AND HISTORY

Microwave-protective suits, of one form or another, have been available for more than 20 years. They were primarily designed to be used as barriers to RFR in the spectrum of about 1 to 10 GHz (wavelengths of 30 cm down to 3 cm). The U. S. Navy approved one such suit for regular Navy issue in the early 1970s. Those early suits were highly conductive and efficiently reflected microwave beams, but they were eventually shown to be flammable by A. W. Guy and C. K. Chou in 1987 when they compared the older suits to a new one designed (by Milliken) to be less flammable. The new suit showed slightly less RFR protection but much less flammability. After 1987, interest in RFR protective suits decreased to the point that the new suit was withdrawn from the market.

About 5 years later, interest in area was re-kindled with the promulgation of C95.1-1991. Limits on body-to-ground currents and contact currents were seen to cause problems with many occupational procedures and situations that had never before been scrutinized in terms of RFR-induced body currents. Surveys of Navy ships found that measurable body-to-ground current could be detected at most topside deck locations within the general vicinity of high-frequency transmitting antennas (nearly everywhere). Other broadcasting facilities were also found to produce body currents.

### RECENT EVALUATIONS

In 1992, researchers at Brooks Air Force Base sponsored a project at the Naval Aerospace Medical Research Laboratory to determine the current availability and effectiveness of microwave protective suits. The only commercially available suit at that time was distributed by Maxwell Safety Products. The fabric looked much like cotton broadcloth and had a very high (megohms) DC conductivity as measured with a simple ohmmeter. Initially, I was not impressed with the appearance of the protective suit, but the first SAR comparison experiments at 2.3 GHz showed good results.

Shortly after the initial 2.3 GHz irradiations, we were asked by Maxwell Safety Products to participate in a Cooperative Research and Development Agreement (CRDA) with them to explore the potential usefulness of the commercially available suit in the high-frequency (HF) and very-high-frequency (VHF) spectra. The CRDA was approved early in 1993, and the work was completed before the end of March and covered the range from 2.0 to 400 MHz with groundplane, near-field exposures of our recently developed full-size human model. Ankle SAR in the model was compared for several configurations of the protective suit. The results of

those HF and VHF experiments were very interesting; they have been published in the June, 1994 issue of Applied Occupational and Environmental Hygiene. They showed that just wearing the coverall portion of the suit caused ankle SAR to increase over the no-suit condition. However, addition of a bootie reduced ankle SAR by a significant factor but did not totally eliminate it.

We explained these results as a "skin-effect" phenomenon in which RF current flow in a conductor occurs predominantly in the periphery of the conductor. This effect is noticeable even at 60 Hz, but is much more dominant in the RF spectrum. In the protective suit irradiation, current flow to the groundplane first increased with the addition of just the coverall portion because the suited human model acted as a bigger "pick-up" antenna and shunted more current to ground through the tissue-equivalent ankles. The large area of capacitive coupling between the body and the suit provided a low-impedance path to the ankles. Ankle SAR, therefore, increased. Adding the booties completed another current path to ground, and by virtue of the "skin-effect," a majority of current was conducted through the fabric rather than the ankle. This effect was observed over the entire spectrum that we studied (2-400 MHz), although body-to-ground current at 2 MHz was relatively low for our irradiation system. These results showed that a protective suit need not be highly conductive (as might be desirable theoretically) to provide useful reductions in SAR and that protection was available at frequencies much lower than microwaves.

Additional microwave tests (1-15 GHz) were conducted in 1993 and typically showed the protective suit to provide 10 to 20 dB reductions in localized SAR for beamed CW irradiation on the frontal body surface. Pulsed microwave tests were also conducted at 1.2 and 5.6 GHz. Results of those tests showed that instantaneous peak power densities of hundreds of watts per square centimeter was required to cause motion-induced surface arcing on the suit.

#### CONDUCTIVE GLOVES AND SOCKS TESTED

In 1991, I was struck with the idea to use conductive gloves rather than rubber gloves to protect from RF burns to the hand. Such burns are not rare in the Navy shipboard occupational environment. We tested this idea on a Navy hydrofoil and found that wearing a stainless steel chain-mail (meat-cutter's) glove prevented a finger burn even though arcing occurred during the intermittent touching of a metal object near the ship's HF fan antenna. Consistent with this idea is the use of conductive socks to reduce ankle SAR for deck-coupled workers in HF fields. We tested this idea at our outdoor groundplane irradiation system at 29.9 MHz. We found that a highly conductive silver-plated nylon "sock" protected the "ankle" of the full-size human model from the normally observed rapid temperature rise. Conductive gloves and socks could serve as protective suits in miniature,

protecting certain body parts such as fingers, wrists, and ankles from SAR-producing current flow or RF shocks and burns. In past years, conductive garments have been produced to protect electronic circuits, to protect recently amputated stumps, but never to protect workers' fingers, wrists, and ankles from RFR currents. Unfortunately, there are presently no suitable conductive fabrics available for making gloves or socks. Even if such fabrics were available, many opinions about worker protection would have to change before conductive gloves and socks could be regularly used.

Aboard Navy ships, for example, no gloves are allowed to be used by topside workers who handle crane-manipulated loads. Any arcing, moreover, would not be allowed under present policy even if it produced no RF burns or high SAR. Arcing is known to occur in high fields and has always been associated with startle reactions. The combination of high fields, bright startling arcs, and RF burns have produced a mind-set that all arcing is bad. Therefore, even if a worker were protected from the RF burn and high SAR, it is unlikely that workers would be allowed to work where arcing occurred.

#### CONCLUSION

Use of protective clothing will increase in future years. European telephone companies seem to be on the leading edge of this increase. Those companies have a need to regularly conduct work on RFR transmitting towers. As RF technology continues to grow in areas such as cellular telephones, computer networks, and military technology, the number of workers needing protection and number of different exposure configurations requiring attention will grow. To allow the most efficient operation of the various systems, periods of downtime must be minimized, and workers will be required to don protective suits much more frequently. More information is needed to corroborate previously obtained data and establish even wider areas of usefulness (frequencies and/or power levels) of protective clothing.

At present, I know of only one manufacturer of RFR protective suits, NSP Safety Products, Nordendorf, Germany. In time, this situation will likely change and will require even more testing and corroboration to support strong programs of worker protection throughout the military and private sectors.



## Measurement of Shielding Effectiveness of Microwave-Protective Suits

Arthur W. Guy, Ph.D.  
Bioelectromagnetics Consulting  
Seattle, Washington

This presentation describes tests of the effectiveness of a number of protective suits designed to shield the human body from exposure to high-intensity microwave fields done by Guy et al., (1987). Four suits were evaluated: the Wave Guard suit used by AT&T; the suit used by the U.S. Navy; and two relatively new suits, one manufactured by the Milliken and Body Guard companies in the United States, the other manufactured by the Invertag Electronics and Telecommunication Company in Switzerland and called the Invascreen Protective System. The attenuations of the suits were initially tested by measuring the waveguide transmission loss through the fabric at various locations on the suit. A signal generator was used to transmit a signal through a waveguide to a power meter, where the power was noted and compared with the value obtained when the fabric was placed between the flanges of the waveguide. All of the suits were also tested on a full-scale phantom human body composed of synthetic muscle tissue enclosed in a 0.3-cm-thick fiberglass shell. The phantom body was instrumented with special diode electric-field sensors at ten different locations on the body where surface electric-field-strength measurements were made, from which the surface specific absorption rates (SAR's) of energy were determined as a function of position. These measurements were made for the model both with and without the suit while under exposure to a relatively pure plane-wave electromagnetic field at a frequency of 2450 MHz, with power densities up to  $65 \text{ mW/cm}^2$ . The exposures were conducted in a large (12 ft x 24 ft x 12 ft) anechoic chamber with an absorber designed to eliminate internal reflections over a frequency range of 450-MHz through 100 GHz. The 2450-MHz fields were provided by a 10-kW klystron source.

Using the waveguide-transmission-loss test, both the Wave Guard and the U.S. navy suit fabrics were found to provide at least 40-dB attenuation. The Milliken material provided at least 30-dB attenuation independent of fabric orientation. The attenuation of the Invascreen material was quite poor, showing an orientation dependence from 17-19 dB for parallel polarized E-field exposure.

Since the waveguide method provides only a comparison between the attenuations of various fabrics and does not evaluate the other factors, such as seams and overall suit design, that affect shielding properties, the suits were put on a full-sized man model filled with phantom muscle, and tests with ten diode E-field sensors were conducted. The attenuations at the forehead, neck, heart, liver, shoulder, elbow, wrist, groin, knee, and ankle were calculated by comparison of two sets of diode sensor readings one taken with and one taken without the suits on the exposed model.

The attenuation in terms of body surface SAR at the ten diode antenna measurement points for each suit is given in Table 1. The Wave Guard suit provided attenuations between 20 and 35 dB for most parts of the body. A few low attenuation values (13.2-16 dB) were obtained at locations on the head and ankle owing to the open head hood and the opening of the pant leg at the ankle. The Milliken suit (with the Wave Guard hood) provided quite good attenuation (20-35 dB) for parallel electrical-field exposure, but low attenuation (2-19 dB) for perpendicular polarized field exposure owing to the poor design (multiple openings) of the suit. The Invascreen suit was well designed to prevent leakage; however, the intrinsic poor attenuation of the fabric material resulted in poor shielding (18.7-24.5 dB for parallel E field of exposure and 0.4-21.1 dB for perpendicular E-field exposure). The highest attenuation was provided by the Navy suit, which had a range of 34.5 to 48.7 dB for exposures in both the parallel and perpendicular orientations with respect to the E Field. This effective shielding is due to the complete enclosure of the man inside the suit and minimal fabric openings.

Therefore, in terms of shielding effectiveness, the Navy suit was the best, the Wave Guard was the second best, and the Milliken and Invascreen were the least effective. However, the flammability of the Navy

and Wave Guard suits presents a fire risk. Open-flame tests indicated that the Milliken fabric material is the most fire retardant.

An ideal combination would be the high attenuation and the minimal-opening design of the Navy suit and the fire-retardant properties of the Milliken fabric. An adequate compromise would be to tailor a suit of the Navy design with Milliken material; such a suit should pose no fire hazard and provide at least a 30-dB attenuation.

**Table 1. Attenuation in Decibels of Microwave Protective Suits at Ten Points on Body Of Phantom Man**

Suit	Pol.	1	2	3	4	5	6	7	8	9	10
Navy	Ver.	48.7	43.3	38.9	43.1	46.9	43.5	42.6	42.7	38.7	40.5
Navy	Hor.	43.2	44.3	42.4	45.5	41.6	35.4	43.6	34.5	36.4	39.6
Wave Guard	Ver.	22.9	21.0	32.1	32.8	33.7	31.6	26.5	34.5	35.0	16.0
Wave Guard	Hor.	14.5	23.2	23.6	23.5	24.6	24.4	23.9	25.7	32.9	13.2
Milliken	Ver.	24.3	28.7	30.4	33.7	32.8	33.9	20.3	27.8	29.1	28.3
Milliken	Hor.	9.9	10.1	10.0	11.2	13.4	10.4	11.1	13.5	19.2	2.0
Invascreen	Ver.	23.3	24.5	23.4	22.4	21.8	21.3	21.5	24.2	19.5	18.7
Invascreen	Hor.	21.1	16.9	13.6	13.5	17.2	8.2	16.3	13.3	0.4	9.6

#### Reference

Guy A.W., Chou C.K., McDougall J.A., and Sorensen, C., 1987, Measurement of Shielding Effectiveness of Microwave-Protective Suits. IEEE Trans on Microwave Theory and Techniques, Vol MTT-35, No 11, Nov pp984-994